UNIVERSITÀ DEGLI STUDI DI MILANO

DIPARTIMENTO DI SCIENZE FARMACOLOGICHE E BIOMOLECOLARI

CORSO DI DOTTORATO IN
SCIENZE FARMACOLOGICHE SPERIMENTALI E CLINICHE
CICLO XXIX

Thromboxane Prostanoid Receptor: function, activation and possible target for cardiovascular protection

BIO/14

Tutor
Prof. Angelo SALA

Coordinatore del Corso di Dottorato
Prof. Alberto CORSINI

Silvia CARNEVALI
Matr. R10563

A.A.
2015-2016

Index

Abstract

In the last few years cardiovascular diseases are considered one of the major cause of death, and one of the main player is TXA_2 (Thromboxane A_2), a product of arachidonic acid metabolism generated from the activity of thromboxane synthase on prostaglandin H_2 intermediate via cyclooxygenase (COX). TXA_2 is responsible for platelets activation and aggregation, thrombus formation, and thus it can cause stroke and myocardial infarction. TXA_2 exerts its actions through the TP receptor, a widely expressed GPCR (G protein coupled receptor) present in many cell types among different organ systems. During my thesis I worked to shed light on the mechanism of activation of TP receptor WT (wild type), and two of its mutants (TPαE129V and TPαR130V) of the highly conserved motif E/DRY, in order to assign each receptor state to the CTC (Cubic Ternary Complex) model. In particular, using the new technique SPASM (Systematic Protein Affinity Strength Modulation), the goal was to understand the conformational state of TPαWT and mutants in basal condition, *i.e.* their coupling or uncoupling states with G proteins. The results obtained suggest that TPαE129V (SAM-super active mutant) is in an 'active-like' conformation corresponding to the RG state (inactive, coupled to G protein), on the contrary, TPαR130V (loss of function mutant) seems to display an inactive R conformation (uncoupled to G protein), as envisioned by CTC model.

The study of TPα receptor induced us to consider a second focus in my thesis: TPα receptor as a possible target for new chemical entities with both COX-2 selectivity (COXIB) and TP antagonist activity. New compounds were obtained modulating the structure of existing drugs (lumiracoxib and RC 0) to obtain novel multitarget NSAIDs (Nonsteroidal Anti-inflammatory Drug) endowed with balanced COXIB and TP receptor antagonist properties. Antagonistic activity on the TP receptor was examined for all compounds by evaluating the inhibition of platelets aggregation induced by the stable TXA_2 receptor agonist U46619. COX-1 and COX-2 inhibition were assessed in human washed platelets (challenged by the calcium ionophore

A23187) and human lympho-monocytes suspension (stimulated with lipopolysaccharides), respectively. COX selectivity was determined by calculating IC_{50} values ratio (COX-2/COX-1) obtained from concentration-response curves. Among the lumiracoxib derivatives, the tetrazole compound **18** and the trifluoromethan sulfonamido-isoster **20** were the more active antagonists at the TP receptor, preventing human platelet aggregation and intracellular signalling, with pA_2 values statistically higher than lumiracoxib. Comparative data regarding COX-2/COX-1 selectivity showed that while compounds **18** and **7** were rather potent and selective COX-2 inhibitors, compound **20** was somehow less potent and selective for COX-2. Among the RC 0 derivatives, of particular interest resulted compounds SWE 74, CP 7 and CP 8, because they demonstrated to be fairly selective for COX-2 enzyme, but they appeared to be the weakest TP receptor antagonists among the 35 compounds tested. On the other hand, the last compound of interest was SWE 96, a molecule possessing a good activity on TPα receptor, but lacking selectivity in term of COX-2 inhibition, that is behaving like traditional NSAIDs. All the other derivatives tested were not selective COX-2 inhibitors and/or did not inhibit platelet aggregation.

Taking advantage of what we learned in terms of structural requirements for COX-2 selective inhibition and TP antagonism, additional studies will certainly be carried out to improve the pharmacodynamic profile of these molecules before a careful evaluation can be considered in an *in vivo* animal model.

Riassunto

Negli ultimi anni i disturbi cardiovascolari sono considerati una delle principali cause di morte, e uno dei principali protagonisti è TXA_2 (Trombossano A_2), un prodotto del metabolismo dell'acido arachidonico generato dall'attività della trombossano sintasi sull'intermedio prostaglandina H_2 via cicloossigenasi (COX). Il TXA_2 è responsabile dell'attivazione e aggregazione piastrinica e della formazione di trombi, può quindi causare ischemia e infarto del miocardio. Il TXA_2 esercita la sua attività attraverso il recettore TP, una GPCR (recettore accoppiato alla proteina G) ampiamente espressa e presente in molti tipi di cellule in diversi sistemi d'organismo. Durante la tesi, ho lavorato per chiarire il meccanismo di attivazione del recettore TP nativo (WT) e di due suoi mutanti (TPαE129V e TPαR130V) appartenenti al motivo altamente conservato E/DRY, al fine di assegnare ciascuno stato recettoriale al modello CTC (Cubic Ternary Complex). In particolare, usando la nuova tecnica SPASM (Systematic Protein Affinity Strength Modulation), l'obiettivo consisteva nel capire lo stato conformazionale del TPαWT e dei mutanti in condizioni basali, *i.e.* il loro stato di accoppiamento o non accoppiamento con le proteine G. I risultati ottenuti suggeriscono che il mutante TPαE129V (SAM-Super Active) sia in una conformazione "active-like", corrispondente allo stato RG (inattivo accoppiato alla proteina G); al contrario, il mutante TPαR130V (loss of function) sembra porsi in una conformazione inattiva, R (non accoppiato alla proteina G), come risulterebbe dal modello CTC.

Lo studio del recettore TPα ci ha indotto a considerare un secondo obiettivo nella mia tesi: il recettore TPα quale possibile bersaglio per nuove entità chimiche che posseggano sia selettività verso l'enzima COX-2 (COXIB), sia un'attività di antagonismo verso il recettore TP. I nuovi composti sono stati ottenuti modulando la struttura di farmaci esistenti (lumiracoxib e RC 0) per ottenere nuovi FANS (Farmaci Antinfiammatori Non Steroidei) dotati di antagonismo al recettore TP e selettività COX-2 bilanciate fra loro. L'attività antagonistica verso il recettore TP è stata

misurata per tutti i composti valutando l'inibizione dell'aggregazione piastrinica indotta dall'analogo stabile del trombossano A_2 (U46619). Le inibizioni verso COX-1 e COX-2 sono state valutate rispettivamente in piastrine lavate umane (stimolate con calcio ionoforo A23187) e in sospensione di linfo-monociti umani (stimolati con lipopolisaccaride). La selettività verso COX-1 o COX-2 è stata determinata calcolando il rapporto dei valori di IC_{50} ottenuti dall'analisi delle rispettive curve concentrazione-risposta. Tra i derivati del lumiracoxib, i più potenti antagonisti del recettore TP erano il composto tetrazolico **18** e il trifluorometano sulfonamidico-isoestere **20**, che riducevano l'aggregazione piastrinica e il 'signaling ' intracellulare, con valori di pA_2 statisticamente superiori a quelli calcolati per il lumiracoxib. La selettività COX-2/COX-1 calcolata ha mostrato che, mentre i composti **18** e **7** erano inibitori di COX-2 abbastanza potenti e selettivi, il composto **20** era invece meno potente e selettivo verso COX-2. Tra i derivati della molecola RC 0 (35 composti), sono risultati essere di particolare interesse i composti SWE 74, CP 7 e CP 8, perché sono piuttosto selettivi verso l'enzima COX-2, ma tra i più deboli antagonisti del recettore TP. D'altra parte, l'ultimo composto di interesse si è rivelato essere SWE 96, una molecola che ha perso selettività in termini di inibizione COX-2, comportandosi quindi come i tradizionali FANS, ma dotato di una buona attività sul recettore TPα. Tutti gli altri derivati analizzati si sono dimostrati essere o inattivi nei confronti dell'aggregazione piastrinica e/o non selettivi verso l'enzima COX-2.

Avvantaggiandoci delle conoscenze acquisite in termini di requisiti strutturali, necessari per avere sia selettività COX-2 sia antagonismo TP, siamo consapevoli che, prima di prendere in considerazione una scrupolosa valutazione in modelli animali *in vivo,* saranno necessari ulteriori studi per migliorare il profilo farmacodinamico di queste molecole.

Introduction

Arachidonic acid cascade and eicosanoids

Arachidonic Acid (AA) is a 20-carbon unsaturated fatty acid (AA 5, 8, 11, 14-eicosatetraenoic acid) that is present in all mammalian cell. This 20 carbon fatty acid with four double bonds was first isolated and identified from mammalian tissues in 1909 by Percival Hartley (Hartley, 1909).

AA is released from membranes by the activation of phospholipases A_2 (PLA_2 induced by an elevation in the cytosolic concentration of Ca^{2+}) and it is converted into many biologically active mediators called "eicosanoids" when cells are stimulated by mechanical trauma, oxidative stress, or by specific cytokine, growth factors, and pro-inflammatory mediators (such as histamine, bradykinin and vasopressin) (Corey et al., 1980). The control of AA release from membranes has undergone several paradigm shifts with the continuing identification of new PLA_2 members (Six and Dennis, 2000). Despite this, type IV cytosolic PLA_2 ($cPLA_2$) remains the key player for eicosanoid production because it has been demonstrated that cells lacking $cPLA_2$ are generally devoid of eicosanoid synthesis (Funk, 2001). Eicosanoids are "autacoids", that are chemical transmitter substances produced by cells of the body and released in the extracellular compartment where they act in the immediate surroundings by binding specific membrane receptor and modulating many biological functions. Eicosanoids' half-life is very short and they are not stored within the cells, but are synthesized *de novo* from membrane-released AA when cells are activated, acting as autocrine and paracrine lipid mediators (Funk, 2001).

The biological active compounds derived from free AA can be classified in four major groups: prostanoids, leukotrienes, iso-eicosanoids and epoxyeicosatrienoic acids and dihydroxyeicosatrienoic acids (Fig. 1).

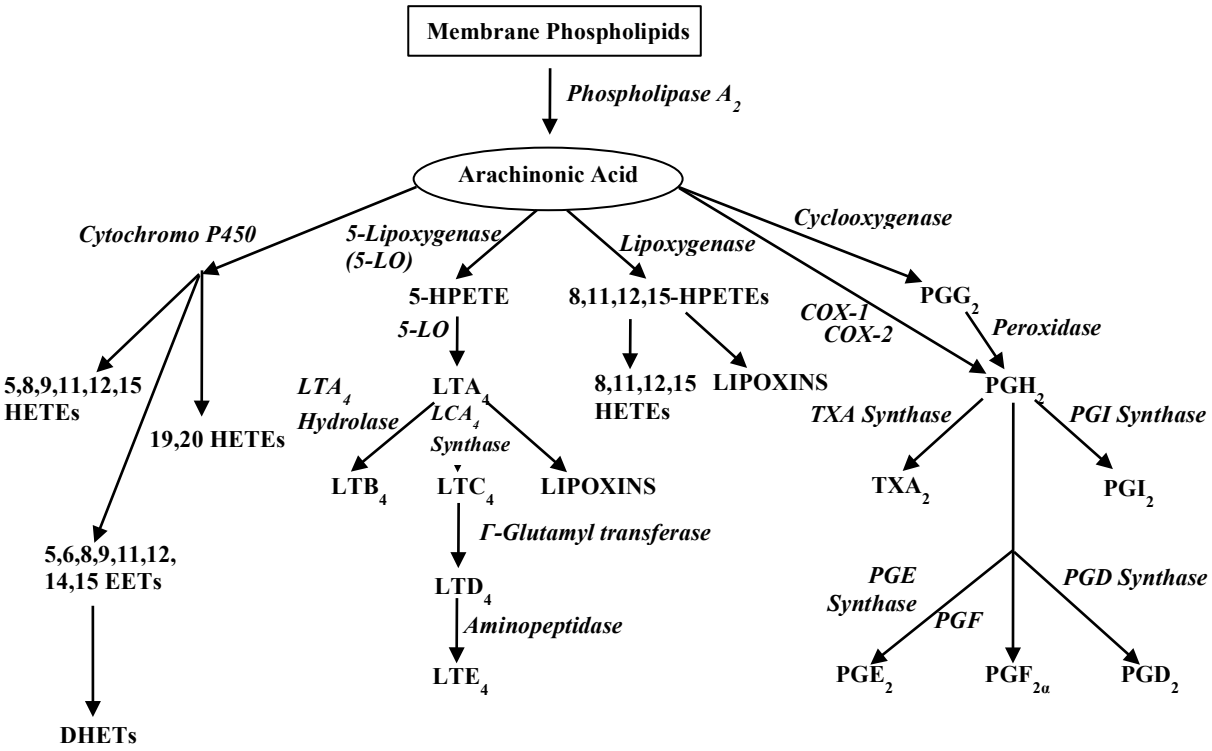

Fig. 1 Arachidonic Acid cascade: Biosynthesis of prostaglandins, thromboxane, leukotrienes, lipoxins and HETEs (*modified from Osterud B. and Bjorklid E., 2003*).

Prostanoids: Prostaglandins And Thromboxane

Prostanoids are formed by the action of prostaglandin G/H synthase, also called cyclooxygenase (COX), on AA. COX, an evolutionarily conserved enzyme, exists as two distinct isoforms, COX-1 and COX-2. The crystal structures of COX-1 and COX-2 are remarkably similar, with one notable amino acid difference that leads to a larger "side-pocket" for substrate access in COX-2 (Smith et al., 2000). COX-1, constitutively expressed in most cells, is the dominant source of prostanoids with house keeping functions, such as gastric epithelial cytoprotection and hemostasis. COX-2, induced by cytokines, stress, and tumor promoters, is the most important source of prostanoids formation in inflammation (Smyth et al., 2009), but is also continuously expressed in cells such as endothelial cells and few other cell types.

COX-1 and COX-2 function as homodimers, and perhaps heterodimers (Yu et al., 2006), inserted in the endoplasmatic reticulum and the nuclear membrane with the substrate binding pocket precisely oriented to take up and transform AA into the unstable cyclic endoperoxides PGG_2 and PGH_2 (Smyth et al., 2009). Downstream

isomerases and synthases complete the conversion and the biosynthesis of the unstable PGG_2 and PGH_2 into TXA_2 and D, E, F, and I series prostaglandins (PGs).

Of particular interest, COX-1 couples preferentially, but not exclusively, with thromboxane synthase, prostaglandin F synthase, and with the cytosolic prostaglandin E synthase (PGES) isozymes, while on the other hand COX-2 prefers prostaglandin I synthase (PGIS) and microsomal (m) PGES isozymes, both of which are induced by cytokines and tumor promoters (Smyth et al., 2009).

Under a physiological and pathological point of view, prostanoids are important players in many events, such as inflammation, cardiovascular system, platelets activation, atherothrombosis events and renal function.

During the inflammatory response, prostanoids biosynthesis is significantly increased and both PGE_2 and PGI_2 are the predominant pro-inflammatory prostanoids. Both markedly enhance edema formation and leukocyte infiltration by promoting blood flow in the inflamed area through a potent vasodilating effect. Finally, the chemotactic function of PGD_2, a major product of mast cells, contributes to inflammation in allergic responses, particularly in the lung (Smyth et al., 2009).

In the cardiovascular system it is known that prostanoids do not circulate and do not impact directly systemic vascular tone because of their short half-life. However, they may modulate local vascular tone at the site of their formation and affect systemic blood pressure through effects on the kidney. Finally $PGF_{2\alpha}$ is a potent constrictor of both pulmonary arteries and veins in humans, while TXA_2 is a vasoconstrictor in the whole animal and in isolated vascular beds (Smyth et al., 2009).

It is well known that activated platelets synthesize TXA_2, further amplifying platelet shape change, activation and recruitment (FitzGerald, 1991). The total biosynthesis of TXA_2 is augmented in clinical syndromes involving platelet activation, including unstable angina, myocardial infarction and stroke. Mature platelets express only COX-1, although megakaryocytes and immature platelet forms also express COX-2 (Rocca et al., 2002). Finally, PGI_2 is a potent inhibitor of platelet activation, synthesized by COX-2, and to a less degree by COX-1, in vascular endothelial and smooth muscle cells.

In atherosclerosis, an inflammatory cardiovascular disease, unstable or ruptured plaques can result in intravascular thrombosis leading to severe clinical

complications. Individual prostanoids are associated with opposite effects in atherothombosis. In mice it has been shown that suppression of TXA_2 biosynthesis, as well as TP antagonism or deletion of the TP receptor, retards atherogenesis (Egan et al., 2005; Kobayashi et al., 2004); conversely, PGI_2 appears atheroprotective (Egan et al., 2004). The effects of PGE_2 on atherotrombosis appear to be more complex: deletion or inhibition of mPGES-1 markedly reduces inflammatory responses in several mouse models, and mPGES-1 deletion also reduces atherogenesis in fat fed hyperlipidemic mice (Wang et al., 2006). Interestingly, in addition to the expected depression of PGE_2 production, deletion of mPGES-1 also increases the biosynthesis of PGI_2.

Renal PGs, especially PGE_2 and PGI_2, but also $PGF_{2\alpha}$ and TXA_2, perform complex and intricate functions in the kidney (Breyer and Breyer, 2000; Hao and Breyer, 2007). Both COXs are typically expressed in renal tissue and it is known that COX-2 derived prostanoids increase medullary blood flow and inhibit tubular sodium readsorption while COX-1 derived products promote salt excretion in the collecting ducts (Smyth et al., 2009).

Thromboxane A2

Thromboxane A2 (TXA_2), as previously reported, arises from the conversion of PGH_2 by thromboxane synthase (TXS), a P450 cytocrome enzyme, that is present in lungs, spleen and macrophages (Needleman et al., 1976). When TXA_2 is formed from PGH_2 by TXS, 12-L-hydroxy-5,8,10-heptadecatrienoic acid (HHT) and malondialdehyde (MDA) are also simultaneously produced (Haurand and Ullrich, 1985; Shen and Tai, 1986). The molar ratio between these products are 1:1:1. TXA_2 is extremely labile as a result of its strained oxetane ring; its half-life in the blood stream is about 30-40 seconds but it appears to be more stable at pH 9-10. TXA_2 is rapidly converted by non-enzymatic addiction of a molecule of water yielding TXB_2, which is lacking biological activity (Armstrong and Wilson, 1995).

Finally, TXS was first found in platelets as a microsomal enzyme (Needleman et al., 1976) and it was then reported also in several other tissues (Sun et al., 1977) like lung, platelets, kidney, stomach, duodenum, colon and spleen.

Physiological and Pathophysiological functions of thromboxane A_2

TXA_2 activity is mediated through the specific G protein-coupled, thromboxane-prostanoid receptor (TP) that is expressed on the plasma membrane of the cells. Only cells that express the TP receptor are able to respond to TXA_2. Indeed, platelets, which are the major producer of TXA_2, also express the TP receptor, and represent the biological system where TXA_2 exerts the most important functional role.

Indeed, the TP-TXA_2 system plays a critical role in hemostasis by representing a major factor in platelet activation: TXA_2 synthesis and subsequent TP receptor activation lead to platelet shape change, adhesion and secretion, which in turn lead to platelet aggregation, promote thrombus formation and cause additional TXA_2 formation. When occurring in the lumen of critical vascular beds, these events may lead to acute myocardial infarct or stroke (Nakahata, 2008).

TXA_2 is also a potent contractile agent of vascular smooth muscle cells (Yamamoto et al., 1993), thus leading to vasoconstriction, and for this reason has also been involved in hypertension (Geoffroy et al., 1989; Liel et al., 1993). In addition to vascular smooth muscles, TXA_2 causes contraction of different types of smooth muscles, including bronchial (Devillier and Bessard, 1997) or intestinal smooth muscles (Schultheiss and Diener, 1999), and TXA_2-induced contraction of bronchial smooth muscles may, in some instances, contribute to asthma (Martin et al., 2001).

TXA_2, and TP have an important role in pro-inflammatory events also occurring in endothelial cells. TXA_2 enhances the surface expression of adhesion proteins, such as intracellular adhesion molecule-1 (ICAM-1), and TXA_2 is involved in endothelial cell migration and angiogenesis (Daniel et al., 1999).

However, in normal conditions TXA_2 pro-aggregatory and vasoconstricting activity is balanced by PGI_2 that, upon binding to its receptor IP, promotes anti-aggregatory and vasodilating activities (Kawabe et al., 2010).

TXA_2 is also involved in nephritis and nephrotic disease of kidney, and may play a role in the allergic response in asthma, rhinitis and atopic dermatitis (Nakahata, 2008).

Leukotrienes

Leukotrienes (LTs) are formed by the action of 5-lipoxygenase (5-LO) on AA released from membrane phospholipids. There are at least six different types of mammalian lipoxygenases, which are named according to the carbon position at which a single oxygen molecule is incorporated. Among them, 5-LO, expressed mainly in granulocytes, macrophages and mast cells, is the most studied one (Samuelsson et al., 1987). AA is first oxidized at the C-5 position by the dual enzymatic activity of 5-LO to yield 5-HpETE followed by an unstable intermediate, leukotriene A4 (LTA_4); 5-HpETE acts in concert with five-LO-activating protein (FLAP) in a Ca^{2+} dependent manner. LTA_4 is either converted into LTB_4 by LTA_4 hydrolase or conjugated to reduced glutathione by leukotriene C4 synthase to yield cysteinyleukotriene (CysLT) 4 (LTC_4). LTC_4 is then exported from the cell and converted into LTD_4 and LTE_4, the most stable CysLT (the cysteinyleukotrienes are: LTC_4, LTD_4 and LTE_4), by extracellular peptidases (Liu and Yokomizo, 2015).

LTs are involved in various inflammatory diseases, including asthma, allergic rhinitis, atopic dermatitis, allergic conjunctivitis, rheumatoid arthritis and chronic obstructive pulmonary disease (Ohnishi et al., 2008).

Asthma is a complex and chronic disorder of the airways that is characterized by airflow obstruction, allergic airway inflammation, and airway hyperresponsiveness. Airway inflammation plays a critical role in the pathogenesis of asthma, which is characterized by the infiltration of inflammatory cells such as neutrophils, eosinophils, and lymphocytes. Studies performed in asthmatic patients suggest a potential role for LTB_4 (Csoma et al., 2002; Wenzel et al., 1995) and, even if the real role of LTB_4 remains unclear, it is thought to be a proinflammatory mediator that is responsible for the recruitment, activation, and survival of leukocytes, including neutrophils and eosinophils (Bruijnzeel et al., 1990; Sumimoto et al., 1984). CysLTs, on the other hand, being the most potent known bronchoconstrictors in humans are thought to play a pivotal role in the pathogenesis of acute and chronic asthma. Indeed, in addition to their bronchoconstricting activity, CysLTs also play an important role in airway remodelling by promoting the proliferation of airway smooth muscle cells and epithelial cells, and by increasing collagen deposition (important feature of chronic asthma) (Hay et al., 1995).

Allergic rhinitis is believed to share a common pathophysiology and immunopathology with asthma, and symptoms of allergic rhinitis, including itching, sneezing and nasal obstruction can coexist with, and have an effect on, bronchial asthma (Peters-Golden et al., 2006). Most of the cells involved in pathophysiology of allergic rhinitis produce and release CysLTs. Moreover, severe nasal obstruction in patients with seasonal allergic rhinitis is associated with increase excretion of urinary LTE_4 (Higashi et al., 2003). Finally, given that peripheral blood neutrophils isolated from patients produce more LTB_4 after calcium ionophore stimulation than those isolated from healthy controls (Sousa et al., 2002), also LTB_4 may play a role in this pathology.

Iso-Eicosanoids

Iso-eicosanoids represent a growing family of eicosanoid isomers, generated non-enzymatically from lipid peroxidation of esterified AA. They include isoprostaglandins or isoprostanes of the D_2, E_2 and $F_{2\alpha}$ series, isothromboxanes and isoleukotrienes (Maclouf et al., 1998). Of particular interest are the isoprostanes because they may have a role in cardiovascular disease.

Isoprostanes are generated *in vitro* as well as *in vivo*, primarily independent of COXs activity, via free radical-induced peroxidation of unsaturated fatty acid (Morrow et al., 1990a). Under physiological conditions, these prostaglandin-like compounds can only be detected as esterified at very low concentrations, in the nanomolar range, or as free compounds in the picomolar range in biological fluids, for example plasma and urine (Morrow et al., 1990b). In condition of oxidative stress, the burst of free radical formation leads to a significant increase in isoprostane levels (Morrow et al., 1992; Morrow et al., 1990b).

Isoprostanes are formed *in situ* on arachidonoyl-containing lipids and then subsequently released in free form into the circulation via an enzyme-dependent mechanism (Morrow et al., 1992; Morrow et al., 1994). Even if seems that this process is dependent on the activity of PLA_2**,** little is known about the mechanisms responsible for the secretion of isoprostanes from intracellular space to the extracellular *milieu*. Once reached the systemic circulation, isoprostanes, such as 8-iso-$PGF_{2\alpha}$, are partially metabolized by mechanisms involving, for example,

peroxisomal β-oxidation (Schwedhelm et al., 2000). Finally, isoprostanes and isoprostane metabolites are freely filtered in the glomerular apparatus of the kidneys and excreted in urine (Bauer et al., 2014).

Experimental data strongly suggest that isoprostanes signalling is exclusively regulated via the interaction with the TP receptor. In the context of isoprostane/TP signalling, an association of TP receptors with G-proteins such as G_q, G_i and G_{11} has been described (Acquaviva et al., 2013; Kinsella et al., 1997). Moreover some experimental results from *in vitro* studies indicate that isoprostanes are partial agonists at TP receptors and that the biological activity of isoprostanes may be additionally mediated via an isoprostane-specific receptor. However, so far, no molecular evidence has been found for the existence of such an isoprostane-specific receptor (Audoly et al., 2000; Bauer et al., 2014; Benndorf et al., 2008).

Isoprostanes participate in oxidative injury by modulating platelet activation and adhesion (Minuz et al., 1998). In addition to altered platelet behaviour, isoprostanes enhance the interaction of monocytes with ECs (Huber et al., 2003; Leitinger et al., 2001) and this process is mediated by TP receptor-dependent activation of PKA and p38 (Huber et al., 2003; Leitinger et al., 2001). Finally, it has been described that high concentrations of isoprostanes cause a significant vasoconstriction of a wide range of different blood vessels (Kromer and Tippins, 1996; Sakariassen et al., 2012; van der Sterren and Villamor, 2011).

Epoxyeicosatrienoic Acids and Dihydroxyeicosatrienoic Acids

Epoxyeicosatrienoic acids (EET) are epoxide derivates of arachidonic acid. They are formed by cytochrome P450 (CYP) epoxygenases and function as lipid mediators. Each CYP epoxygenases produce several regioisomers, with usually one predominant form. Epoxidation can occur at any of the four double bonds of AA, giving rise to four regioisomers, 5,6-, 8,9-, 11,12-, and 14,15-EET. As the regioisomers have a number of similar metabolic and functional properties, they are generally considered as a single class of compounds (Spector, 2009) responsible for autocrine and paracrine effects (Larsen et al., 2008).

EETs are synthesized in the endothelium and activate large-conductance Ca^{2+}-activated K^+ channels, causing hyperpolarization of the vascular smooth muscle and

vasorelaxation (Campbell and Falck, 2007). Thus, EETs function as an endothelium-derived hyperpolarizing factor (EDHF) in a number of vascular beds, including the coronary and renal circulation, producing decrease in blood pressure (Carroll et al., 2006). After all, EETs have beneficial and positive effects: it has been reported that EETs promote anti-inflammatory and antiapoptotic actions in the endhotelium (Larsen et al., 2007) and in kidney (Imig, 2005) and also 11,12- and 14,15-EET are cardioprotective during reoxygenation of ischemic myocardium, decreasing infarct size (Gross et al., 2008; Seubert et al., 2007).

Dihydroxyeicosatrienoic acids (DHETs) are formed by the activity of soluble epoxide hydrolase (sEH) on EETs. DHETs are known to attenuate many of the functional and positive effects of EETs, but no specific function has so far been detected (Spector and Norris, 2007). For this reasons the inhibition of sHE is being evaluated as a mechanism for increasing and prolonging the beneficial actions of EETs. However, some caution is suggested by the findings that 11,12-DHET activates Ca^{2+} activated K^{+} channels in coronary artery myocytes and induces coronary vasodilatation (Lu et al., 2001). The sHE inhibitors were initially developed as antihypertensive agents (Chiamvimonvat et al., 2007), but recent data indicate that they may also prevent cardiac hypertrophy (Xu et al., 2006), decrease vascular smooth muscle proliferation (Ng et al., 2006), improve renal hemodynamics (Roman, 2002), and decrease hypertensive renal damage (Huang et al., 2007; Spector and Norris, 2007).

Pharmacological Modulation of Arachidonic Acid

NSAIDs: Nonsteroidal anti-inflammatory drugs

NSAIDs are among the most commonly prescribed medications purchased over the counter to treat acute and chronic pain and inflammation associated with a range of medical condition (Pawlosky, 2013). It is estimated that NSAIDs are prescribed to about 25% of Canadians for short-term use, but overall use is likely much higher with over-the-counter availability (Pawlosky, 2013).

The main mechanism of the analgesic and antipyretic action of NSAIDs appears to be prostaglandin biosynthesis inhibition.

Like any medication, the benefits of NSAIDs should be considered in tandem with the potential adverse effects. Side effects range from the mild and common to the severe and infrequent: dyspepsia, gastric or duodenal ulceration, sodium retention and subsequent hypertension, as well as increased incidence on cardiovascular adverse event (like infarct and stroke). These are the results of the homeostatic role of COX-1 enzyme, being responsible for the production of prostaglandins and thromboxane, which are involved in routine physiological functions such as gastroprotection, platelet aggregation and renal blood flow.

The most widely known NSAID is Aspirin, the only NSAID known to react binding covalently (and time-dependently) with the cyclooxygenases. Aspirin acetylates Ser-529 in COX-1 (Ser-516 in COX-2), inhibiting irreversibly its enzymatic activity. This unique feature, which, together with the limited capacity of platelets for *de novo* protein synthesis, is responsible for the inhibition of platelet TXA_2 biosynthesis even when used at sub-optimal doses for its anti-inflammatory action, and underlies aspirin's position as the only COX inhibitor with proven cardioprotective activity (Patrono et al., 2001).

COXIB

In the early 1990s, when it was proven that there were two COX isoforms, it was proposed that the analgesic, anti-pyretic and anti-inflammatory effects of non-steroidal anti-inflammatory drugs (NSAIDs) could be attributed to COX-2 inhibition, whereas the anti-thrombotic effects, as well as the unwanted renal and gastrointestinal (GI) side effects, might be dependent upon COX-1 inhibition (Rovati et al., 2010). Thus, NSAIDs, that were initially classified on the basis of their chemical and pharmacological properties, were later reconsidered mainly on their COX-1/2 selectivity (Grosser et al., 2006; Warner et al., 1999). Indeed, it was the beginning of a new era for the non steroidal anti-inflammatory drugs: the opportunity to selectivity target one of the two isoforms gave rise to a wide research, aimed at the identification of a safer NSAID, particularly in terms of gastrolesivity and renal function (Masso Gonzalez et al., 2010; Pal and Hossain, 1985). The research was, therefore, focused on COX-2-selective drugs (COXIBs), considered as second generation NSAIDs (FitzGerald and Patrono, 2001) that would retain the anti-

inflammatory and analgesic activities without blunting the gastroprotection sustained by COX-1-derived mucosal PGE_2 synthesis (Cannon and Breedveld, 2001; DeWitt, 1999). As platelet COX-1 was demonstrated to be the major responsible for pro-aggregating TXA_2 synthesis, a marked COX-2 inhibition was considered to be an ideal choice, because gastrointestinal (GI) bleeding that often accompanied the lack of cytoprotection was also amplified by the suppressed formation of TXA_2 (Whittle, 2003), and the resulting altered hemostasis.

However, while on one side a large number of clinical trials, VIGOR (Bombardier et al., 2000), CLASS (Silverstein et al., 2000), TARGET (Schnitzer et al., 2004) largely confirmed a GI safer profile by COXIBs, on the other side increasing evidence for potential cardiovascular (CV) risk associated with COXIBs emerged (Howard and Delafontaine, 2004), mainly ascribed to a COX-2-dependent inhibition of the antiaggregating endothelial-derived prostacyclin (PGI_2) (McAdam et al., 1999). The so called 'balance-tipping' or "imbalance" theory, suggested that any drug that reduces endothelial COX-2-derived PGI_2, without affecting platelet COX-1-derived TXA_2, will predispose to a prothrombotic state (Fitzgerald, 2004). As a consequence of this unanticipated but potentially serious side effect, rofecoxib from Merck and valdecoxib from Pfizer were withdrawn from the market (FitzGerald, 2007; Grosser et al., 2006).

Nevertheless, it remained open the possibility to use a new and safer pharmacological approach combining the anti-inflammatory activity of COXIBs together with a cardioprotective component (Rovati et al., 2010).

Arachidonic acid metabolites receptor

All AA metabolites exert their biological effects by binding to G protein-coupled receptors (GPCRs). In particular two receptors have been identified for LTB_4: the BLT1 and BLT2, and similarly for CysLTs the CysLT1 and CysLT2 receptors have also been characterized. Concerning the prostanoids, a single gene product has been identified for prostacyclin and $PGF_{2\alpha}$: the I prostanoid receptor (IP) and the F prostanoid receptor (FP) respectively, while are known four distinct PGE_2 receptors

(the EP1-4), two PGD_2 receptors (DP1 and DP2) and two T prostanoid receptors for (TPα and TPβ) for TXA_2.

LTB_4 exerts its biological effects through its two GPCRs expressed on the surface of cells. BLT1 is the high-affinity LTB_4 receptor, BLT2 is its low affinity receptor and, in human genome, the genes that encode these receptors are located in very closed proximity to each other (Kamohara et al., 2000; Yokomizo et al., 1997; Yokomizo et al., 2000). The human *LTB4R* gene encodes a BLT1 protein comprising 352 amino acid residues (NCBI Reference Sequence: NP_858043) and it shares relatively high sequence homology with BLT1 of other species; similarly, BLT2 is also highly conserved, showing 92% homology with murine BLT2 at the amino acid level (Iizuka et al., 2005; Kamohara et al., 2000; Yokomizo et al., 2000). BLT1 is predominantly expressed on leukocytes (granulocytes, monocytes, macrophages, eosinophils, dendritic cells, mast cells and differentiated T-cells) (Serhan and Prescott, 2000), whereas human BLT2 is ubiquitously expressed throughout the body (Kamohara et al., 2000; Yokomizo et al., 2000). Finally, several studies showed that BLT1 and BLT2 couple to G_i- and/or G_q-proteins, depending on the particular cell type (Brink et al., 2003; Kamohara et al., 2000; Sabirsh et al., 2004; Yokomizo et al., 1997). These two GPCRs activate various kinases, which, in turn, phosphorylate downstream signalling molecules.

Recent molecular cloning and functional studies of CysLTs receptors have provided new insights into their biological function(s). The human *CysLT1* gene is located on the X chromosome (Xq13-Xq21) and encodes a protein of 337 amino acids (Lynch et al., 1999). The gene encoding human CysLT2 is located on chromosome 13q14 and the open reading frame encodes a protein of 347 amino acids (Heise et al., 2000; Nothacker et al., 2000). The homology between the two human receptor subtypes is only 31%. It has been demonstrated that CysLT1 mRNA is expressed in normal lung smooth muscle cells and interstitial macrophages, but little or no expression is detected in normal airway epithelial cells; CysLT1 expression has been detected also in eosinophils, monocytes, macrophages and pre-granulocytic $CD34^+$ cells isolated from normal peripheral blood (Figueroa et al., 2001; Lynch et al., 1999). CysLT2 in humans is expressed at high levels by the spleen and peripheral blood leukocytes, as well as in coronary smooth muscle cells, endothelial cells, Purkinje fiber cells, and

human umbilical vein endothelial cells (HUVEC) (Heise et al., 2000; Kamohara et al., 2001; Nothacker et al., 2000; Takasaki et al., 2000). Uniquely, this receptor is also expressed in the heart, adrenal gland, in the brain and in the spinal cord (Heise et al., 2000; Nothacker et al., 2000). Taken together, these findings suggest that the expression of CysLT receptors is regulated by various cytokines, and it is intimately associated with the pathogenesis of many allergic diseases (Liu and Yokomizo, 2015).

As previously reported prostanoid receptors are pharmacologically classified into those specific for TX, PGI, PGE, PGF, or PGD, designed TP, IP, EP, FP, and DP receptors, respectively, with EP receptors being further divided into four subtypes identified as EP1, EP2, EP3, and EP4 (Coleman et al., 1994; Kennedy et al., 1982). All receptors are G protein-coupled, rhodopsin-type receptors with seven transmembrane domains and each is encoded by a distinct gene. The different variants of EP3, that are generated by alternative splicing of exons encoding the carboxyl-terminal tail, were also identified and these isoforms show similar ligand binding characteristics but distinct signal transduction properties. In addition to this family of E prostanoid receptors, there is also a separate receptor for PGD_2 (Hirai et al., 2001). This receptor, called CRTH2, was originally cloned as an orphan receptor expressed in T helper (Th) 2 lymphocytes and it has been shown to bind PGD_2 with an affinity as high as that of the DP receptor. CRTH2 belongs to the family of chemokyne receptors and mediates chemotaxis of Th2 lymphocytes as well as of eosinophils and basophils in response to PGD_2 (Narumiya, 2007).

Several studies revealed that the eight types or subtypes of prostanoid receptors can be divided into three groups on the basis of their modes of signal transduction: IP, DP, EP2 and EP4 mediate an increase in the intracellular level of cAMP and have been classified as ”relaxant” receptors; TP, FP and EP1 induce elevation of intracellular Ca^{2+} and have been denoted as “contractile” receptors; EP3 elicits a decrease in the intracellular concentration of cAMP and has been termed an “inhibitory” receptor (Narumiya et al., 1999). This functional grouping of prostanoid receptors is based on the coupling of each receptor to only one of the three signalling pathways, increase or decrease in the intracellular cAMP level or elevation in the intracellular Ca^{2+} concentration; it does not exclude the possibility that these

receptors are able to couple to more than one G protein and therefore to different signal transduction pathways (Narumiya, 2007). It has been suggested that the prostanoid receptors might be ubiquitously distributed throughout the body because of the wide range of prostanoid actions, and northern blot analysis and *in situ* hybridization studies revealed that, even within the same organ, transcripts of different receptor genes were distributed differentially.

G protein-coupled receptors (GPCRs)

GPCRs represent the largest superfamily of receptors in mammalian genome with about 850 members. Out of this number about 350 receptors are potentially drug targets, but for about 100 GPCRs, the so called orphan receptors, neither the endogenous ligand nor the physiological function are yet known (Fredriksson et al., 2003; Lagerstrom and Schioth, 2008). GPCRs are responsible for signal transduction from the extracellular space to the inside of the cells. Since GPCRs are involved in mediating cell signal processes, they are implicated in many diseases and are the targets of a number of drugs used therapeutically. It has been estimated, that about 60% of all prescription drugs today target GPCRs (Schoneberg et al., 2004), being developed for just 50 established GPCR targets out of all the known members of this family, making GPCRs one of the most important class of current pharmacological targets.

Several classification systems have been used to sort out this superfamily. Some groups the receptors considering their ligand, and others using both physiological and structural features. One of the most frequently used classification system lists the receptors based on sequence and structural similarity; using this approach these receptors can be clustered into 5 families: class A, the rhodopsin family (701 members); class B the secretin family (15 members); class C, the glutamate family (15 members); the adhesion family (24 members), the frizzled/taste family (24 members).

The first high resolution three dimensional GPCR crystal structure is that of rhodopsin, solved in 2000 with a resolution of 2.8 A. This structure came from the three-dimensional crystal of bovine rhodopsin and confirmed the general architecture

of the seven transmembrane helices. The three dimensional structure of GPCR has been hardly obtained, but in 2008, using x-ray crystallography, the structure of A2α adenosine, β1 and β2-adrenergic receptors (AR) have been solved at high resolution.
The GPCR proteins are also called seven transmembrane (7TM) receptors because of their common structural signature of seven hydrophobic α-helices that cross the plasma membrane connecting, by alternating intracellular and extracellular loop (ICLs and ECLs), the extracellular amino terminus and the intracellular carboxyl terminus. GPCRs share the greatest homology within the TM segments. The most variable structures among the family of GPCRs are the carboxyl terminus, the intracellular loop spanning TM5 and TM6, and the amino terminus.
Although structural similarity of GPCRs, the natural GPCR ligands are very different, ranging from subatomic particles (a photon), to ions (H^+ and Ca^{++}), to small organic molecules, to peptides and proteins. Indeed the ligands of the GPCRs have different nature: they could be ions, organic odorants, amines, peptides, proteins, lipids, nucleotides, and even photons are able to communicate through these proteins. The location of the ligand binding domains for many GPCRs has been determined and, while many small organic agonists bind within the TM segments, peptide hormones and proteins often bind to the amino terminus and to extracellular sequences joining the TM domains.
GPCRs are able to functionally bind different kinds of G proteins with their intracellular domains (both the COOH terminus and the intracellular loops), and therefore, we can observe a great diversity in the functional coupling of the GPCRs with a number of alternative signaling pathways, interacting directly with a number of other proteins.

Thromboxane A_2 receptor

The thromboxane prostanoid (TP) receptor is a G-protein coupled receptor and is classified as family A of GPCR, the rhodopsin family. It derives its name from its preferred endogenous agonist, TXA_2, even if it is activated also by other AA derivates, such as isoprostanes and 20-hydroxyeicosatetraenoic acid (20-HETE).

In 1989, Narumiya and colleagues purified for the first time the human TP protein, following the development of specific agonists and antagonists in the 1980s (Ushikubi et al., 1989). Based on the sequence of the purified protein, a seven-TM/G protein coupled receptor, human TP cDNA was cloned from placenta (Hirata et al., 1991). Later Raychowdhury, Yukawa, Collins, McGrail, Kent and Ware (1994) (Raychowdhury et al., 1994) cloned another human TP cDNA from human endothelial cell differing from the first only in its C-terminus; this cDNA represents alternative splicing products of the TXA_2 receptor gene. Now, the TP originally cloned from human placenta is called TPα (composed by 343 amino acids in length), and the TP originally cloned from endothelial cells is called as TPβ (407 amino acids in length) (Nakahata, 2008). The cDNA encoding TPα and TPβ represent alternative splicing products of the TP gene, which is located at chromosome 19p13.3. It is present as a single copy, spans over 15 kb and contains 3 exons divided by 2 introns (Nusing et al., 1993).

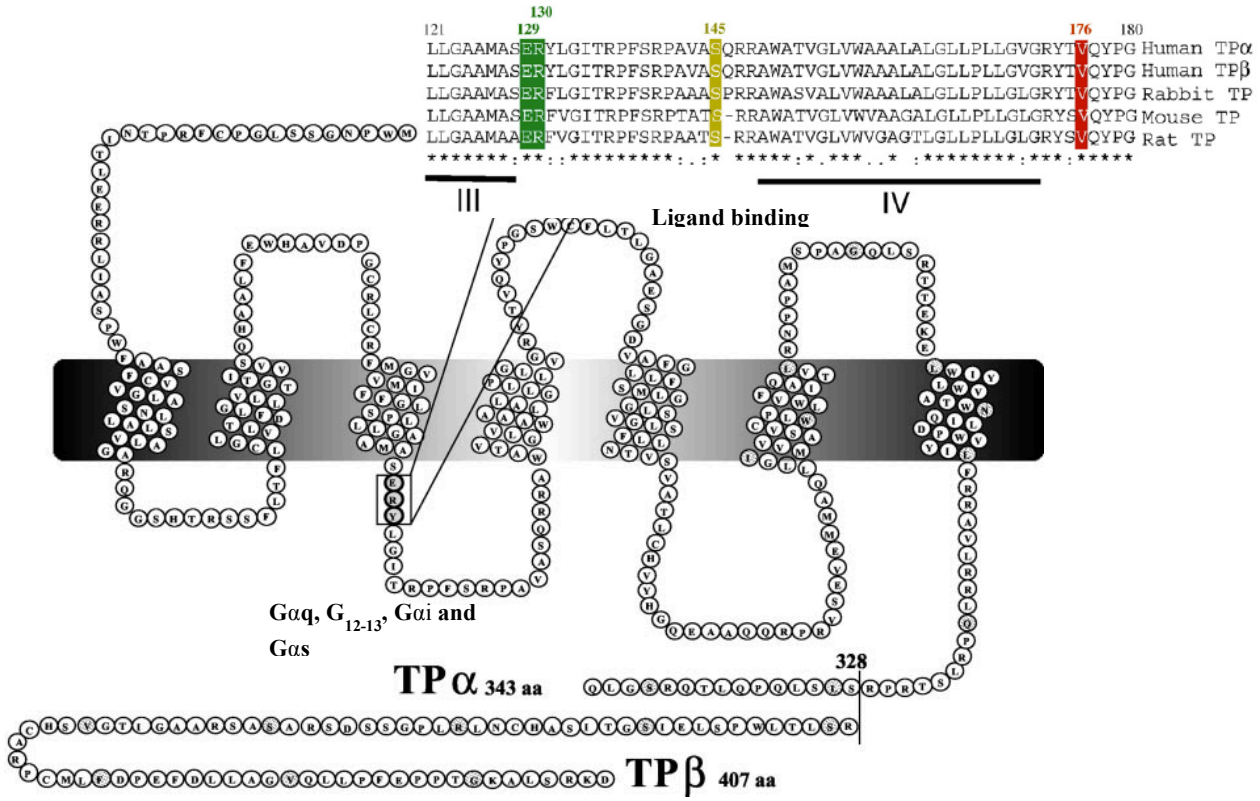

Fig. 2 Amino acid sequences of TPα and TPβ showing the position of the highly conservative ERY motif at the N-terminal end of the second intracellular loop. The different cytoplasmatic C-terminus end of TPα and TPβ are shown. The blocked area represents plasma membrane with seven putative transmembrane domains (*modified from Capra V., et al. 2004 and Nakahata N., et al. 2008*).

Comparison of the two receptor isoform sequences reveals that even though the first 328 amino acids are the same for both (Raychowdhury et al., 1994), the β isoform exhibits an extended C-terminal cytoplasmic domain (Fig. 2). Because of their amino acids sequences the ligand binding sites are assumed to be identical in both splice variants. Therefore, differences in function between TPα and TPβ must be derived from the difference in their C-terminal regions.

Although a detailed analysis of the protein expression of TPα and TPβ should be necessary, the mRNAs for both splicing variants have been detected in most tissues and cells, including platelets, placenta, vascular smooth muscle cells, brain, small intestine and thymus (Miggin and Kinsella, 1998). However, it is worth noting that expression of each TP isoform transcript is not equal within or across different cell types. Thus, while platelets express high concentrations of the TPα mRNA, they possess only residual mRNA coding the TPβ (Habib et al., 1999).

Historically, TP receptor involvement in blood platelet function has received the greatest attention. Nevertheless, it is now clear that TP receptors exhibit a wide distribution in different cell types and among different organ systems (Nakahata, 2008). Over the years, different biological roles for TP receptor signaling have been established in both homeostatic and pathological processes. Thus TP receptor activation is thought to be involved in thrombosis/hemostasis, modulation of the immune response, acute myocardial infarction, inflammatory lung disease, hypertension, nephrotic disease, *etc*.. Based on this consideration, attempts have been made to define the distinct signaling pathways by which TP receptors elicit their biological and pathological effects. In this regard, it is well documented that TP receptors have the capacity to activate a multitude of different signaling cascades which regulate cellular ion flux, cytoskeletal arrangement, cell adhesion, motility, nuclear transcription factors, proliferation, cell survival, and apoptosis. They are known to couple to at least four G proteins, which in turn activate numerous downstream effectors, including second messenger systems such as IP3/DAG, cAMP, small G proteins (Ras, Rho), phosphoinositide-3 (PI3) kinase, as well as protein kinase C (PKC) and protein kinase A (PKA) (Nakahata, 2008).

Furthermore, it has also become apparent that the signaling preferences between these different TP receptor-mediated pathways vary in both cell- and organ-specific

manner. Consequently, TP receptor activation in one cell type may lead to quite different signaling events than its activation in other cell types (Miggin and Kinsella, 1998).

The highly conserved E/DRY motif

As discussed above, despite the primary structure of the GPCRs is characterized by a common structural motif of 7TM regions, there is no evidence of an overall sequence homology. Nevertheless, is possible to identify a number of highly conserved stretch of residues such as the triplet of amino acids glutamic acid/aspartic acid-arginine-tyrosine. This so called E/DRY or DRY motif is located at the boundary between TM3 and ICL2 of class A GPCRs (rhodopsin family) and is thought to play a central role in regulating GPCR conformational states (Rovati et al., 2007) (Fig.2).

Moreover, it has been proposed that there are two different subgroups of receptors within class A GPCRs that make different use of the E/DRY motif, independently of the G protein type (G_s, G_i, or G_q) to which the receptor couples. In phenotype 1 receptors (P1-type), the consensus picture, derived in part from the rhodopsin structure, is that the basic arginine (denoted residue 3.50) forms stable intramolecular interactions with the neighboring aspartic acid or glutamic acid (3.49) and/or with another charged residue (6.30) on helix 6 (Ballesteros et al., 2001; Teller et al., 2001), thereby constraining GPCRs in the inactive (R) conformation. In particular, the crystal structure of the ground state of rhodopsin indicates that the arginine is engaged in a double salt bridge with the adjacent glutamic acid (3.49) and with the glutamic acid (6.30) on helix 6 (Palczewski et al., 2000; Teller et al., 2001).

Mutation of the glutamic acid/aspartic acid of the E/DRY motif has been proposed to induce a conformational change that rearranges the arginine from its polar pocket, resulting in the ability of some GPCRs to adopt an active conformation (R*) (Cotecchia et al., 2002; Scheer et al., 1996; Scheer et al., 1997a). Thus, this first phenotype is characterized by an increase of agonist-independent basal receptor activity (constitutive activity CA), upon mutation of glutamic acid/aspartic acid 3.49 (constitutive active mutant, CAM). Example of receptors members of this subgroup

are: α1-adrenergic receptors (α1-AR), β2-AR, α2-AR and vasopressin type II receptors (V2R) states (Rovati et al., 2007).

The second phenotype (P2-type) does not exhibit increased CA upon mutation of E/D$^{3.49}$ (constitutive inactive mutant, CIM). Nonetheless mutations can still affect receptor function as glutamic acid/aspartic acid non conservative (*i.e.*, charge-neutralizing or hydropathy-reversing) mutations have a number of effects that support an important role in stabilizing receptor conformation. Receptors part of this P2-type group are: rhodopsin, muscarinic M1 and M5, cannabinoid 2 (CB2R), α2A-AR, V1AR, and also TP.

Finally, it has been demonstrated that nonconservative mutations of R$^{3.50}$ show variable effects on function of P1-type receptors, but invariably exert strongly disruptive effects on P2-type receptor activity. This correlation between the effects of glutamic acid/aspartic acid and arginine mutations within P1 and P2 groups of receptors is a key aspect of this phenotypic division. It is interesting that R$^{3.50}$ mutations also show two patterns of effects on agonist binding. The first (in P1-type receptors) preserves high-affinity agonist binding and G protein coupling, whereas the second (in P2-type) disrupts high-affinity agonist binding and, conceivably, G protein coupling (examples TP and α2A-AR) (Rovati et al., 2007). The effect of nonconservative R$^{3.50}$ mutations in P2-type GPCRs to disrupt receptor function concomitant with the decreased agonist affinity, is in agreement with the loss of G protein coupling.

There is an apparent paradox between the increased or unchanged agonist affinity and loss of function. There are two possible explanations for this: R$^{3.50}$ may serve as an effector for G protein activation as suggested by Acharya and Karnik (1996) and Chung et al., 2002 (Acharya and Karnik, 1996; Chung et al., 2002a) or, alternatively, it mutation may produce a "constitutively desensitized" phenotype, reported as loss-of-function mutant due to decreased expression at the plasma membrane (Barak et al., 2001).

ERY motif in TP receptor

In TP receptor, as in the vast majority of class A (rhodopsin family) GPCRs**,** is present the highly conserved sequence Glu/Asp-Arg-Tyr triplet of residues. In particular, in TP receptor, this motif is composed by residues E129, R130 and Y131 and, like in all receptor where it is present, it is located between the TM3 and the ICL2. Of interest Arg ($R^{3.50}$) is conserved in 96% of the receptors of this class (Mirzadegan et al., 2003), suggesting a central role for this residue in the transition from the inactive to the active state of the receptor. Indeed, the central $R^{3.50}$ forms a network of interactions with the adjacent $E^{3.49}$ (E129) (intrahelical salt bridge) and with another residue in position 6.30, *i.e.* E240, (interhelical hydrogen bridge) that is thought to lock and to stabilize the receptor in its inactive conformation (R). The ligand interaction, with the ligand binding site in the extracellular domain of the receptor, induces a conformational change that disrupt the constrains of the ionic lock between TM3 and TM6 and cause the activation of the receptor (R*), which, in turn, start the signal transduction (Rovati et al., 2007).

In TP receptor the glutamic acid in position 129 ($E^{3.49}$) is able to maintain receptor in the inactive states (R) likely through a salt bridge with the near arginine 130 ($R^{3.50}$), and has a role in maintaining the receptor in the functional tridimensional state. Indeed, non-conservative mutations of $E^{3.49}$ (E129V) generated a receptor with increased efficacy and potency after agonist activation, but without any increase in CA compared to WT. In addition, this mutant clearly showed an increased affinity for full and partial agonists (Ambrosio et al., 2010; Capra et al., 2004). For these characteristics, this active variant has been named SAM (superactive mutants) (Ambrosio et al., 2010; Capra et al., 2013). This phenomenon has already been observed for α_{2A}AR (Chung et al., 2002b) and m_1AchR (Lu et al., 1997) and it has been interpreted as a possible conformational change in the agonist-binding pocket. E129V represents a good example of a mutation in the E/DRY motif that does not increase basal activity, while augmenting agonist-stimulated receptor signaling. These results led us to hypothesize a conformational change of the receptor toward an ‘active-like’ conformation. Interestingly, a conservative mutation in this position, E129D, having conserved hydropathic characteristic, had no effect in terms of TP receptor functionality.

We also previously studied mutant at position 3.50. Non conservative mutation of $R^{3.50}$ (R130V) resulted in receptors with no increased in CA, but with a statistically significant impairment in agonist-induced total IP production (loss of function phenotype), demonstrating that this residue is indeed important for receptor functionality (Capra et al., 2004). Conservative mutations, such as R130K, did not affect receptor signaling. Interestingly, R130V mutant showed a loss of high affinity agonist binding (Capra et al., 2004). Thus, these data, the loss of function phenotype and the loss of the high-affinity agonist binding, suggest a 'defective' G protein coupling. This might be ascribed either to disruption of the physical interaction between receptor and G protein or to a reduced receptor affinity for its cognate G protein. However, the exact role of Arg in the E/DRY motif is still under discussion: it has been suggested that Arg may catalyze GDP release (Acharya and Karnik, 1996) or may be involved in receptor isomerization (Scheer et al., 2000), but it is also possible that this residue is directly involved in G protein recognition and coupling (Burstein et al., 1998; Chung et al., 2002b).

In conclusion, the ERY motif in TP receptor is directly involved in governing G protein coupling/recognition. Hence, mutations of the E129 residue do not induce CA, whereas agonist-induced responses might be altered in a mutation-specific manner. Indeed, some nonconservative mutants might yield receptors with more efficient signaling properties, an observation that seems to suggest a conformational change toward an 'active-like' conformation. On the other hand, the central arginine of the ERY motif seems to be more directly involved in receptor-G protein coupling/recognition, so that nonconservative mutations of this residue invariably impair agonist-induced receptor responses and, accordingly, reduce affinity for agonist binding. Finally, it has been suggested the essential role of the hydropathic characteristic of the residues involved in G protein-receptor binding: substitutions with residues having conserved hydropathic characteristic (E129D and R130K) had no effect on TP receptor functionality (Moro et al., 1993; Scheer et al., 1997b; Wess, 1998).

The equilibrium models between receptor, ligands and G-proteins

As already discussed, heptahelical receptors represent the most versatile form of transmembrane signaling protein and one of the largest families of potential targets for pharmacological drugs (Lefkowitz, 2007). Therefore, it is not surprising the widespread interest in the mechanism(s) by which GPCRs mediate their effects. In the late 80's, the concept of drug-receptor went through a big change with: 1) the recognition that receptors exhibit constitutive activity in the absence of agonist, 2) the parallel discovery of inverse agonists, and 3) analysis of pharmacological data obtained by mutated receptors with molecular biology. This led to a number of receptor theories of increasing complexity with the intent to reconcile experimental data to mathematical models. The first mathematical model that try to describe the mechanism of action of GPCR is based on Clark's theory "the occupancy theory", the second level of model complexity is the ternary complex model (TCM), and some years after, with new pharmacological discoveries, was postulated the extended ternary complex model (ETC). Finally the cubic ternary complex model (CTC) is now under discussion.

Despite the explosion of GPCR crystal structures of both active (R*) and inactive (R) receptor states (more than 30 structures from Class A, B, C and Frizzled), little additional progress has been made in unraveling the mechanism(s) through which GPCR become active (Bhattacharya and Vaidehi, 2014), as well as in providing a full account of the ensemble of basal and active states (Audet and Bouvier, 2012). Indeed, one of the most intriguing and complex issues regarding receptor function and activation is the definition of the conformational landscape of different receptor states (Deupi and Kobilka, 2010) and describing them with a mathematical model. Thus, it's important trying to reconcile biochemical, structural and theoretical data on GPCR conformations and try to understand in particular the role of highly conserved E/DRY motif.

Classical Model

The simplest mechanistic model of receptor–ligand equilibrium is Clark's classical model (1937) (Clark, 1937). Clark's model consists of two elements: a ligand, A, and

a receptor, R. The receptor is assumed to possess a single site for the binding of the ligand. Following the laws of mass action, a receptor and a ligand combine to form a receptor–ligand complex, AR. Two receptor species are present—the free and inactive receptor R, and the receptor–ligand complex AR at equilibrium. The presence of these two species defines the extent of the classical model's complexity.
Classical model was modified by Ariëns (Ariëns, 1954) and Stephenson (Stephenson, 1956) to accommodate antagonists and partial agonists action and represents the simplest mechanistic models of ligand-receptor interaction.

Ternary Complex Model

In 1980, DeLéan and colleagues introduced the next step of model complexity: the Ternary Complex Model (TCM), in which the components that interact are three—a ligand, a receptor, and a transducer. This is the first theoretical model of receptor function that included auxiliary membrane-associated proteins, in this case the G proteins. Evidence for the importance of G proteins in receptor function dates back to Rodbell et al. (1971) (Rodbell et al., 1971), who demonstrated that the hormonal stimulation of the AC receptor-linked system is dependent upon the presence of GTP. Subsequently, Sternweis et al. (1981) (Sternweis et al., 1981) isolated a membrane-bound protein with GTPase activity, a guanine nucleotide-binding protein or G- protein that acts as an intermediary between receptor and effector. Thus, in the adenylyl cyclase (AC) system the role of the hormone is indirect, the hormone acts on the receptor that acts on the G protein that acts on an effector system. For such G protein mediated receptor systems, the classical model has been proven to be inadequate (Kenakin and Morgan, 1989; Leff et al., 1990).
In the TCM, receptors possess two binding sites: one for the ligand, A, and one for the G-protein, G. This model generalized the classical model by allowing receptors to interact with ligands as well as G proteins. In its full version, the ternary complex at equilibrium is comprehensive of four receptor species: R, AR, RG, and ARG (Weiss et al., 1996a) (Fig. 3A). The TCM formulated by DeLéan accommodates for a complex (non monotonic binding curves) behavior for agonists and partial-agonists, but not for antagonists, that could not be explained with existing theories (De Lean et al., 1980b). Essentially, agonists bind the receptor R with low affinity

and the receptor-G protein complex (RG) with high affinity.

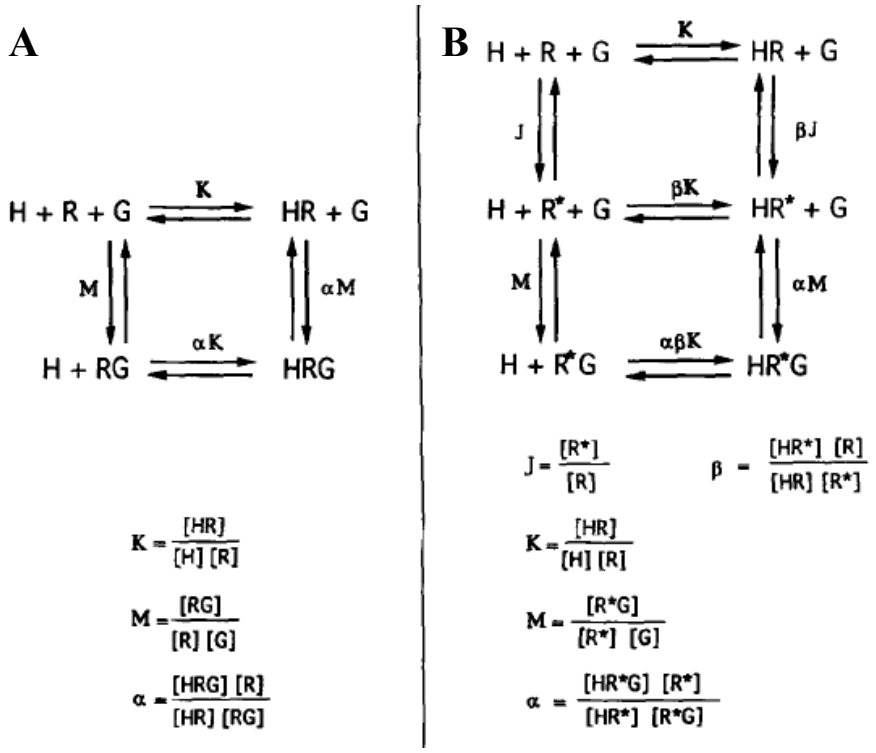

Fig. 3 The Ternary Complex Model. (A) the classical form of TCM. H= hormone; R=receptor; G= G protein. (B) in the proposed modified version of TCM, R undergoes an allosteric transition with a constant J which leads to the formation of an R* intermediate. The latter, in turn, interacts with the other components H and G, in a fashion similar to R in the classical form of the model (*from Samama P., et al. 1993*).

Extended Ternary Complex Model

At the beginning of the '90s, Samama and colleagues were working on β2-adrenergic receptor and replaced four amino acids of C-terminal portion of the third intracellular loop. These amino acids were substituted with residues derived from the corresponding region of the α_{1B}-AR and were chosen to mirror the replacements previously found to constitutively activate the α_{1B}-AR. This conservative substitution leads to agonist-independent activation of the AC. The mutant receptors exhibited (Samama et al., 1993b) :

- an increased basal activity, more than three times higher than the wild type;
- an increased affinity for agonists, correlated with their intrinsic activity at the wild-type receptor, and which does not depend on G protein interaction;
- an increased potency of agonists for stimulation of CA;
- an increased intrinsic activity of partial agonists.

Therefore, the almost simultaneous discovery of Constitutive Active Mutant (CAMs) receptors (Cotecchia et al., 2002; Kjelsberg et al., 1992; Robinson et al., 1992) and inverse agonist (Costa and Herz, 1989; Costa et al., 1992) led to the idea that the active state is an intrinsic property of the receptor itself rather than of RG complex. This made it apparent that a ligand-driven isomerization step was necessary and the receptor activity depended on the equilibrium between inactive (R) and active (R*) receptor species, as postulated by the two-state model of ligand-gated ion channel receptors (Del Castillo and Katz, 1957). The properties of these mutant receptors can not be adequately rationalized within the theoretical framework of the TCM, which postulates that: receptor activation requires the agonist-promoted formation of an active "ternary" complex among agonist, receptor, and G protein (De Lean et al., 1980a).

Based on such experimental results, Samama and colleagues, by combining the two-state receptor model with the TCM, formulated the Extended Ternary Complex Model (ETC) (Lefkowitz et al., 1993; Samama et al., 1993a) (Fig. 3B).

In this model, six receptor species exist at equilibrium, R, R*, HR, HR*, R*G, and HR*G (R= receptor; H= hormone/ligand; G= G protein). In the ETC, receptor activation is a necessary precondition for G-protein coupling. The receptor can exist in equilibrium between two conformations, R and R*. Only the R* is able to bind the G protein, so that HR*G is the only possible ternary complex formed, and R* can be regarded as the "active state" (Samama et al., 1993a).

Thus, two additional constants determine the formation of the ternary complex J and β:

J, dimensionless, describes the spontaneous isomerization R↔ R*;

β, is also a dimensionless constant that describes the extent to which the binding of H affects this equilibrium.

In this model, the capacity of ligand to induce the formation of the ternary complex depend on two factors: its ability to facilitate the transition of R to the active state R*, which is gauged by the constant β, and its ability to stabilize the ternary complex HR*G, gauged by the constant α. While β only depends on ligand and receptor, α also depends on the G protein. Thus, the overall molecular efficacy of the ligand H is now given by the product αβ. In Fig. 3B αβ = [HR'G][R]/[HR][R*G], which means

that αβ is an equilibrium constant describing the implicit exchange reaction: [HR]+[R*G] [HR*G]+[R]. Thus, the larger αβ is, the more likely it is to find H associated in the productive ternary complex [HR*G], rather than in the inactive binary complex [HR].

It is worth examining how this extended TCM is related to previous models of hormone action. If J grows to a very high value, all receptors exist in the R* state, and the model contracts to the TCM in the usual form (lower loop of Fig. 3B). If M assumes a very small value (or, equivalently, if G = 0, *i.e.* in the absence of G protein or presence of GTP), the model becomes analogous to the so-called allosteric receptor model for a monomeric receptor (upper loop), proposed by several investigators (Del Castillo and Katz, 1957).

Indeed, in a single receptor protomer context (no dimers), ETC describes the receptor interaction with the four orthosteric ligand types, *i.e.* agonists, partial-agonists, antagonists and inverse agonists. Within this context, agonists (full or partial) shift the equilibrium in favour of R* promoting activation of the receptor, while inverse agonists shift the equilibrium in favour of R inhibiting basal activity. Antagonists will show no preference for the two states of the receptor, thus leaving the equilibrium unaltered and the receptor activity unaffected. This model has several advantages, as it describes different receptor states when the receptor is ligand bound and it allows for selective affinity for different receptor species (as the TCM), but also allows for efficacy to be vectorial, *i.e.* positive ($a > 1$) or negative ($a < 1$) (Kenakin, 2004), providing an explanation for CA.

Cubic Ternary Complex Model

The ETC had rapidly evolved in the Cubic Ternary Complex model (CTC) described by Weiss and colleagues (Weiss et al., 1996a; Weiss et al., 1996b; Weiss et al., 1996c), mainly because ETC is thermodynamically incomplete. The CTC model is an equilibrium model that generalizes traditional binary mass action occupancy models of receptor–ligand interactions. CTC is symmetric, comprehensive with respect to several other previous pharmacological models, and can be generalized to equilibrium involving multiple ligands (including biased agonists), G proteins (or other transducers) and receptors. Furthermore, based on the principle of free energy

coupling (Weber, 1972), CTC is thermodynamically complete as it describes all the possible three-ways interactions between receptor, ligand and G protein.

In its most general form, the CTC model represents a membrane system consisting of multiple receptor types that interact with a diverse set of transducer molecules (G-proteins) and ligand molecules (hormones). In the CTC model each receptor is allowed to bind to only one G-protein and/or hormone at a time, but different receptors are allowed to compete for G-proteins and ligands. Thus, G-proteins and ligands are envisioned as forming a common pool accessible to each receptor. In addition, each receptor can exist in two distinct conformations, active and inactive, each of which is able to interact with ligand and G-protein.

The assumption of the CTC model is that:

i. Receptors have two distinct binding sites: an external site accessible to agonists and antagonists, and an internal site available to G proteins;

ii. External ligands (agonists and antagonists) and G proteins exist in separate phases and do not encounter each other;

iii. Receptors exist in two states with respect to their ability to activate G proteins and initiate biological responses: active and inactive;

iv. The interactions of external ligands, G proteins, and receptor activation states are assumed to be governed by the laws of mass action;

v. All possible two-way and three-way interactions between external ligands, G-proteins, and receptor activation states are assumed to be potentially significant and are represented by coefficients in the model.

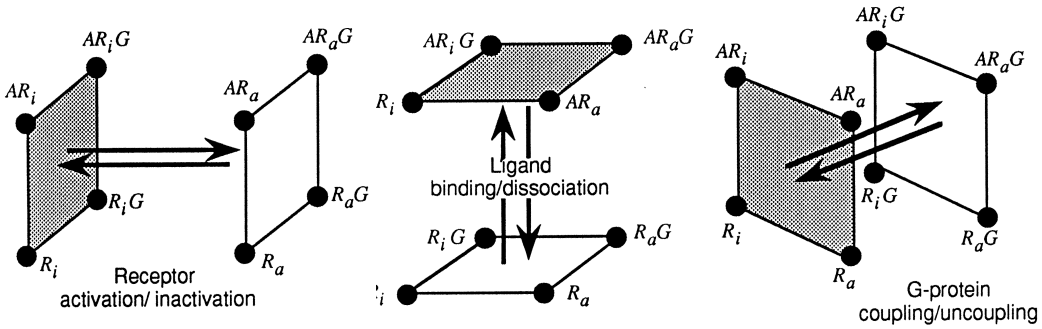

Fig. 4 Transformations allowed in CTC model (Ri=inactive receptor; Ra= activated receptor; A=ligand; G=G protein) (*from Weiss J.M., et al. 1995*).

Let Ri and Ra denote the inactive and active conformations of a receptor R. Let A denote a ligand and G a G protein. The basic building block of the cubic ternary complex model consists of eight distinct types of receptor species: Ri, Ra, ARi, ARa, RiG, RaG, ARiG, and ARaG. A geometric representation of the model can be obtained by identifying each vertex of a cube with a different receptor species. The edges of the cube define all the allowed transitions between receptor species (Fig. 5A).

It is not obligatory in the CTC that ligand binding and receptor activation occur together: ligand can bind without activating the receptor and receptors may spontaneously activate without previously binding to ligand.

Allowable transformations include:

i. change of receptor state, inactive to active or *vice versa*;

ii. binding or dissociation of G-protein;

iii. binding or dissociation of ligand.

In this geometric representation, each transformation is a transition between pairs of species occupying parallel faces of the cube. The three sets of parallel faces of the cube correspond to the three allowed transformations (Fig. 4).

Each face of the cube consists of a set of receptor species sharing a common feature. The shared feature thus provides a label for that face. Using this scheme, the six faces of the typical cubic building block can be labeled as the inactive face, active face, G protein face, G protein-free face, ligand face, and ligand-free face (Fig. 5A).

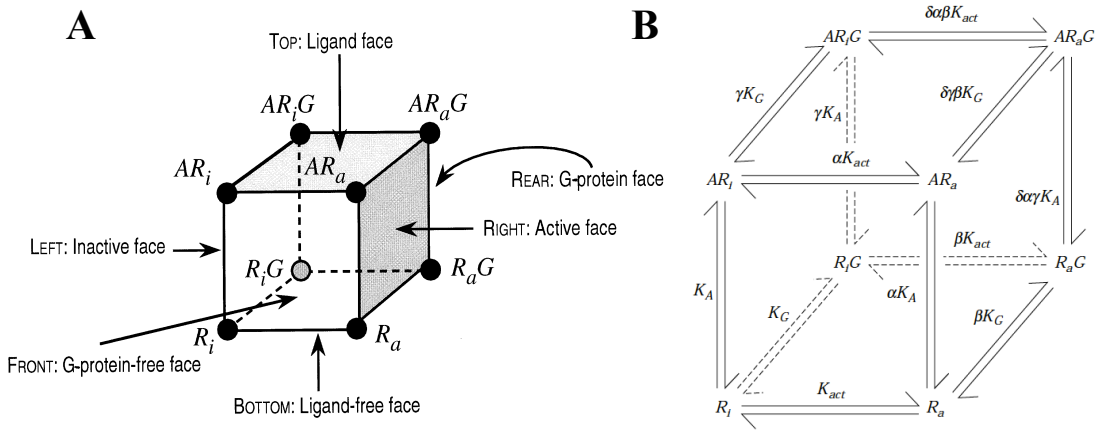

Fig. 5 (A) Schematic view of the cube; (B) CTC model with equilibrium association constants (*from Weiss J.M., et al. 1995 and 1996*).

Aim of the Study

GPCRs regulate virtually all known physiological processes in mammals (Lefkowitz, 2007), and the high number of drugs that target these receptors as agonists or antagonists recognize their significance to the current clinical practice of medicine (Tyndall and Sandilya, 2005). Moreover, from a molecular-structure point of view, an emerging opinion from several studies is that GPCRs are not simple "on-off" switches but adopt a continuum of conformations (Bockenhauer et al., 2011).

Aim of the first part of my thesis work was to focus on the molecular mechanisms of TP activation, in particular the role of GPCR structural conformations in G protein selection and, possibly, to position the conformational states of the two ERY motif mutants TPαE129V and TPαR130V within a mathematical framework such as the CTC model, a thermodynamically complete model by which all the possible three-ways interactions between receptor, ligand and G protein are described.

In the second part of my project we considered the possibility to combine a TP antagonist component to a COXIB. Hopefully, the new pharmacological agent, with a selective COX-2 inhibitory activity and balanced TP antagonistic activity, would able to provide protection against the potentially harmful TP receptor activation by mediators sensitive and insensitive to aspirin/NSAIDs, such as the platelet-derived TXA_2 and the nonenzymatic product isoprostanes. New compounds were obtained modulating the structure of lumiracoxib, a highly potent COXIB (Rordorf et al., 2005), in collaboration with professor Massimo Bertinaria (University of Torino), and also modulating the structure of a well known NSAID (RC 0), in collaboration with doctor Eugen Proschak, professor at the Frankfurt University.

Results

An emerging view from several studies is that GPCRs are not simple "on-off" switches, but rather they adopt a continuum of conformations (Bockenhauer et al., 2011). One of the focuses of my thesis was to assess the TPα, WT and mutants (TPαE129V and TPαR130V), coupling with their cognate G proteins in order to identify different conformational states of TP receptor.

A useful method to directly link ligand-specific changes in GPCR conformations to differential downstream responses is based on a recently developed technique, termed SPASM (Systematic Protein Affinity Strength Modulation), a FRET based method able to distinguish between G protein binding from G protein activation (Malik et al., 2013). The SPASM sensors involve the fusion of a native peptide from the C terminus of a Gα subunit to the C terminus of the intact GPCR. Each SPASM sensor contains, from N to C terminus: a GPCR, mCitrine (FRET acceptor), ER/K linker, mCerulean (FRET donor), and a 27-amino acid peptide (x-pep where x denotes the type of Gα subunit q and s) derived from the α5-helix of the Gα C terminus. With these sensors high FRET signal is generated when Gα C terminus binds GPCR (active conformation, donor and acceptor in close proximity), while low FRET signal is expected when GPCR is in its inactive conformation (Gα C terminus doesn't bind GPCR and mCit is not close to mCer). In addition, we generated a construct lacking the 27 amino-acid peptide from Gα, but containing only FRET donor and acceptor fluorophores (called 'no-pep'), which was used to test the functionality of our constructs in second messenger generation experiments (inositol phosphate levels and cAMP accumulation) and to measure background (non specific) FRET in FRET experiments (Malik et al., 2013).

Cloning of TPαWT, TPαE129V and TPαR130V in the FRET vectors

In order to apply this technique to our system of interest, we cloned HA TPαWT, HA TPαE129V and HA TPαR130V genes in the three different pCDNA5/FRT vectors all containing acceptor and donor sequence, but each containing the specific 27 amino-acid C terminal sequence of $G\alpha_q$, $G\alpha_s$ and no Gα (kindly provided by Dr Sivaraj Sivaramakrishnan, Michigan University). Thus, we obtained 9 FRET based SPASM sensors: 3 no-pep (sensors control), 3 q-pep and 3 s-pep, one for each receptor, *i.e.* TPαWT, TPαE129V and TPαR130V.

TPα receptor expression and cellular localization

The following step was to control the correct plasma membrane localization of each sensor in transiently transfected HEK293-T cells. To do this, we take advantage of one of the fluorescence probe (donor) present in the SPASM vectors. Indeed, we analysed the intensity of emitted fluorescence of transfected cells by fluorescence microscopy. After 30h-32h from transfection with the different plasmids, HEK293-T cells were excited with light at 492nm and emission fluorescence signal was recorded at 500-600nm (these are the specific wavelengths for the FRET acceptor mCitrine). The fluorescent signal was compared with cells visualized by halogen light to verify the transfection efficiency, proteins expression level and to control plasma membrane localization.

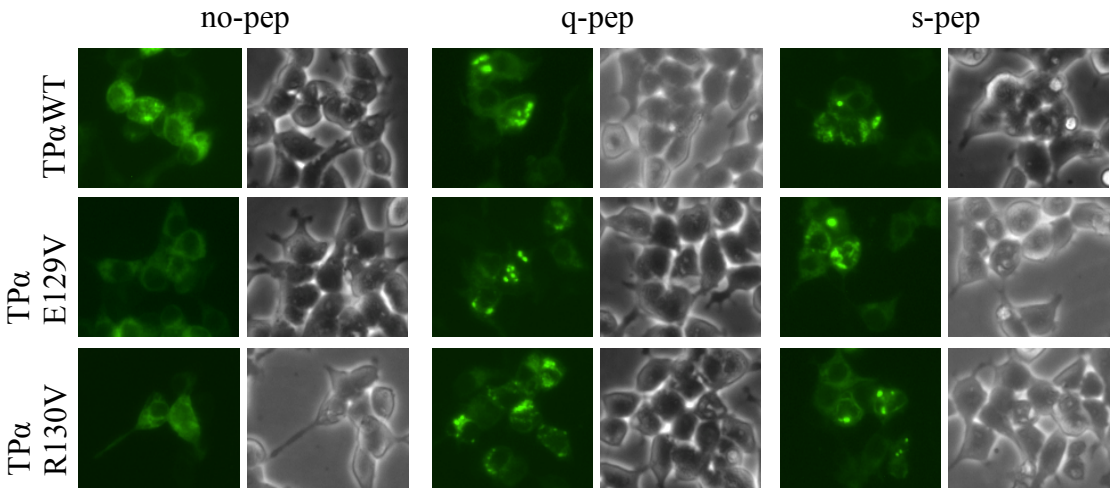

Fig. 6 TPα SPASM sensors localization at the plasma membrane in HEK293-T live cells.

As shown in figure 6, the WT 'no-pep' construct is well expressed in term of transfection efficiency (number of cells transfected) and in term of level of protein expression. In particular it is possible to observe that the fluorescence signal is homogeneous in almost 40% of the cells, moreover the fluorescence is mainly localized at the plasma membranes. As far as the q-pep and s-pep fusion proteins is concern, despite the intensities of fluorescence constructs are similar to TPα WT 'no-pep', however a weak signal is also present inside the cytoplasm. This result is likely due to proteins retention, thus creating inclusion bodies that do not allow the correct translocation of the protein to the plasma membrane.

We also analysed the fluorescence of 3HA TPαE129V and 3HA TPαR130V no-pep, q-pep and s-pep receptors (Fig. 6). As expected, both 'no-pep' constructs were well expressed at the cell membranes, but as for TPα WT constructs, again the q-pep and s-pep of the two mutant proteins were less expressed at the plasma membrane, while a fluorescence signal was also present into the cytoplasm. Finally, as an internal control, we also visualized the fluorescence in mock-transfected cells, and, as expected, no fluorescence signal was indeed present (data not shown).

Thus, from these observations we can affirm that each point mutation doesn't modify protein localization, but the presence of the $G\alpha_q$ and $G\alpha_s$ peptides cause a weak formation of inclusion bodies into the cytoplasm.

Western Blot Analysis

To support the fluorescent imaging observations, HEK293-T cells, individually transfected with the different SPASM sensors, were subjected to SDS-PAGE separation and western blot analysis using anti-HA antibodies. Western blot analysis is a useful technique to detect protein expression, and can provide both qualitative and semi-quantitative data. Thus, we prepared membrane enriched cellular fractions (27000 g), a preparation that can give also information of the correct cellular localization of our constructs. As it is clear from figure 7, the molecular weight (MW) of each sensor is about 110 kDa, as predicted from amino acid sequences. In addition, it is possible to observe two distinct bands at 100 and 120 kDa respectively, the higher one probably representing a glycosylated form of the

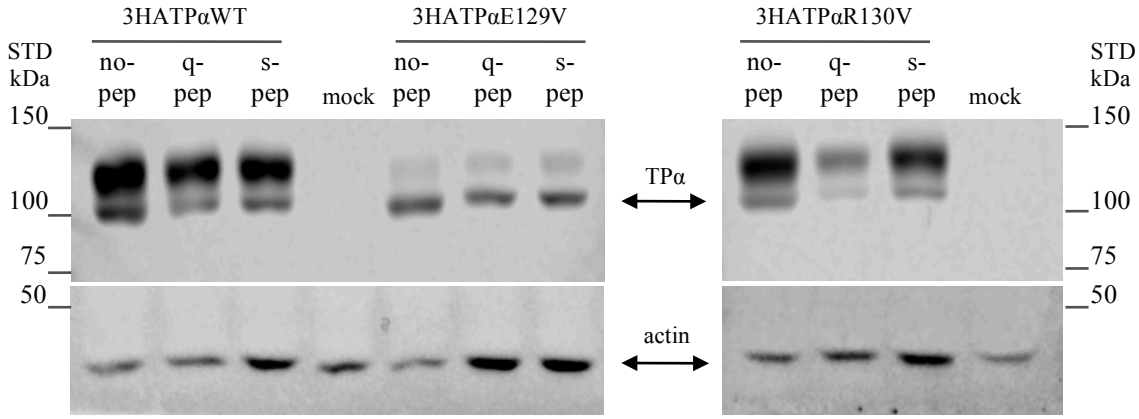

Fig. 7 Western blot analysis for 3HA TPαWT and mutants SPASM sensors identification in enriched membrane samples of HEK293-T cell transiently transfected.

receptor. Intensity of the bands confirms that the proteins are well expressed in membrane, despite the presence of the SPASM probes and a partial retention into the cytoplasm. Of particular interest is the signal of the three 3HA TPαE129V sensors in which the intensities of the glycosylated forms are weaker compared to the corresponding WT signals. This data seem to confirm an increased difficulty for the mutated receptor to localize at the plasma membrane. As for 3HA TPαR130V sensors, the figure 7 clearly shows that while the 3HA TPαR130V 's-pep' signal is quite similar to that of 'no-pep' sensor, the intensity of the two bands corresponding to the q-pep fusion protein are both weaker than the 'no-pep' and 's-pep' constructs, confirming an impairment also for this construct to be correctly translated and localized at the plasma membrane.

Functional assays

Gq-dependent signaling of TPα WT and mutants no-pep receptors

To check the pharmacological profile of our constructs, we compared the functionality of WT and mutant TPα receptors with our 'no-pep' SPASM sensors by performing U46619-induced total IP concentration-response curves. As mentioned before, only the 'no-pep' fusion proteins are able to activate the signal transduction pathway, while in the 'q-pep' and 's-pep' sensors the presence of the specific Gα

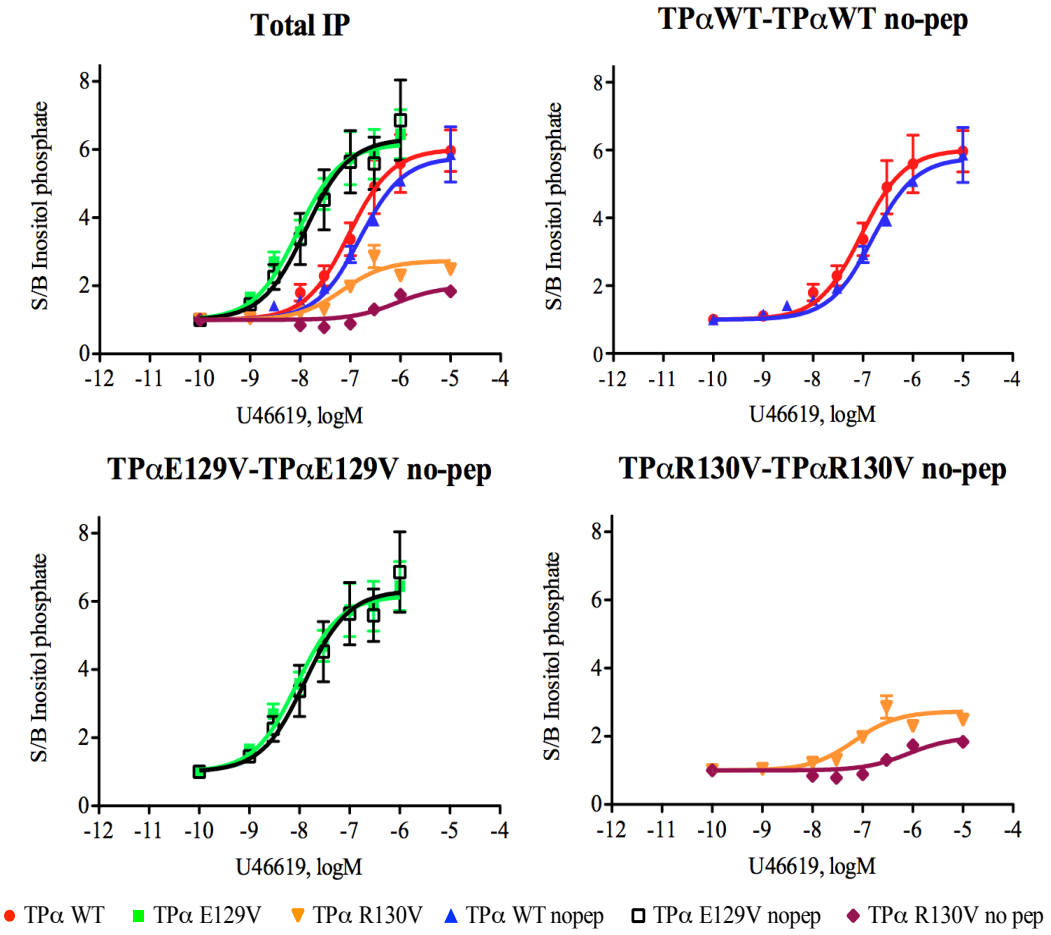

Fig. 8 Concentration-response curves of agonist induced total IP formation in HEK293-T cells expressing TPαWT, TPαE129V and TPαR130V with and without SPASM no-pep sensors. IP accumulation was measured after incubation of increasing concentrations of U46619 agonist for 30 min. Values of EC_{50} were obtained by simultaneous analysis with the Prism computer program of at least three independent experiment each performed in duplicate. EC_{50} values were obtained by simultaneous analysis performed using GraphPad Prism 4.00. Curves are computer-generated.

Tab. 1 EC_{50} IP values of TPαWT, TPαE129V and TPαR130V with and without SPASM no-pep sensors.

Receptor	EC_{50} (nM ± %CV)
TPαWT	93.4 ± 47
TPαWT no-pep	155 ± 20
TPαE129V	8.9 ± 41
TPαE129V no-pep	13 ± 66
TPαR130V	70 ± 45
TPαR130V no-pep	816.6 ± 90

component at the C terminus competitively inhibit the coupling of the receptor with the endogenous G proteins. Computer-assisted analysis of total IP formation (Fig. 8) shows that HEK293-T cells transiently expressing the WT and E129V TPα respond to U46619 stimulation with a marked elevation of total IPs (6 fold increase over basal) while, as expected, cells expressing the R130V mutant respond poorly to the same agonist (about 2 fold increase over basal). Furthermore, U46619 potency at the two mutants reflect the SAM and the loss of function nature of TPαE129V and TPαR130V, respectively. In fact, about a 10 fold difference in EC_{50} values was found between TPαWT and TPαE129V mutant (93.4 nM ± 47 %CV and 8.9 nM ± 41 %CV, respectively), while EC_{50} value of TPαR130V is not statistically different from that of WT receptor (70 nM ± 45 %CV), in line with results previously published by us (Ambrosio et al., 2010; Capra et al., 2013; Capra et al., 2004). Similar results have been obtained for the different 'no-pep' SPASM sensors: EC_{50} values of 155 nM ± 20 %CV, 13 nM ± 66 %CV and 817 ± 90 %CV for TPα WT, TPα E129V and TPαR130V, respectively (Tab. 1). Overall, these experiments confirm that each 'no-pep' TPα SPASM sensor respond to U46619 stimulation similarly to the corresponding TPα receptors control constructs.

Gs-dependent signaling of TPα WT and mutants no-pep receptors

To further expand the observations about TPαWT and mutants G_q signal transduction pathways, we investigated if IP accumulation behaviour was maintained also at the level of the secondary TPα transductional pathway, *i.e.* the coupling of the TPα to heterotrimeric $G\alpha_s$ protein. For the same reason as for IP assay, we can test only the 'no-pep' constructs in comparison to receptors without the SPASM sensors. Thus, TPα receptor was assessed for its ability to induce cAMP accumulation following stimulation with increasing concentrations of the stable TXA_2 analogue U46619. Figure 9 shows the concentration-response curve of agonist-induced cAMP production in cells expressing human TPαWT, E129V and R130V mutants in the presence of 100 μM of the Ca^{2+} chelator BAPTA/AM to prevent non-specific activation of adenylate cyclase (AC). Computer assisted analysis of U46619-induced concentration-response curve for TPαWT receptor revealed an EC_{50} value of 147 nM

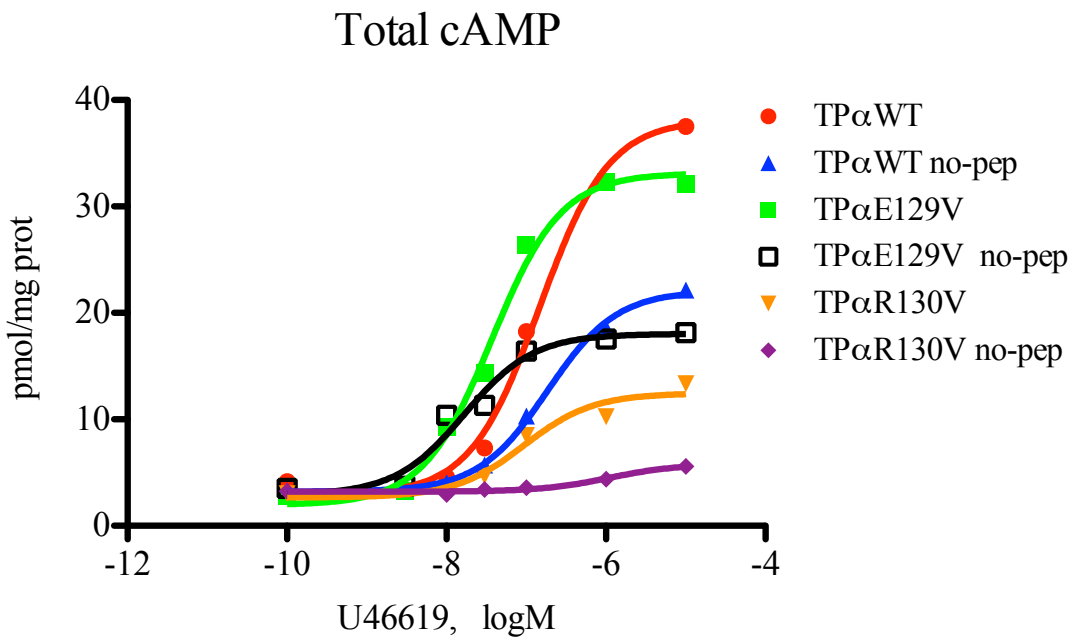

Fig. 9 Concentration-response curves of agonist-induced total cAMP production in HEK293-T cells expressing the TPαWT, TPαE129V and TPαR130V with and without SPASM no-pep sensors. cAMP was measured in basal condition or after stimulation with increasing concentrations of the agonist (U46619) for 10 min. EC_{50} values were obtained by simultaneous analysis performed using GraphPad Prism 4.00. Curves are computer-generated.

Tab. 2 U46619 induced cAMP accumulation: EC_{50} values in HEK293-T cells transiently transfected with TPαWT, TPαE129V and TPαR130V with and without SPASM no-pep sensors.

Receptor	**EC_{50} (nM ± %CV)**
TPαWT	147 ± 86
TPαWT no-pep	187 ± 28
TPαE129V	37.2 ± 34
TPαE129V no-pep	16.7 ± 93
TPαR130V	94 ± 97
TPαR130V no-pep	111± 57

± 86 %CV. As expected, TPαE129V mutant was found to be more potent than the WT receptor, with an EC_{50} value lower than that of the TPαWT (37.2 nM ± 34 %CV), again substantiating it classification as a SAM and in line with results previously published by us (Ambrosio et al., 2010). On the other hand, the EC_{50} value of TPαR130V was 94 nM ± 97 %CV, similar to the WT receptor. All the SPASM "no-pep" sensors have a comparable EC_{50} of their respective control: 187 nM ± 28 %CV, 16.7 nM ± 93 %CV, 111 nM ± 57 %CV for TPαWT no-pep, TPαE129V no-pep, TPαR130V no-pep, respectively.

In term of efficacy, the E_{max} value of TPαWT and TPαE129V were similar (38 pmol/mg prot. ± %CV and 33 pmol/mg prot. ± 3 %CV, respectively), again in line with the results obtained in term of total IP accumulation. The efficacy of TPαR130V (12.5 pmol/mg prot. ± 7 %CV) was about three fold lower compared to the WT, confirming its classification as a loss of function mutant. Furthermore, unlike in the IP assay, all the SPASM sensor efficacy values were lower than their controls (Tab. 2): 22 pmol/mg prot. ± 2 %CV TPαWT no-pep ($p < 0.01$), 18 pmol/mg prot. ± 5 %CV TPαE129V no-pep ($p < 0.01$) and 5.8 pmol/mg prot. ± 5 %CV TPαR130V no-pep.

In conclusion, these experiments demonstrate that each 'no-pep' TPα SPASM sensor can activate the TPα secondary G_s signal pathway similarly to the corresponding control receptors. However, the significant reduction in maximal efficacy showed by the different SPASM sensors let us hypothesize that the presence of SPASM construct can negatively influence the protein activity, further decreasing the efficiency in G_s coupling.

Basal FRET signaling of TPαWT, TPαE129V and TPαR130V no/q/s-pep sensors

The SPASM sensors are designed for FRET-based detection of GPCR conformations that favour G protein interactions. Several studies have shown that peptides derived from the Gα C terminus interact with the GPCR following stimulation with canonical agonist (Hamm et al., 1988; Rasenick et al., 1994), and that, ligand-stimulated GPCR preferentially interacts with a particular Gα C terminus (Conklin et al., 1993;

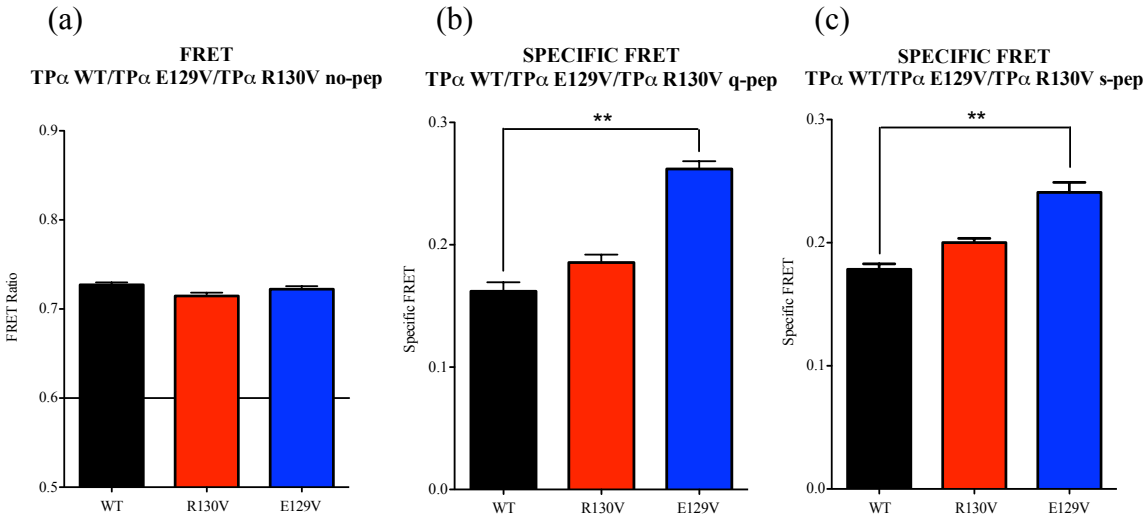

Fig. 10 Basal FRET measurement of TPαWT and ERY mutants no-pep, q-pep and s-pep. (a) FRET Ratio (mCitrine/mCerulean, 525nm/475nm) of TPαWT and ERY mutants no-pep. (b-c) Specific FRET, that is Gq/Gs-pep FRET signal subtracted of the corresponding no-pep value, of TPαWT and ERY mutants q-pep and s-pep, respectively. ** $p < 0.01$ vs TPαWT.

Tab. 3 FRET Ratio values of TPαWT, TPαE129V and TPαR130V no-pep sensors.

Receptor	FRET Ratio (525nm/475nm) ± SD
TPαWT no-pep	0.73 ± 0.025
TPαR130V no-pep	0.71 ± 0.02
TPαE129V no-pep	0.72 ± 0.03

Tab. 4 Specific FRET of TPαWT, TPαE129V and TPαR130V q-pep and s-pep sensors.

Receptor	SPECIFIC FRET (525nm/475nm) ± SD
TPαWT q-pep	0.162 ± 0.037
TPαR130V q-pep	0.186 ±0.028
TPαE129V q-pep	0.262 ± 0.034**
TPαWT s-pep	0.169 ± 0.018
TPαR130V s-pep	0.200 ± 0.019
TPαE129V s-pep	0.240 ± 0.034**

** $p < 0.01$ vs TPαWT

Conklin et al., 1996). Thus, the Gα C terminus peptides used in this study are 27 amino acids long, essentially encompassing the entire α5-helix of a specific Gα subunit (Oldham and Hamm, 2008). This particular length of the peptide is used to potentially preserve the α helical structure of the G protein C terminus.

FRET-based detection involves excitation of sample at 430nm (mCerulean-FRET donor excitation wavelength), and recording emission from 450nm to 600nm (475nm and 525nm are the emission peaks of mCerulean (donor) and mCitrine (acceptor), respectively).

Thus, we compared basal FRET signal, in term of acceptor/donor ratio (525nm/475nm), in absence of agonist of the three control 'no-pep' TPα receptors. As expected, no difference in the FRET ratios were observed (0.73 ± 0.03 SD; 0.71 ± 0.02 SD and 0.72 ± 0.03 SD for TPαWT, TPαR130V and TPαE129V 'no-pep' constructs, respectively) (Fig. 10 and Tab. 3). Next, we recorded basal FRET signal of TPαWT and mutant receptors with 'q-pep' and 's-pep' peptide in term of specific FRET, *i.e.* FRET ratio of TPα q/s-pep subtracted of the FRET ratio of its corresponding 'no-pep' constructs. Specific FRET values measured for TPαWT q-pep, TPαR130V q-pep and TPαE129V q-pep (Fig. 10b) are reported in table 4. Interestingly, mutant specific FRET value calculated for TPαE129V q-pep is statistically higher ($p < 0.01$) compared to WT (0.262 ± 0.034 and 0.162 ± 0.037 respectively), suggesting that TPαE129V mutant is somewhat more pre-coupled to its cognate G_q protein. Similar results were obtained for TPαE129V s-pep (Tab. 4). Indeed, specific FRET values calculated are 0.169 ± 0.018 SD, 0.200 ± 0.019 SD and 0.240 ± 0.034 SD for TPαWT, TPαR130V and TPαE129V respectively (Fig. 10c).

COXIB-FIRST PART: Lumiracoxib derived compounds

Chemistry

Compounds **7** (2-[(2-chloro-6-fluorophenyl)amino]-5-methyl-benzoic acid) and **32** (2-(((4-chlorophenyl)sulfonyl)amino)-5-methyl-benzoic acid) were synthesized according to the procedure described in Hoxha et al., 2016 (Hoxha et al., 2016). The

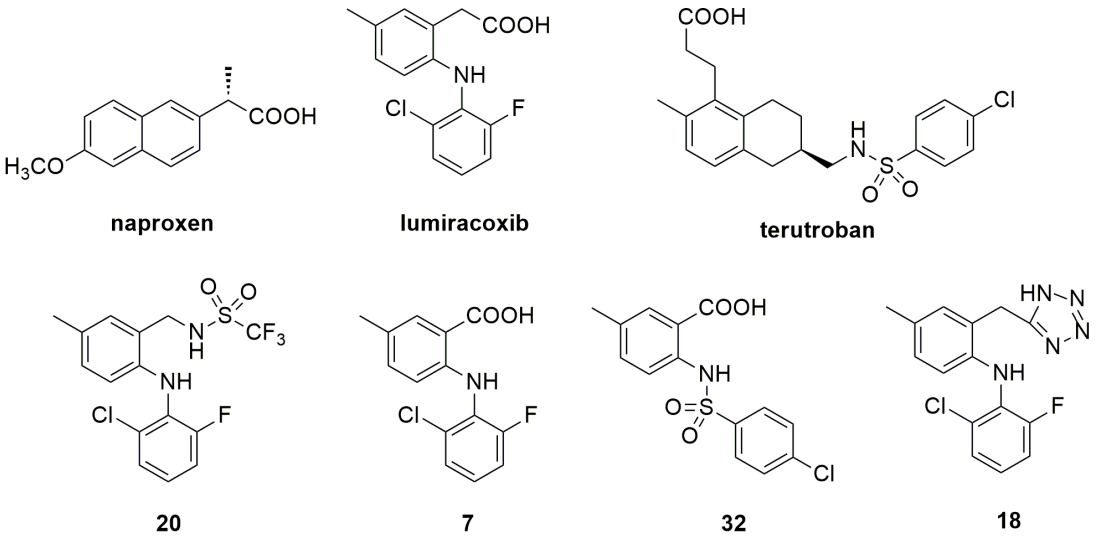

Fig. 11 Chemical structures of reference compounds naproxen, lumiracoxib and terutroban, as well as of the newly synthesized compounds **7, 18**, **20,** and **32**.

synthesis of lumiracoxib analogue **7** was accomplished as previously described (Bertinaria et al., 2012). Briefly, the Chan-Lam coupling was used by reacting 2-amino-5-methylbenzoic acid with 2-chloro-6-fluorophenylboronic acid in the presence of 1,8-diazabicylo-[5,4,0]undec-7-ene (DBU) and a stoichiometric amount of copper acetate in dioxane solution. Compound **32** was synthesized by reacting 2-amino-5-methylbenzoic acid with 4-chlorobenzensulfonyl chloride in the presence of excess Na_2CO_3 in water at 60 – 80 °C. The product was isolated and recrystallized from ethanol. Compounds **18** (N-(2-Chloro-6-fluorophenyl)-4-methyl-2-(1H-tetrazol-5-ylmethyl)-benzenamine) and **20** (N-[[2-[(2-Chloro-6-fluorophenyl)amino]-5-methylphenyl]methyl]-1,1,1-trifluoromethanesulfonamide) were obtained as previously reported (Bertinaria et al., 2012) (Fig. 11).

Physico-chemical characterization of compounds

The compounds selected for this study present most of the structural characteristics predicted for lumiracoxib analogs suitable as COX-2 inhibitors from a recent *in silico* study (Bartzatt, 2014). Their structures contain: 1) two aromatic rings; 2) at least two oxygen atoms (with the exception of compound **18**); 3) at least one carboxyl group or a carboxyl isosteric group; 4) at least one -OH or -NHn group.

Tab 5. Topological polar surface area (tPSA), solubility in simulated gastric fluid (SGF) and phosphate buffered solution (PBS), dissociation constants and lipophilicity descriptors of compounds under study.

Compound	tPSA[a]	Solubility (μM) ±SD		pK_a ±S.D.[b]	clog P [c]	$logD^{7.4}$ ±S.D.[d]
	($Å^2$)	*SGF*	*PBS*			
Lumiracoxib	49.3	23.4 ±0.7	442.1 ±21.4	4.15 ±0.03[e]	4.66	1.19 ±0.05
7	49.3	8.7 ±0.1	440.2 ±3.9	4.31 ±0.05	5.84	1.86 ±0.03
18	61.1	54.1 ±5.4	533.9 ±16.2	4.85 ±0.01[e]	4.85	1.60 ±0.03
20	58.2	13.9 ±1.6	60.7 ±2.3	6.70 ±0.01[e]	6.16	> 3.5
32	83.5	19.3 ±4.9	553.1 ±15.0	4.33 ±0.01	4.54	0.87 ±0.04

[a] Topological polar surface area values calculated using ChemBioDraw v.12 CambridgeSoft.
[b] Data obtained by potentiometric titration (SIRIUS GlpKa).
[c] Values calculated by using Bio-Loom for Windows v.1.5 BioByte Corp.
[d] Data obtained by shake-flask method.
[e] According to ref. (Rao and Oprian, 1996).

Inspection of data reported in table 5 evidences that the topological polar surface area (tPSA) of the studied compounds is similar or higher than that of lumiracoxib; in particular, the value of tPSA for the tetrazole analog **18** (61.1) is very close to the mean value found for a set of 36 NSAIDs (63.2) and of lumiracoxib analogs (70.5) (Bartzatt, 2012; Bartzatt, 2014). The measured solubility indicates that **18** is more soluble than lumiracoxib both in simulated gastric fluid and in phosphate buffered saline. Its solubility double that of the reference drug when the simulated gastric fluid is considered as the medium. This may be an advantage following oral administration. Derivatives **7** and **32** also show a similar solubility with respect to lumiracoxib at physiological pH, their solubility is slightly lowered when the pH is brought down to 1.5. Compound **20** is the least soluble derivative of the series at pH 7.4, nevertheless it retains a fair solubility in simulated gastric fluid medium (0.59 fold that of lumiracoxib).

The pKa values of **7**, **18** and **32** are slightly higher than that of lumiracoxib. Derivative **20** presents a significantly lower acidity with respect to that of the reference drug, this property reflects in a distribution coefficient measured at pH 7.4 greater than 3.5, consequently **20** is more lipophilic than lumiracoxib in physiological condition. Compounds **7** and **18** are 1.56 and 1.34 fold more lipophilic than lumiracoxib and this may favour cellular permeability. All the compounds were

also shown to be stable in human serum with > 98 % unchanged form detected after 24 h incubation (data not shown). From this preliminary characterization we could assume that the tetrazole derivative **18** shows the best drug-like properties among the compounds of this series.

Inhibition of TP receptor functional activity in human platelets

A series of newly synthetized compounds, *i.e.* compound **18**, **20**, **7**, and **32**, as well as a non-selective COX inhibitor (naproxen) and a potent and selective COX-2 inhibitor (lumiracoxib) (Fig. 11) were studied for TP receptor antagonism in platelets from healthy human volunteers. The extent of aggregation was detected by Born-turbidimetric assay. Blood was collected in the presence of 100 µM acetylsalicylic acid to render the platelets unresponsive to the challenge with arachidonic acid (1-3 µM), but fully responsive to the calcium ionophore A23187 (3 µM; data not shown). Representative traces of washed platelet aggregation obtained with 0.1 µM of the stable TXA_2 analogue U46619 in the presence of increasing concentrations (0.3-20 µM) of compounds **18** and **20** are portrayed in figure 12. When platelets were

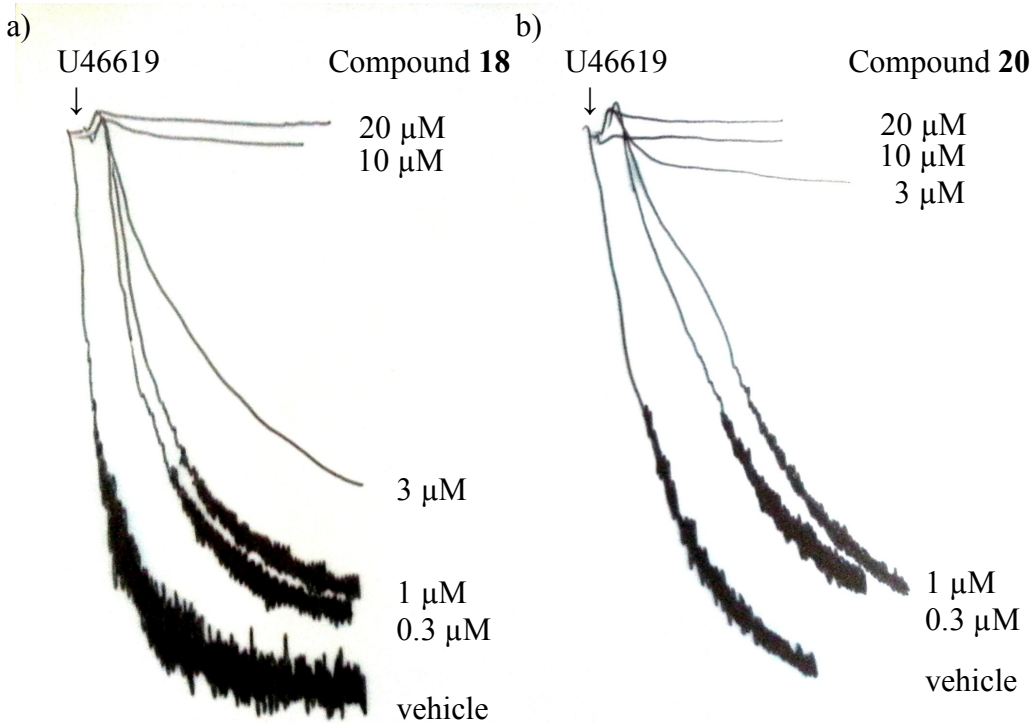

Fig. 12 Representative original traces of acetylsalicylic acid-treated human platelets demonstrating the effect of compounds 18 and 20 on the TP-dependent aggregation. Washed platelets were challenged with 0.1 µM U46619 (arrow) in the presence of vehicle (0.2 % DMSO) or the indicated concentrations of compounds **18** (a) and **20** (b). Each aggregation was registered for 5 minutes.

challenged with increasing concentrations of U46619, a concentration-dependent platelet aggregation occurred, which revealed a potency value of 59 nM ± 19 %CV (Fig. 13), in perfect agreement with our previous results (Selg et al., 2007). This response was thus truly independent of endogenous TXA_2 formation. The sensitivity of platelets to U46619 did not change during the time required for the experiment and none of the tested compounds caused any aggregating response by itself. Figure 12 also shows the inhibition curves of U46619-induced (0.1 μM) platelet aggregation due to increasing concentrations of the newly synthetized compounds as well as the reference compounds. Table 6 reports their respective pA_2 values calculated accordingly to equations 1-3 (see Methods section). Among the different molecules tested, compounds **18** and **20** were found to be the most potent in terms of TXA_2 antagonism with pA_2 values comparable to that of diclofenac, but, at least for compound **20**, statistically different from that of lumiracoxib (pA_2 = 5.9, 95% CI - Confidence Interval 5.4-6.4 for compound **20** - pA_2 = 5.0, 95% CI - Confidence Interval 4.7-5.2 for lumiracoxib).

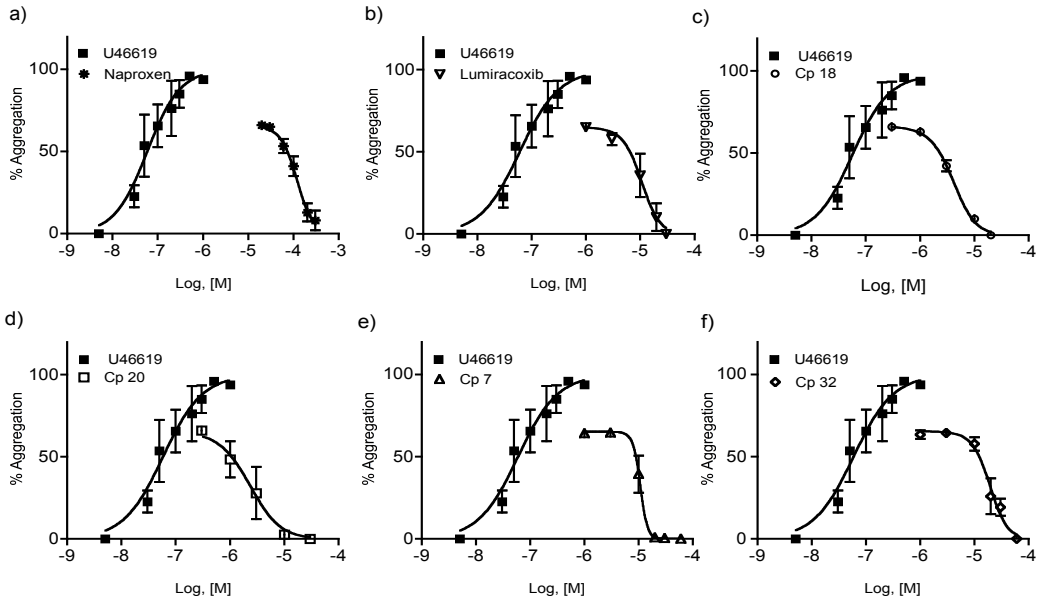

Fig. 13 Antagonism of human platelet aggregation induced by U46619 by the indicated compounds. Concentration-response curves of U46619-induced washed platelet aggregation from human blood and inhibition curves of: naproxen (a), lumiracoxib (b), compound **18** (c) compound **20** (d), compound **7** (e) and compound **32** (f). EC_{50}'s were calculated using a four parameters logistic model, while pA_2's were calculated accordingly to the set of equations 1-3 as described in Materials and Methods. Values shown represent platelet aggregation (mean ± SE) expressed as % maximal aggregation induced by 0.1 μM U46619. Blood was treated with 100 μM acetylsalicylic acid. Experiments have been performed at least three times in duplicates. All curves shown were computer generated.

Tab. 6 TP receptor antagonism at human washed platelet aggregation and total IP production in transfected HEK293 cells. pA_2 values were determined by measuring inhibition of aggregation response to the stable agonist U46619.

Compound	$pA_2 \pm$ %CV	
	Human washed platelet aggregation	Total IP production in HEK293 cells
Lumiracoxib	5.0 ± 2.5	4.6 ± 5.2
Diclofenac	5.4 ± 4.9	5.3 ± 4.7
Naproxen	4.1 ± 2.5	3.9 ± 16.3
Terutroban	9.4 ± 4.1	9.3 ± 2.8
18	5.6 ± 3.5	5.5*± 2.2
20	5.9* ± 4.1	5.7* ± 2.3
7	5.0 ± 1.8	4.9 ± 5.1
32	4.8 ± 2.4	4.8 ± 2.5

* 95% CI *vs*. lumiracoxib, see results

Inhibition of TPα functional activity in HEK293

All compounds were also tested for their ability to inhibit the total inositol phosphate (IP) production following classic TP receptor coupling with G_q. The human TPα receptor transiently expressed in HEK293 cells was activated by the stable TXA_2 analogue U46619 (0.1 μM, 30 min) in the absence and presence of 30 min pretreatment with increasing concentrations of the reported antagonists (Fig. 14). TP receptor activation by U46619 resulted in a robust increase in total IP production with a calculated EC_{50} of 29.3 nM ± 10 %CV, as previously reported (Ambrosio et al., 2010; Capra et al., 2013; Fanelli et al., 2011). No response has been obtained from mock-transfected cells. The pA_2 values calculated for each compound are presented in table 6. It is worth notice here that the results obtained in total IP production inhibition are in full agreement with those obtained in aggregation studies. Compounds **18** and **20** were again the most potent molecules, with pA_2 values similar to that of diclofenac and both statistically different from that of lumiracoxib (pA_2 = 5.5, 95% CI, 5.2-5.8 for compound **18** - pA_2 = 5.7, 95% CI, 5.4-6.0 for compound **20** - pA_2 = 4.6 95% CI, 4.1-5.1 for lumiracoxib), in good agreement with affinity binding data previously obtained in HEK293 cells (Bertinaria et al., 2012).

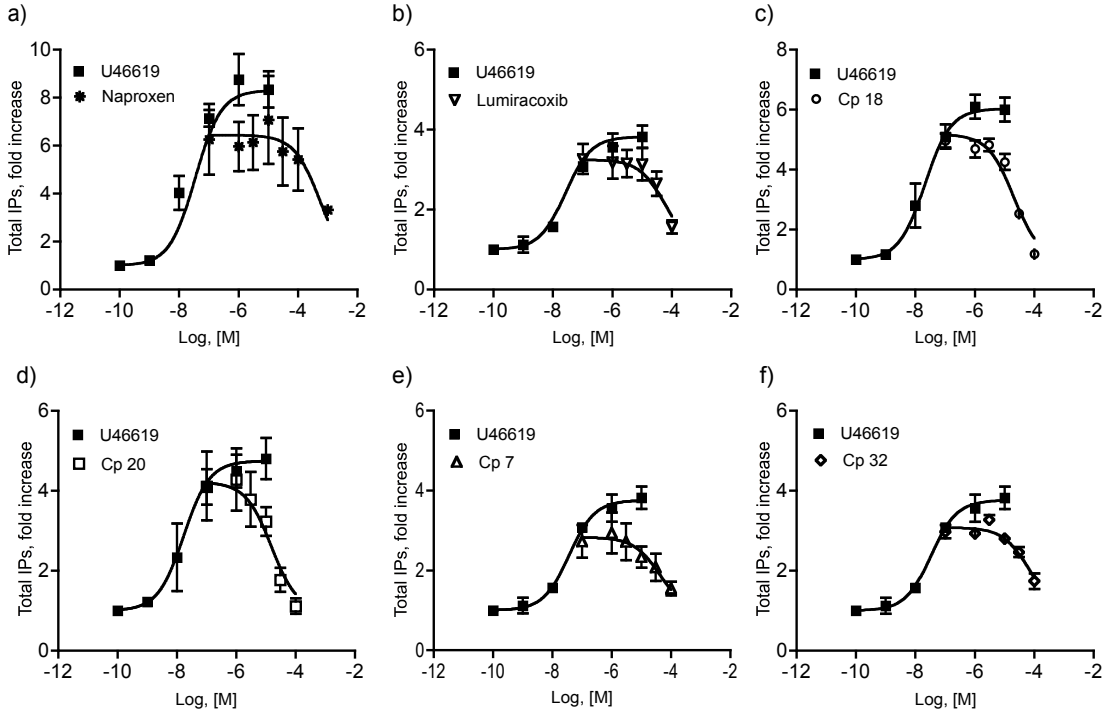

Fig. 14 Antagonism by the indicated compounds of total IP production induced by the TXA_2 analog U46619 in HEK cells transiently transfected with the alpha isoform of the human TP receptor. Concentration-response curves of U46619-induced total IP production and inhibition curves of naproxen (a), lumiracoxib (b), compound **18** (c), compound **20** (d), compound **7** (e), and compound **32** (f), obtained in the presence of 0.1 μM U46619. EC_{50}'s were calculated using a four parameters logistic model, while pA_2's were calculated accordingly to the set of equations 1-3 as described in Materials and Methods. Values shown represent the mean percentage of fold increase over basal ± SE. Experiments were performed at least three times in duplicate. All curves shown were computer generated.

COX-2/COX-1 selectivity

Newly synthesized compounds should maintain the COX-2 selectivity of the parent lumiracoxib and therefore their capacity to act as COX-2 inhibitors was determined on isolated human lympho-monocytes following treatment with acetylsalicylic acid. COX-2 expression was stimulated overnight with 10 μg/mL of lipopolysaccharide, and the PGE_2 produced was determined by enzyme immunoassay and mass spectrometry, whereas COX-1 inhibitory activity was determined in washed human platelets as TXB_2 production, measured by mass spectrometry.

All the compounds tested inhibit the COX-2 enzyme in a concentration-dependent manner with lumiracoxib and diclofenac displaying the highest absolute potency (Tab. 7), while compound **32**, containing the 4-chlorobenzensulfonamide moiety present in the very potent TP receptor antagonist terutroban (Simonet et al., 1997),

Tab. 7 COX-2 and COX-1 inhibitory activities determined by *in vitro* assay in lympho-monocytes and washed human platelets.

Compound	COX-2 inhibition IC_{50} (μM) ± %CV	COX-1 inhibition IC_{50} (μM) ± %CV	COX-2/COX-1 selectivity
Lumiracoxib	0.0035 ± 26	3.22 ± 22	910
Diclofenac	0.0011 ± 30	0.0083 ± 6.2	7.6
Naproxen	0.19 ± 66	0.11 ± 10	0.58
Terutroban	inactive at 10 μM	N.D.	-
18	0.014 ± 23	13.2 ± 22	942
20	0.42 ± 32	16.1 ± 6	38
7	0.025 ± 46	25.5 ± 10	1020
32	1.20 ± 45	inactive at 60 μM	-

N.D. - Not Determined

being the less potent molecule of the series (Tab. 7). Among the other molecules, the tetrazole derivative **18** and compound **7** inhibited COX-2 in a very similar way with potencies of 0.014 and 0.025 μM, respectively, while compound **20** showed a potency similar to that of naproxen (Fig. 15 and Tab. 7).

Diclofenac displayed by far the highest potency as COX-1 inhibitor in washed platelets, with values in the nM range, followed by naproxen (Tab. 7). Once again the tetrazole derivative **18** and compound **7** behaved very similarly with IC_{50} values of 13.2 μM and 25.5 μM, respectively, while this time compound **20** showed an IC_{50} of 16.1 μM, close to that of **18** and **7**; compound **32**, resulted inactive in terms of COX-1 inhibition (Fig. 15 and Tab. 7).

Naproxen and lumiracoxib were expected to be, respectively, the less and the most selective COX-2 inhibitors (Fig. 15 and Tab. 7) in perfect agreement with previously published data summarizing the selectivity profiles of various NSAIDs, including COXIBs (Fig. 16) (FitzGerald and Patrono, 2001). Furthermore, figure 15 and table 7 clearly indicate that compounds **18** and **7** are the most selective COXIBs among the multitarget molecules synthetized. Of notice, the sulfonamide derivative **20**, despite being only about 40 times more selective for COX-2 with respect to COX-1 inhibition at calculated IC_{50}, presented a very steep slope of the concentration-response curve (Hill coefficient >>1). This characteristic has no direct impact on the Therapeutic Index of the molecule, and, thus, on its safety, but rather suggest that it is possible to find a dose of compound **20** that is selective for COX-2. Thus, at

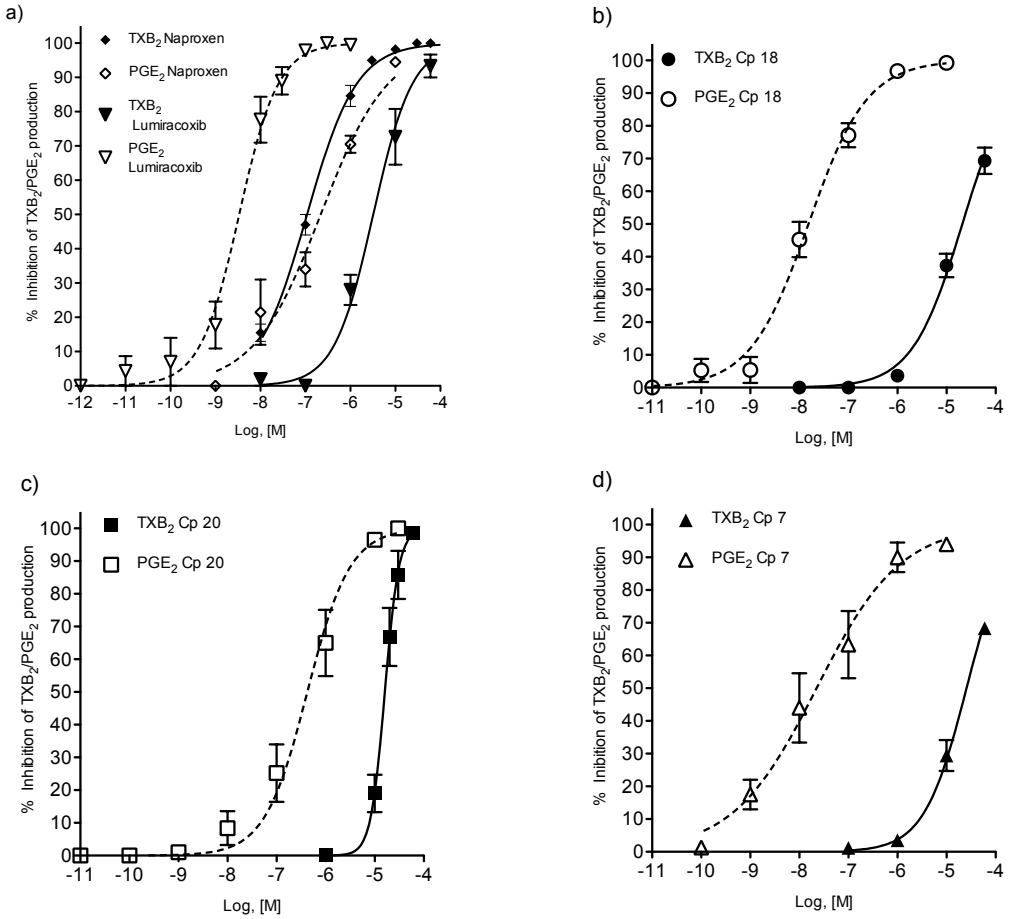

Fig. 15 Inhibition of COX-1 and COX-2 activity by the indicated compounds in comparison to the reference compounds naproxen and lumiracoxib (a). COX-1 activity was assessed in terms of inhibition of TXB_2 production induced by calcium ionophore in human washed platelets; COX-2 activity was assessed in terms of inhibition of PGE_2 production induced by LPS in isolated human monocytes. Data are expressed as percent inhibition of TXB_2 or PGE_2 release versus untreated controls. Error bars represent mean ± SE of at least three independent experiments, each performed in duplicate.

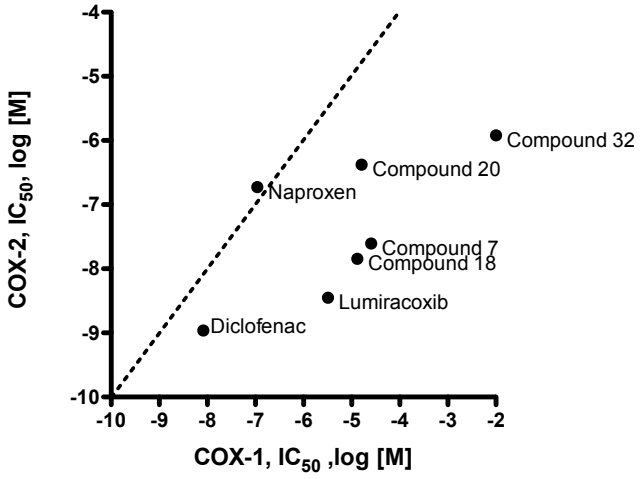

Fig. 16 COX-2/COX-1 selectivity. IC_{50} values obtained for the various compounds are plotted to appreciate their selectivity: the diagonal line indicates equivalence, therefore compounds with high selectivity for COX-2 over COX-1 are plotted below the line.

concentrations ten times its IC_{50} for COX-2 inhibition, about 95% of COX-2 is inhibited, while no inhibition of COX-1 is observed (Fig. 15c).

COXIB-SECOND PART: RC 0 Derivates

Inhibition of TP receptor functional activity in human platelets for RC 0 derivatives compounds

A group of newly synthesized RC 0 derivatives, as well as RC 0, were studied for TP receptor antagonism in platelets from healthy human volunteers. Washed platelets were stimulated with 0.1µM of the stable TXA_2 analogue U46619, and the extent of aggregation was detected by Born-turbidimetric assay for 5 minutes. The sensitivity

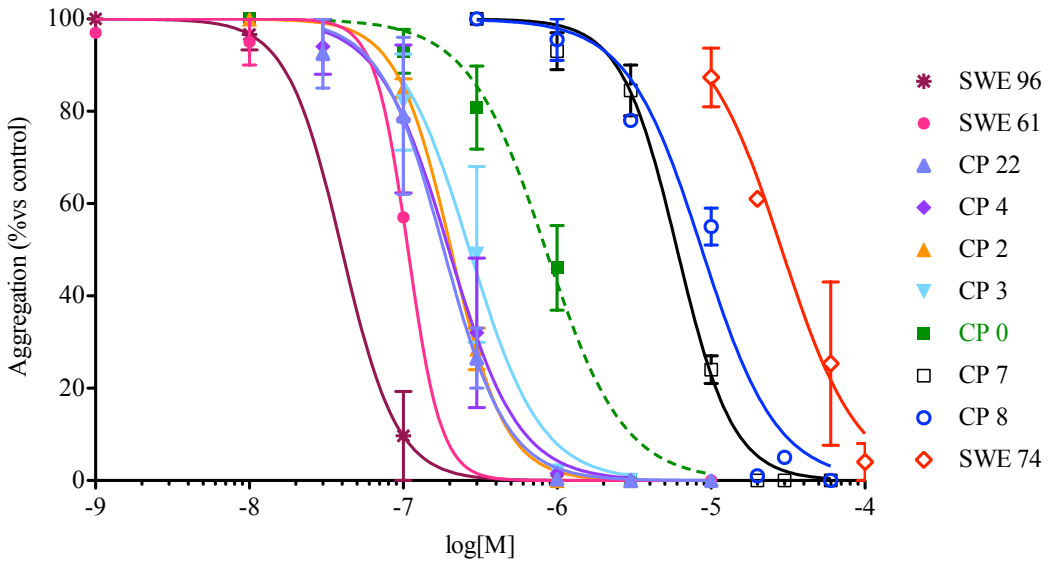

	SWE 96	SWE 61	CP 22	CP 4	CP 2
EC50	3.991e-008	1.073e-007	1.833e-007	1.977e-007	2.047e-007

CP 3	CP 0	SWE 74	CP 8	CP 7
2.695e-007	8.441e-007	2.885e-005	8.728e-006	6.028e-006

Fig. 17 Concentration-response curves of human platelet aggregation induced by 0.1µM U46619. SWE 96-61-74, RC 0 (reference compound), CP 22-4-2-3-7-8 and SWE94 EC_{50} were calculated using a four parameters logistic model. Values represent mean ±SE, expressed as % maximal aggregation. Experiments have been performed at least three times in duplicates. EC_{50} were obtained by a nonlinear regression sigmoidal dose-response curve performed using GraphPad Prism 4.00. All curves shown were computer generated.

of platelets to U46619 did not change during the time required for the experiment, as assessed at regular intervals, and none of the tested molecules caused any aggregation response by itself.

Table 8 reports the IC_{50} values of the inhibition curves of U46619-induced (0.1μM) platelets aggregation due to increasing concentration of the newly synthesized compounds as well as the reference compound RC 0. Among the different molecules tested, compounds SWE 96-61, belonging to the same class of molecules, and CP 2-3-4-22, belonging to a second set of molecular group (in green in the table), in term of RC 0 substituents, were found to be more potent TXA_2 antagonists than RC 0 with lower IC_{50} values (Fig. 17). Among these compounds, SWE 96 is clearly the most potent molecule screened, being also more potent than reference compound RC 0 (SWE 96 IC_{50}: 0.039μM (0.02-0.79) against RC 0's IC_{50} 0.84μM (0.65-1.09).

COX-2/COX-1 selectivity for RC 0 derivatives compounds

The goal of newly synthesized compounds is to maintain or improve the COX-2 selectivity of the parent RC 0 that is to act as COX-2 selective inhibitors. This activity was determined on isolated human lympho-monocytes suspension. COX-2 expression was stimulated overnight with 10 μg/ml of LPS, and the PGE_2 produced was determined by LC/MS/MS analysis, whereas COX-1 inhibitory activity was assessed in washed human platelets determining TXB_2 production following the stimulation with 2 μM of calcium ionophore A23187 for 10 min. TXB_2 production was quantified by LC/MS/MS analysis.

All the compounds tested inhibited the COX-2 activity in a concentration-dependent manner with RC 0 displaying a potency, in term of IC_{50}, of 0.11 μM (0.06-0.19). Compounds SWE 74-68-86 resulted more potent than RC 0 (in red in Tab. 8), with IC_{50} of 0.05μM (0.04-0.07), 0.01μM (0.002-0.01) and 0.04μM (0.03-0.07) respectively, but unfortunately SWE 68 and SWE 86 lacked the required selectivity, showing IC_{50} for COX-1 inhibition of 0.01μM (0.008-0.011) and 0.05μM (0.04-0.06) respectively. Of particular interest resulted the compounds SWE 74, CP 7 and CP 8, in which the IC_{50} for the inhibition of PGE_2 production were 0.05 μM (0.04-0.07), 0.54 μM (0.44-0.65) and 1.8 μM (1.34-2.39) respectively, while their potency in term of COX-1 inhibition, *i.e.* TXB_2 production, were 5.82 μM (3.25-10.4), 123 μM (76-

197), 19 μM (15,4-23,5) respectively (Fig. 18). Indeed, based on their activities against COX-1 and COX-2 these three RC 0 derivatives could be described as COXIB, because the ratio between the IC_{50}s for COX-1 and COX-2 was higher that 25.

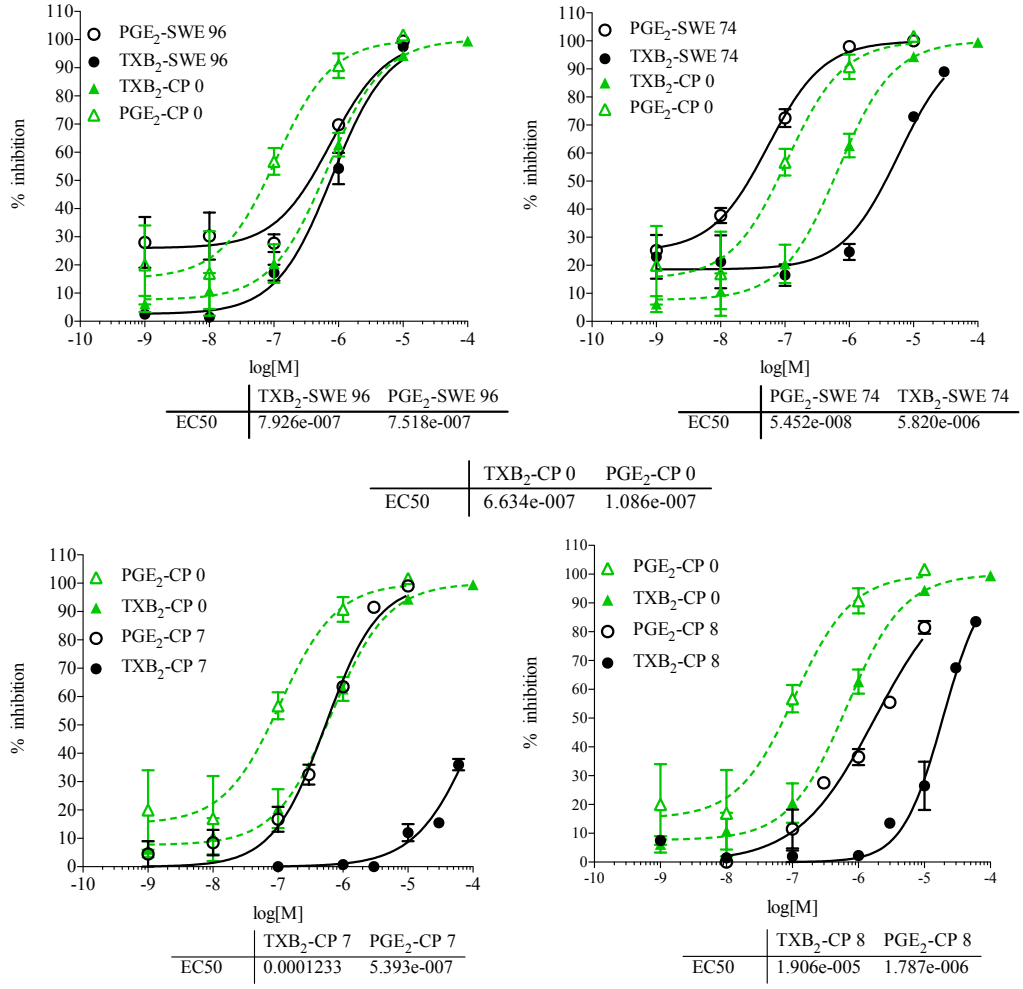

Fig. 18 COX-1 and COX-2 inhibition. EC_{50} were obtained by a nonlinear regression sigmoidal dose-response curve performed using GraphPad Prism 4.00. compared to the reference compound RC 0. COX-1 activity was assessed in term of inhibition of TXB_2 production induced by calcium ionophore in human washed platelets; COX-2 activity was assessed in terms of inhibition of PGE_2 production induced by LPS in isolated human lympho-monocytes suspension. Data are expressed as percent inhibition of TXB_2 and PGE_2 release versus untreated controls. Error bars represent mean ± SE of at least three independent experiments, each performed in duplicate.

Tab. 8 (a) Human washed platelets TPα receptor antagonism: inhibition of U46619 induced aggregation. (b-c) COX-2 and COX-1 activities determined by *in vitro* assay for detection of PGE_2 and TXB_2 in lympho-monocytes suspension and washed human platelets, respectively. (d) COX-2 and COX-1 IC_{50} ratio.

Compound	(a) Aggregation IC_{50} (μM)	(b) PGE_2 IC_{50} (μM)	(c) TXB_2 IC_{50} (μM)	(d) PGE_2/TXB_2
Oxaprozin	**0.84**	**0.11**	**0.61**	**0.18**
SWE96	**0.04**	**0.75**	**0.79**	**0.95**
SWE61	**0.11**	0.31	0.14	2.21
SWE74	**28.85**	**0.05**	**5.82**	**0.01**
SWE95	0.53	0.49	0.56	0.88
SWE27	0.65	0.99	0.08	12.38
SWE101	0.71	0.51	1.19	0.43
SWE50	1.94	0.43	0.64	0.67
SWE47	2.50	3.70	5.74	0.64
SWE41	0.80	0.27	0.36	0.75
SWE37	2.14	1.13	0.29	3.90
SWE60	1.03	0.92	1.25	0.74
SWE68	2.74	**0.01**	0.01	1.44
SWE73	0.46	1.50	0.98	1.53
SWE86	2.02	**0.04**	0.05	0.84
SWE87	0.68	1.40	0.77	1.82
SWE100	1.47	8.23	4.81	1.71
SWE104	1.75	0.57	0.94	0.61
SWE105	0.85	0.22	0.18	1.22
SWE11	12.79	4.19	4.55	0.92
SWE21	2.39	3.25	2.12	1.53
FK40	1.01	0.10	0.02	5.00
AF872	43.13	0.13	0.098	1.33
SWE102	10.36	7.81	8.34	0.94
FEK30	1.02	0.99	3.05	0.32
FEK36	1.19	3.29	5.55	0.59
FEK42	1.64	2.49	7.22	0.34
CP2	**0.20**	2.37	0.22	10.77
CP3	**0.27**	3.96	0.18	22.00
CP4	**0.19**	12.28	3.22	3.81
CP7	**6.03**	**0.57**	**123.3**	**0.00**
CP8	**8.73**	**1.79**	**19.06**	**0.09**
CP15	3.27	87.42	11.62	7.52
CP5	0.80	16.31	1.90	8.58
CP21	0.94	81.45	8.61	9.46
CP22	**0.18**	9.03	35.37	0.26

Discussion

Cardiovascular disease (CVD) is a highly prevalent pathology, and one of the major cause of death in recent years. It was estimated that 17.5 million people died for CVDs in 2012, representing 31% of all global deaths (WHO, World Health Organization).

In CVD pathologies, one of the main player is TXA_2, a product of AA metabolism arising from the activity of TXS on COX-derived PGH_2 intermediate. TXA_2 is the major agonist of TPα receptor, which is expressed in prevalence in platelets membrane and in many other tissues and cells like smooth muscle cells of the vessel, lung, kidney and spleen. From a patophysiological point of view, TPα mediates platelet activation and aggregation, thrombus formation and vascular constriction, and indeed it can cause stroke and myocardial infarction.

TPα is a GPCR of the rhodopsin family, and, as the vast majority of proteins in this class, it has a highly conserved triplet of amino acids (Glu/Asp-Arg-Tyr), the so called E/DRY motif, located at the boundary between TM3 and ICL2. As discussed above, these residues received considerable attention with respect to the regulation of GPCR conformational states.

In the first part of my thesis, we tried to shed light on the mechanism of activation of GPCRs and on the different conformational states they can adopt, since an emerging view from several studies has postulated that GPCR are not simple "on-off" switches, but rather adopt a continuum of conformations (Bockenhauer et al., 2011). The focus of this part of my thesis was therefore to assess the TPαWT and its mutants (TPαE129V and TPαR130V) for their coupling with the cognate G protein in order to identify possible different states of the different constructs and verify if, in basal condition, they exist in a conformational state that was already theorized in the CTC model of Weiss and colleagues. Furthermore, because the comprehension of the TP mechanism of activation will help to define its role in CVDs, in the second part of my thesis we focused our attention on the identification of new compounds

targeting both TPα and the COX-2 enzyme (a key player in inflammatory, fever and pain events) in order to obtain a new pharmacological class of agents possessing both a selective COX-2 inhibitory activity (COXIB-second generation of NSAIDs) and a TP antagonist activity. The combination of these two properties should, hopefully, allow us to identify a new nonsteroidal anti-inflammatory drug with the same gastro-intestinal safety of COXIB, but devoid of their potential CV side effects (Rovati et al., 2010).

As for the first goal of my thesis, *i.e.* to explore TPα mechanism of action, we used the FRET based SPASM technique, a novel tool useful to detect the ligand- or mutation-induced stabilization of GPCR conformations that promote interactions with G proteins in live cells (Malik et al., 2013), thus capable to distinguish between G protein binding from G protein activation.

Before performing the basal SPASM experiment, *i.e.* in the absence of agonist, we validated the nine fusion proteins obtained from the cloning of TPαWT and the two mutants TPαE129V and TPαR130V in the three different SPASM sensors, in term of cellular localization and functionality. As expected, laser scanning fluorescence microscopy confirmed the correct localization at the plasma membrane, despite the $G\alpha_q$ and $G\alpha_s$ sensors showed some protein retention, as evidenced by the presence of inclusion bodies into the cytoplasm (Fig. 6). This result is not totally unexpected as the SPASM sensors, composed by the FRET acceptor mCitrine and the donor mCerulean, also encompass the 27 amino acids of $G\alpha_q$ or $G\alpha_s$ C terminus, which might prevent the normal and correct folding of the TPα receptor. Indeed, western blot analysis of cell membrane enriched samples confirmed that each SPASM sensors is found in the correct cell fraction and has the expected molecular weight (Fig. 7). However, the significant reduction of the density of the higher molecular weight band in TPαE129V construct, likely to represent a glycosylated form of the receptor, with respect to WT seems to confirm a grater difficulty for the mutated receptor to reach the plasma membrane.

The last step of sensors validation was to perform the functional assays: we compared the functionality of WT and mutant TPα receptors with the respective 'no-pep' SPASM sensors by constructing U46619-induced total IP and cAMP concentration-response curves in order to test $G\alpha_q$ and $G\alpha_s$ signal transduction

pathway, respectively. As discussed above, only the 'no-pep' fusion proteins are able to activate the signal transduction pathway, while in the 'q-pep' and 's-pep' sensors the presence of the specific Gα component at the C terminus competitively inhibit endogenous G protein interactions. In both functional assay the potencies and the efficacies of each SPASM sensor were comparable to that of the corresponding TPα construct without the SPASM component and there was no change in the functionality of the receptor, thus confirming the gain and the loss of function nature of TPαE129V and TPαR130V, respectively (Fig. 8-9).

After SPASM sensors validation, FRET experiments were performed with both 'q-pep' and 's-pep' sensors. As shown in figure 10 all TPα no-pep fusion proteins (TPαWT, TPαE129V and TPαR130V no-pep) showed the same basal FRET signal. Unexpectedly, TPαE129V q-pep specific FRET value resulted significantly higher than the one calculated for the WT and R130V receptors (Fig. 10b). Similar behaviour has been obtained for TPαE129V s-pep (Fig. 10c). Indeed**,** these results seem to indicate that TPαE129V mutant, in absence of any agonist stimulation, is somewhat more pre-coupled to its cognate G_q and G_s proteins than TPαWT and TPαR130V. Considering that TPαE129V is characterized by high agonist binding affinity and by an agonist-induced increased efficacy and/or potency in signaling without any increase in basal activity, *i.e.* SAM (Capra et al., 2004), it is possible to postulate that this mutant, in basal condition, is in a RG state (inactive coupled to G protein), as postulated by the CTC model. On the other hand, TPαR130V confirms to be a typical loss of function mutant, indeed reflecting the R (inactive, uncoupled form to G protein) conformational state of the CTC model.

Considering that the mutant SPASM constructs TPαR130V 'q-pep' and 's-pep', and even more the TPαE129V 'q-pep' and 's-pep' are somewhat retained in the cytoplasm, to confirm our SPASM data we are planning to apply another FRET-based technique, *i.e.* the "acceptor photobleaching fluorescence resonance energy transfer", to our SPASM sensors. In this case FRET measurements will be performed before and after the laser-induced acceptor photobleaching, and have the unique advantage over the conventional FRET of assaying only surface receptors (Konig et al., 2006). In this type of analysis, fluorescence emission by a donor fluorochrome is quenched due to direct transfer of excitation energy to an acceptor fluorochrome.

Upon laser-induced acceptor photobleaching, this FRET is blunted and the donor signal is de-quenched, meaning that there was energy transfer, and, thus, close proximity between donor and acceptor fluorophores. On the other hand if the donor intensity does not increase after acceptor photobleaching, it means that there was no energy transfer, and thus, no proximity between donor and acceptor. Since this technique assumes to measure FRET in a defined cell area using laser scanning confocal microscopy, this will, hopefully, overcome the problem of protein retention of $G\alpha_q$ and $G\alpha_s$ SPASM sensors. Indeed, selecting specific plasma membrane area, the FRET signal detected with this technique will be related only to the proteins with correct folding and correct cellular localization. This technique has been recently used to study homodimerization of TPα receptor in our lab (Capra et al., 2016), and has been demonstrated to generate highly reproducible results compared to conventional FRET.

In the second part of my thesis work, I focused on the identification of new antinflammatory compounds targeting TPα and COX-2 enzyme. Our working hypothesis is that the addition of a TP antagonist component to a COXIB may provide protection against all the harmful activities of a classical COXIB due to its inhibition of endothelial cell-derived PGI_2 production without affecting platelet-derived TXA_2 synthesis (McAdam et al., 1999). In addition, the presence of a receptor antagonist will also prevent TP activation by mediators insensitive to aspirin or other NSAIDs, such as the nonenzymatic products of AA metabolism isoprostanes.

Today, there is no safe NSAIDs and their main side effects include GI and renal toxicity (Salvo et al., 2011). COXIB therapy is currently used in chronic pain control in selected patients with higher risks of GI complications but lower risk of CV events as an alternative to conventional NSAIDs associated to gastroprotective therapy. However, these subjects will experience an increased CV-risk as a result of the selective inhibition of endothelial PGI_2 production, potentially exposing them to serious CV events. Therefore, there is still an unmet need for an adequate pain therapy combined with minimal GI damage and CV toxicity. In addition, traditional NSAIDs are known to interfere with the cardioprotective effect of low-dose aspirin, somehow endangering the benefit of their association (Catella-Lawson et al., 2001).

Finally, a number of TXA_2 biosynthesis inhibitors and/or receptor antagonists have been developed and studied, showing their ability to provide additional CV protection on top of that of aspirin (Cayatte et al., 2000; Sakariassen et al., 2012), even though they have always suffered from being perceived as a more expensive alternative to the economical and active aspirin. In particular, the potent and selective TP antagonist terutroban (Gaussem et al., 2005) has been shown to be an effective antithrombotic agent in peripheral arterial disease (Fiessinger et al., 2010) and to improve endothelial function in atherosclerotic patients (Lesault et al., 2011). Somehow unexpectedly, the PERFORM Phase III clinical trial with terutroban in patients with cerebral ischemic events did not meet the predefined criteria for non-inferiority to aspirin, while showing similar rates of primary endpoint between the two drugs (Bousser et al., 2011).

We recently reported a full *in vitro* pharmacological characterization (Hoxha et al., 2016) of selected molecules from a series of lumiracoxib derivatives previously synthetized in collaboration with the University of Torino (Bertinaria et al., 2012). The non-selective first generation NSAID naproxen, the most selective COX-2 inhibitor lumiracoxib and the TP antagonist terutroban have been considered as reference compounds. Among the molecules tested, the tetrazole derivative compound **18** and the trifluoromethansulfonamido-isoster compound **20**, are the most active and present a fairly balance between COX-2 inhibitory activity and TP receptor antagonism. However, TP receptor inhibitory potency remain in the micromolar range, preventing, at this stage, a real *in vivo* relevance for these molecules. The data generated during my thesis work have shown that compounds **7** and **32** did not possess better TP antagonist properties than the reference compound lumiracoxib, while losing most of their potency as COX inhibitors albeit preserving COX-2 selectivity. The replacement of 2-fluoro-6-chloro-phenyl substituent present on the amino nitrogen in compound **7** with the *p*-chlorophenylsulfonyl substructure, typical of terutroban, generated compound **32** where two phenyl rings are linked by a sulfonamide group instead of the classic amino group. However, this modulation did not meet our expectations, as compound **32** did not show better properties with respect to compounds **18**, **20** and **7**. These data suggest that COX-2 selectivity might be determined by the presence of the 2-amino-5-methyl benzen carboxylic acid

moiety, while potency could be regulated by the nature of the substituent present on the amino nitrogen. The first observation is in agreement with literature data highlighting the importance of methyl substitution for COX-2 selectivity (Blobaum and Marnett, 2007).

On the other hand, compounds **18** and **20** have gained in TP receptor antagonist activity, with compound **20** statistically different from lumiracoxib in both inhibition of human platelets aggregation and IP generation in a transfected system, despite still far from required values for an *in vivo* application. These functional results are in good agreement with affinity binding data previously reported for these compounds (Bertinaria et al., 2012), and support the strategy of isosteric replacement of the carboxylic function of lumiracoxib, either with linear or cyclic substructures for the successful generation of molecules endowed with improved TP antagonism. Compound **18** and particularly compound **20** displayed better balanced activities, better approaching the ideal value of 1 of the ratio between the calculated potencies at both pharmacological targets when compared to lumiracoxib or diclofenac. However, compound **20** lost most of its COX-2 inhibitory activity and COX selectivity compared to compound **18,** suggesting that a higher acidity of carboxylic acid isoster is needed to maintain a high level of COX-2 inhibition. Concerning COX-2 activity, it is interesting to note that shortening the alkyl chain connecting the acidic moiety to the benzene ring reflects in a loss of activity (see derivative **7** and lumiracoxib). This observation clearly indicates that the acidic moiety should be separated from the benzene ring by one carbon atom to reach optimal binding to COX-2 pocket, in agreement with the postulated binding pose of diclofenac and lumiracoxib at the COX-2 binding site (Rowlinson et al., 2003). Interestingly the distance of the acidic unit from the benzene ring might also influence the antagonism at the TP receptor (compare derivatives **18** and **20** vs **7** and **32** in table 6). The stringent structural requirements for COX-2 inhibition are apparently in contrast with the need of compounds endowed with more flexible and extended structures, which proved more efficient as TP receptor antagonists. In this context, the use of different carboxylic acid bioisosters, together with docking studies on both COX-2 and TP receptor models could be envisaged for the development of new molecules (Ballatore et al., 2011; Yamamoto et al., 1993).

Thus, despite compounds **18** and **20** have gained in TP receptor antagonist activity, they are still far from the required values for an *in vivo* application. However, the information derived from the characterization of this first series of molecules has been used as the starting point of a new strategy to design more potent molecules that might change the way we treat chronic inflammatory diseases.

Thus in collaboration with Goethe University in Frankfurt, we started to design and test a second class of compounds which are, in fact, derivatives of a different NSAID that we will call RC 0. From a docking study, conducted by professor Proschak, it seems that RC 0 could be a good scaffold to make a new drug able to target both COX-2 and the TP receptor. This compound has been shown to be effective and well tolerated in the clinical management of signs and symptoms of adult rheumatoid arthritis, osteoarthritis, ankylosing spondylitis and soft tissue disorders such as bursitis and tendonitis. Even if the literature shows that RC 0 can produce mild gastrointestinal complaints such as nausea, diarrhoea, constipation and occasionally vomiting similar to other NSAIDs, this drug exhibits a good tolerability profile, in both healthy human subjects and in patients with inflammatory painful disorders. Furthermore, RC 0 possesses many positive characteristics, for example it has a high oral bioavailability (95%) and it has a long plasma half-life (about 50-60 hours), which allows a once a day administration. Moreover, RC 0 is >99,5% bound to albumin and the quote of unbound RC 0 is increased at higher concentrations after single or repeated doses. This increase in free (unbound) RC 0 results in an increase in clearance. Finally, RC 0 is metabolised in the liver by oxidative and conjugative pathways and is eliminated by the renal and faecal routes. These dual metabolic and elimination pathways may reduce the risk of disproportionate drug accumulation and toxicity even when RC 0 is used in the elderly and compromised patients. Thus, these findings seem to corroborate our choice to use RC 0 as a starting structure for further development.

Among the 35 compounds tested so far, compounds SWE 74, CP 7 and CP 8 are of particular interest because of their profile as COXIB; in particular, SWE 74 shows an IC_{50} ratio (COX-2 vs COX-1 inhibition) lower than RC 0, that therefore makes it more COX-2 selective than reference compound; CP 7 and CP 8 resulted weaker than RC 0 in term of COX-2 inhibition, but, in particular for CP 7, their activity against

COX-1 was almost absent. This means that it could be possible to use higher concentration without inhibiting COX-1 enzyme, and therefore avoiding GI side effects. Unfortunately all these compounds were the weakest TP receptor antagonist among the compounds tested. Finally, SWE 96 showed a behaviour that was the opposite of that characterizing the previous group: in fact its IC_{50} for the antagonism of the TP receptor is 20 fold lower than RC 0, but it lacks selectivity for the COX-2 enzyme.

In light of the structural information gathered from all the compounds tested, and again in collaboration with professor Eugen Proschak and colleagues, the next step of this project will be to develop a new chemical entity presenting a good balance of the COXIB activity and the TP receptor antagonism, for further testing in an *in vivo* model.

Overall Conclusions

Despite the recent explosion of GPCR crystal structures of both active (R^*) and inactive (R) receptor states, a lot of work will still be necessary to fully unravel the mechanism(s) through which they become active, as well as in providing a full account of the ensemble of basal and active states. Clearly more structural work will be necessary to fully understand the highly regulated process of receptor activation, but the results of this thesis work supports the CTC as the minimum model to explain the complex pharmacological behaviour of GPCRs in general, and of TP receptor and its mutants in particular. From the results of my first project it is possible to postulate that the TPαE129V (SAM) is in an 'active-like' conformation corresponding to the RG state (inactive, coupled to G protein) as already suggested for the β2-AR (Adrenergic receptor). On the contrary, TPαR130V (loss of function mutant) seems to display an inactive R conformation (uncoupled to G protein), as envisioned by CTC model.

In addition, considering the role of TXA_2-TP system in CVDs, the elucidation of the mechanism/s of TP activation could represent the basis for the design of new multitarget antinflammatory compounds. For this reason, the second focus of my thesis was to investigate the TPα receptor as a possible target for new chemical entities possessing both TP antagonist and selective COX-2 inhibitory activities.

The results presented demonstrate that modification of existing drugs (lumiracoxib or RC 0) can lead to new bivalent multitarget molecules with obvious advantages in their pharmacological profiles: a higher TP antagonist potency and a more balanced COX-2 selectivity.

Even if further studies will be necessary to improve the pharmacodinamic profile of these molecules before a careful evaluation can be considered in an *in vivo* animal model, the information relative to the structural requirements for TP antagonism and COX-2 selective inhibition provide an important starting point for the successful development of a new family of GI- and cardiovascular-safe NSAIDs.

Materials and Methods

Abbreviations

BFB	Bromophenol blue (3′,3″,5′,5″tetrabromophenolsulfonphthalein)
bp	bais pair
kb	Kilobases
DMEM	Dulbecco's modified Eagle's medium
DTT	Dithiothreitol
EtBr	Etidium Bromide
FBS	fetal bovine serum
HEK293T (ATCC® CRL-3216™)	human embryonic kidney
I-BOP	(1S*) -7-[3- [3-hydroxy-4- (4-iodophenoxy) -1-butenyl]- 7- oxabicyclo [2.2.1] hept-2-yl]-5 heptenoic acid
IP	inositol phosphate
KDa	KiloDalton
SDS	sodium dodecyl solphate
Tris	hydroxy-methyl-aminomethane
HBSS	Hanks Balanced Salt Solution
U46619	([1R-[1α,4α,5β(Z),6α(1*E*,3S*)]]-7-[6-(3-hydroxy-1-octenyl)- 2 oxabicyclo[2.2.1]hept-5-yl]-5-heptenoic acid)
SQ29,548	([1S-[1α,2α(*Z*),3α,4α]]-7-[3-[[2-[(phenylamino)carbonyl]-hydrazino] methyl]-7-oxabicyclo[2.2.1]hept-2-yl]-5-heptenoic acid)

Materials

Buffers and media

- SDS RUNNING GEL 10%

    4.05 ml H_2O

    3.35 ml Acrylamide/Bis solution 30% (19:1)

2.6 ml LOWER buffer

10 µl TEMED

100 µl ammomium persolfate (AP) 10%

- SDS STACKING GEL

6.4 ml H_2O

1 ml Acrylamide/Bis solution 30% (19:1)

2.6 ml UPPER buffer

10 µl TEMED

50 µl ammomium persolfate (AP) 10%

- LOWER BUFFER: 1.5M Tris + 0,4% SDS pH=8.8

17.17 g Tris

0.2 g SDS

Distilled water up to 100 ml

HCl until pH=8.8

-UPPER BUFFER: 0.5 M TRIS + 0.4% SDS pH=6.8

3.02 g Tris

0.2 g SDS

Distilled water up to 50 ml

HCl until pH=6.8

-AP 10%

20 mg AP + 200 µl H_2O

-SDS-PAGE ELECTRODE BUFFER (10X):

144.7 g Glycin (1.92 M)

30.3 g Tris Base (0.25M)

10 g SDS (1%)

Distilled water up to 1 L

-SDS-PAGE BLOTTING BUFFER (1X):

17.29 g Glycin (192 M)

3.63 g Tris Base (0.025M)

240 ml MetOH (20%)

Distilled water up to 1.2 L

-Laemmly Buffer 10X (10 L):

302.8 g Tris Base

1440.3 g Glycin

Distilled water up to 10 L

-Sample Buffer:

3 ml Tris-Cl (1M)

1 g SDS

5 ml glycerol

20 mM DTT

-Pounceau S:

0.2 % Pounceau S

3% Acetic acid

-TBS (1X):

2.423 g Tris 20mM

29.22 g NaCl 500mM

Distilled water up to 1L

-TBS-T:

TBS 1X

0.1 % Tween 20

-TBS-T 5% milk:

PBST 1X

5% non fat dry milk

-DNA ladder

60 µl DNA Ladder (New England Biolabs) 500ng/µl

100 µl Blu 6X for DNA

440 µl Distilled water

-Bromofenol Blu 6X for DNA

0.25% BFB

30% glycerol

-Cracking solution (2X)

100 mM NaOH

10 mM EDTA pH=8

1% SDS

10% glycerol

BFB

-Buffer A

HEPES-buffered saline

0.2% dextrose (w/v)

500μM ascorbic acid

1.5 μg ml^{-1} aprotinin

1.5 μg mL^{-1} leupeptin at pH 7.45.

-HBSS -/- (1X)

5.3 mM KCl

0.4 mM KH_2PO_4

138 mM NaCl

4.1 mM $NaHCO_3$

0.3 mM Na_2HPO_4

-HBSS +/+ (1X)

HBSS -/- 1X

1.2 mM $CaCl_2$ $2H_2O$

0.5 mM $MgCl_2$ $6H_2O$

0.4 mM $MgSO_4$ $7H_2O$

-Lysis A

0.2% NaCl

-Lysis B

1.6% NaCl

0.2% Sucrose

$[d_4]PGE_2$ and $[d_4]TXB_2$ deuterated standards were from Cayman Chemical (Ann Arbor, MI)

PGE_2 enzyme immunoassay- kit were from Cayman Chemical (Ann Arbor, MI)

Anion exchange resin AG 1X-8 (formate form, 200–400 mesh)

Growth medium

• Growth medium for *E. coli*:

LB-Broth, LB Bouillon

10 g/L Tryptone

5 g/L Yeast extracts

5 g/L NaCl

LB Ampicillin 0.1 μg/μl

LB Agar: LD + 1% Agar

• Growth media for HEK293-T cells:

• DMEM (Dulbecco's Modified Eagle Medium, Gibco. Thermo Fisher-USA) supplemented with 10% FBS and Hepes 20mM. Medium was or was not supplemented with Penicillin/Streptomicin.

• Inositol-free Dulbecco's modified Eagle's medium (DMEM) was obtained from ICN Pharmaceuticals Inc. (Costa Mesa, CA).

Transfection medium and reagents

• Opti-MEM® (Thermofisher, MA, USA): rReduced-Serum Medium is an improved Minimal Essential Medium (MEM) that allows a reduction of Fetal Bovine Serum supplementation by at least 50% with no change in growth rate or morphology.

• Lipofectamine® 2000 (Thermo Fisher, MA, USA), it is a transfection Reagent that has been shown to effectively transfect the widest variety of adherent and suspension cell lines.

• X-tremeGENE™ 9 DNA Transfection Reagent (Sigma Aldrich Co, St Luis, USA) is a polymer reagent for transfecting common cell lines. X-tremeGENE 9 DNA Transfection Reagent is a blend of lipids and other components supplied in 80% ethanol, filtered through 0.2 μm pore size membrane, and packaged in glass vials.

Cell lines

Cell line used is HEK293-T (ATCC® CRL-3216™): an ephitelial human embryonic kidney cell line. Originally referred as 293tsA1609neo, is a highly transfectable derivative of human embryonic kidney 293 cells, and contains the SV40 T-antigen. This cell line is competent to replicate vectors carrying the SV40 region of replication. It has been widely used for retroviral production, gene expression and protein production.

HEK293-T cells were cultured in DMEM containing 10% FCS and kept at 37°C in a humidified atmosphere of 95% air and 5% CO_2. Medium was supplemented with 20mM HEPES and 50units/ml penicillin, 100µg/ml streptomycin.

Transfections were performed using the Lipofectamine 2000 or X-tremeGENE™ reagent following manufacturer's instructions. Briefly, cells were plated into tissue culture dishes in order to obtain a 50–60% confluence at the time of transfection. Transfection has been done with an optimized 2:1 Lipofectamine /DNA ratio or 10µl X-tremeGENE ™/2µg DNA.

Bacterial strains and plasmids

Epicurian Coli (*E. Coli*) chemical DH5α competent cells were from ThermoFisher, Invitrogen company.

Genotype: F^- Φ80*lac*ZΔM15 Δ(*lac*ZYA-*arg*F) U169 *rec*A1 *end*A1 *hsd*R17 (rk^-, mk^+) *pho*A *sup*E44 λ^- *thi*$^-$1 *gyr*A96 *rel*A1.

MAX Efficiency® DH5α™ Competent Cells are a well-known, versatile strain that can be used in many everyday cloning applications. In addition to supporting blue/white screening, *rec*A1 and *end*A1 mutations in DH5α™ cells increase insert stability and improve the quality of plasmid DNA prepared from minipreps.

Features of MAX Efficiency® DH5α™ Competent Cells include: transformation efficiency up to 1×10^9 transformants/µg plasmid DNA, high plasmid yield from the DH5α™ (*end*A1) *E. coli* strain, Blue/white screening capable (*lac*ZΔM15), Greater insert stability due to the presence of *rec*A1.

The Φ80*lac*ZΔM15 marker provides α-complementation of the β-galactosidase gene from pUC or similar vectors, and can therefore be used for blue/white screening of

colonies on bacterial plates containing Bluo-gal or X-gal. DH5α™ cells are capable of being transformed efficiently with large plasmids, and can also serve as a host for the M13mp cloning vectors if a lawn of DH5α-FT™, DH5αF′™, DH5αF′IQ™, JM101, or JM107 is provided to allow plaque formation. These cells are suitable for the construction of gene banks or for the generation of cDNA libraries using plasmid-derived vectors.

Oligonucleotides

TPα (KpnI-) for: CCTGGGGCTGCTGGTGACCGGAACCATCGTGGTGTCCCAGC

TPα (KpnI-) rev: GCTGGGACACCACGATGGTTCCGGTCACCAGCAGCCCCAGG

HindIII-3HA for: CCGCCGAAGCTTATGTACCCATACGATGTTCC

KpnI-TPα rev: CCGCCGGGTACCCTGCAGCCCGGAGCGCTGC

TPα (KpnI-) seq1for: ATTACCCTGGAGGAGAGACG

TPα (KpnI-) seq2for: CCTGGCTGCCGTCTCTGTCG

TPα (KpnI-) seq3rev: GATACCCAGGTAGCGCTCTG

TPα (KpnI-) seq4for: CGCTACACCGTGCAATACCC

Plasmids

pcDNA5 plasmid is a mammalian centromeric expression vector composed by 5446 bp. In the sequence is present the CMV promoter, ampicillin and neomycin-resistance markers.

pSC3.2 (pcDNA3 3HATPαWT KpnI-)
Centromeric vector derived from pcDNA3 3HATPαWT. It has been created by site-directed mutagenesis in order to delete the restriction enzyme sequence for KpnI.

pSC4.4 (pcDNA5 3HATPαWT KpnI- no pep)
Centromeric vector derived from pcDNA5 β3AR_mCit_10nm_mCer_nopep.

3HATPαWT KpnI- amplified by PCR from pSC3.2, digested with HindIII/KpnI, has been cloned in pCDNA5 β3AR_mCit_10nm_mCer_nopep, previously digested with HindIII/KpnI.

pSC5.4 (pcDNA5 3HATPαWT KpnI- q pep)
Centromeric vector derived from pcDNA5 β3AR_mCit_10nm_mCer_nopep.
3HATPαWT KpnI- amplified by PCR from pSC3.2, digested with HindIII/KpnI, has been cloned in pCDNA5 β3AR_mCit_10nm_mCer_qpep, previously digested with HindIII/KpnI.

pSC7.1 (pcDNA5 3HATPαWT KpnI- s pep)
Centromeric vector derived from pcDNA5 β3AR_mCit_10nm_mCer_nopep.
3HATPαWT KpnI- amplified by PCR from pSC3.2, digested with HindIII/KpnI, has been cloned in pCDNA5 β3AR_mCit_10nm_mCer_spep, previously digested with HindIII/KpnI.

pSC10.1 (pcDNA3 3HATPαE129V KpnI-)
Centromeric vector derived from pcDNA3 3HATPαE129V. It has been created by site-directed mutagenesis in order to delete the restriction enzyme sequence for KpnI.

pSC11.1 (pcDNA5 3HATPαE129V KpnI- no pep)
Centromeric vector derived from pcDNA5 β3AR_mCit_10nm_mCer_nopep.
3HATPαE129V KpnI- amplified by PCR from pSC10.1, digested with HindIII/KpnI, has been cloned in pCDNA5 β3AR_mCit_10nm_mCer_nopep, previously digested with HindIII/KpnI.

pSC12.2 (pcDNA5 3HATPαE129V KpnI- q pep)
Centromeric vector derived from pcDNA5 β3AR_mCit_10nm_mCer_qpep.
3HATPαE129V KpnI- amplified by PCR from pSC10.1, digested with HindIII/KpnI, has been cloned in pCDNA5 β3AR_mCit_10nm_mCer_qpep, previously digested with HindIII/KpnI.

pSC7.1 (pcDNA5 3HATPαE129V KpnI- s pep)
Centromeric vector derived from pcDNA5 β3AR_mCit_10nm_mCer_spep. 3HATPαE129V KpnI- amplified by PCR from pSC10.1, digested with HindIII/KpnI, has been cloned in pCDNA5 β3AR_mCit_10nm_mCer_spep, previously digested with HindIII/KpnI.

pSC19.2 (pcDNA3 3HATPαR130V KpnI-)
Centromeric vector derived from pcDNA3 3HATPαR130V. It has been created by site-directed mutagenesis in order to delete the restriction enzyme sequence for KpnI.

pSC20.1 (pcDNA5 3HATPαR130V KpnI- no pep)
Centromeric vector derived from pcDNA5 β3AR_mCit_10nm_mCer_nopep. 3HATPαE129V KpnI- amplified by PCR from pSC19.2, digested with HindIII/KpnI, has been cloned in pCDNA5 β3AR_mCit_10nm_mCer_nopep, previously digested with HindIII/KpnI.

pSC21.1 (pcDNA5 3HATPαR130V KpnI- q pep)
Centromeric vector derived from pcDNA5 β3AR_mCit_10nm_mCer_qpep. 3HATPαE129V KpnI- amplified by PCR from pSC19.2, digested with HindIII/KpnI, has been cloned in pCDNA5 β3AR_mCit_10nm_mCer_qpep, previously digested with HindIII/KpnI.

pSC22.2 (pcDNA5 3HATPαR130V KpnI- s pep)
Centromeric vector derived from pcDNA5 β3AR_mCit_10nm_mCer_spep. 3HATPαE129V KpnI- amplified by PCR from pSC19.2, digested with HindIII/KpnI, has been cloned in pCDNA5 β3AR_mCit_10nm_mCer_spep, previously digested with HindIII/KpnI.

RECOMBINANT DNA TECHNIQUES:

Polymerase chain reaction (PCR)

PCR is carried out using plasmid DNA as template. In this work it has been used Pfu Ultra II polymerase (Agilent technologies).

The reaction mix contain:

10 ng DNA template

5 µl DNA polymerase buffer 1X

1 µl oligonucleotides 20 pmoles each

5µl dNTPs 2 mM each

1 unit DNA Polymerase

2,5 µl DMSO

Water up to 50µl

Reactions are performed using iCycler Thermal Cycler (Biorad) in these conditions:

1. first denaturation 5 min at 95°C
2. denaturation 30 sec at 95°C
3. annealing 1 min at the Tm of the oligonucleotides
4. extension 2 min per kb at 72°C
5. repeat steps from 2 to 4 for 30 times
6. final extension 10 min at 72°C

Tm is the melting temperature. Conditions can be modified according to the oligonucleotides used.

Site-directed mutagenesis PCR

We used kit "QuickChange™ Site-Directed Mutagenesis Kit" provided by Stratagene.

The reaction mix contain:

10 ng plasmidic DNA

5 µl DNA Polymerase buffer 10X

1 µl oligonucleotides (125 ng/µl)

5 µl dNTPs 2 mM each

1 µl Turbo DNA Polymerase (2,5 U/µl)

water up to 50 µl

Reactions are performed using iCycler Thermal Cycler (Biorad) in these conditions:

1. first denaturation 30 sec at 95°C
2. denaturation 30 sec at 95°C

3. annealing 1 min at 55°C
4. extension 2 min per kb at 72°C
5. repeat steps from 2 to 4, 18 times

After the end of reaction, the mix are digested with 1µl of DpnI (10 U/µl) for 1 hour at 37°C.

DNA digestion with restriction enzymes and DNA purification

DNA is digested with specific endonucleases in the conditions suggested by Thermo Fisher Scientific. Samples are added 1/6 of the volume of BFB solution (6X: 0.25% BFB in 30% glycerol), before loading on agarose gel (0.8%-2%). DNA is visualized by Ethidium bromide at the final concentration of 5 mg/ml. To identify the size of the DNA fragments, it is loaded a Molecular Weight Marker by New England Biolabs. DNA is purified from agarose gel using the Gel Extraction Kit (Promega).

Ligation

A suitable amount of digested DNA and cleaved vector are ligated using Quick ligase (New England Biolabs).

Preparation of competent cells and transformation of *E. coli*

E. coli DH5αTM is inoculated into 10 ml of LB medium and grown overnight at 37 °C without agitation. The day after the culture is inoculated into 1 L of LB and grown at 37 °C with agitation until the O.D (l=600 nm) reach 0.4-0.5. At this point cells are kept on ice for 10 minutes, centrifuged at 6000 rpm for 15 minutes at 4 °C and washed two times with 1 L and 500 ml respectively of water ice-cold. Competent cells are fractioned in 50 µl aliquotes and stocked at -80° C. To transform these cells 0.5-1 mg of DNA is added (30 minutes in ice). The bacteria was then subjected to thermic shock at 37 °C for 1 minute or 42 °C for 30 seconds. Cells were transferred again on ice for 2 minutes. Finally, cells are grown in 1 ml of LB medium (without antibiotics) for 1 h at 37 °C and subsequently plated on selective solid medium. Cells are grown overnight at 37 °C.

Cracking procedure of plasmidic DNA extraction from *E. coli*

Cracking procedure is a quick protocol to test the presence of plasmid into *E. coli* cells. Cracking solution was prepared and can be stored at RT up to 2 months. 25 µl of deionized water was transferred into eppendorf tubes (1.5 ml) for each colony of interest. The colony is picked up using p200 pipette and resuspended in deionized water. 25 µl of cracking solution was added, and quickly mixed by vortex. The solution was incubated at RT for 5 minutes and then visualized in gel agarose.

Plasmidic DNA preparation from *E. coli*

QIAfilter Plasmid Kits by Qiagen (Hilden, Germany): cells were grown o/n in 3 ml of LB+Ampicillin liquid media, extraction was performed following the standard protocol provided. An optimal DNA concentration is about 800 ng/ml.

Preparation of cell membranes for western blotting analysis

HEK293-T cells were plated in p100 plates of 60 cm^2 area. The day after, transfection was performed when HEK293-T were at 30% confluence. After two days from transfection, cell membranes preparation was performed for western blotting analysis. HEK293-T cells were washed one time with 5 ml PBS (4°C - non sterile). Cells were resuspended in 800 µl 10 mM Hepes supplemented with Complete 1x (protease inhibitor cocktail tablets provided by Roche) and scraped on ice. Cells were then collected into potter. Plates w ere washed with 800 µl 10 mM Hepes supplemented with Complete 1x and, again, collected into potter. Samples were pottered and centrifuged at 800 g 4°C, 10 minutes. Supernatants were transferred in tubes, centrifuged at 27000 g, 4°C for 30 minutes and pellet were resuspended into Hepes 10 mM + Complete 1x. Samples are stored at -80 °C.

SDS-PAGE and WESTERN BLOT

SDS-PAGE was performed with 6% acrylamide/bis-acrylamide gel (30%) for equal amounts of proteins in each sample; electrophoresis was performed in SDS-PAGE running buffer. Proteins were electro-transferred on nitrocellulose membrane (Biorad) in a Transfer buffer overnight at 40mA or 2 hours at 180mA. Nitrocellulose filters were saturated with 5% non-fat dry milk in TBST for 1 hour and incubated

with primary antibody in 3% non-fat dry milk o/n at 4°C. Filters were washed six times with TBST (5 minutes) and were incubated with secondary antibody again in 5% non-fat dry milk. Filters were washed again six times with TBST, the chemioluminescence reaction was performed and the signals were detected with Clarity™ Western ECL Blotting Substrates (Thermo Fisher Scientific) through ODYSSEY Fc LI-COR.

Anti-HA antibody (anti-HA) and secondary antibodies anti-mouse were both diluted 1:3000. Stripping of membrane was performed for actin detection. Membranes were incubated for 10 minutes at RT with glycine 0.1 M, then with TRIS 0.1 M for 10 minutes at RT. After that, membranes were washed 2 times with TBS-T (10-15 minutes each washing) and saturated with 5% non-fat dry milk in TBST (1 hour). Membranes were incubated with primary antibody (Anti-actin) in 3% non-fat dry milk o/n at 4°C. Membranes were washed six times with PBST for 5 minutes each and were then incubated with secondary antibody (Anti-mouse) again in 5% non-fat dry milk. Membranes were washed six times with TBS-T for 5 minutes and finally visualized using Clarity™ Western ECL Blotting Substrates through ODYSSEY Fc LI-COR.

Western blot antibodies:

Primary antibody:	Dilution	Secondary antibody (SIGMA)	Dilution
a-HA (Biolegend)	1:3000	GAM	1:3000
a-actin	1:5000	GAM	1:3000

Total Inositol Phosphate (IP) determination

The functional activity of the receptor was assessed 48h after transfection by measurement of the total inositol phosphates (IP) accumulation (*phosphatidylinositol* 3, 4, 5-trisphosphate). Indeed if the agonist binds the receptor, it becomes in active state. Confluent cells were labeled with 0.5 μCi of [*myo*-2-^{3}H] inositol (17 Ci/mmol - PerkinElmer Life and Analytical Sciences, Boston, MA) for 24 h in serum-free, inositol-free DMEM (ICN Pharmaceuticals Inc., Costa Mesa, CA) containing 20 mM HEPES, pH 7.4, and 0.5% (w/v) Albumax I. Cells were

washed and incubated with serum-free, inositol-free DMEM containing 25 mM LiCl for 10 min and then incubated with different concentrations of U46619 (Cayman Chemical, Ann Arbor, MI). After 30 min, the reaction was stopped by aspiration of the supernatant and the addition of 0.75 ml of 10 mM formic acid. After 30 min of incubation at room temperature, the solution was collected in 3 ml of 5 mM NH_4OH, pH 8 to 9, and separated with an anion exchange AG 1X-8 column, formate form, 200 to 400 mesh (Bio-Rad, Hercules, CA). Free inositol and glycerophosphoinositol were washed with 40 mM ammonium formate/formic acid buffer at pH 5, and total IP were eluted with 4 ml of a 2 M ammonium formate/formic acid buffer at pH 5. 250 ml aliquots of the total IP fraction were counted by liquid scintillation.

cAMP Assay

cAMP assay detects cAMP accumulation: it was performed 48 hours after transfection using cAMP HTRF Cis Bio, UK. In briefly, confluent cells at 37°C were washed with PBS 1x, cells are incubated for 1 hour at 37°C with 5mM EDTA in PBS. Cells then are centrifuged at 1000rpm for 5 minutes and resuspended into 1ml of DMEM. Cells are counted and plated into 96 wells plates (100 000cell/well into 100 µl/well). The day after, cells are preincubated with 100 µM BAPTA/AM for 60 min, washed with PBS and finally stimulated with different concentrations of the U46619 for 1 hour. Cells are treated with cAMP-D_2 and anti-cAMP cryptate in stimulation buffer SB (SB 1 mM IBMX into physiological buffer) for 1 hour at RT. Reaction runs at 4°C for 1 hour, follow by 1 min centrifugation at 1000 rpm. Supernatants were finally assayed immediately after collection according to the manufacturer's instructions: λ excitation=320 nm and the λ of emission detected are 620nm and 665 nm.

Live Cell Microscopy

Cells were imaged with Axiovert 200 (ZIESS) microscope equipped with a Fluoarc N HBO 103 lamp and AxioCam HRm device camera (Photometrics). Cells were imaged on 6 well plates, 32 h after transfection.

FRET Measurements

FRET spectra were generated by exciting cells at 430 nm (spectral band pass, 8 nm), and scanning emission from 450–600 nm (band pass, 4 nm) on a FluoroMax- 4 fluorometer (Horiba Scientific). For mCitrine-only measurements, cells were excited at 490 nm (band pass, 8 nm), and emission was recorded from 500–600 nm (band pass, 4 nm). Each sample, resuspended in buffer A, 37 °C, was collected within 30 min.

Live Cell FRET Ratio

OD measurements were taken for untransfected and transfected cells in buffer A; appropriate volumes of media were added to achieve an A600 nm reading of 0.3 (Bio-Rad SmartSpec Plus Spectophotometer, 3-mm path length, quartz cuvette). The corrected fluorescence emission spectra were normalized to mCerulean emission (475 nm). 'FRET ratio' was obtained by calculating ratio mCitrine (525 nm)/mCerulean (475 nm).

Isolation of human platelets and analysis of platelet aggregation.

CPD-anticoagulated human blood (Citrate Phosphate Dextrose solution: sodium citrate, dihydrate, 26.3 g/L; dextrose, monohydrate, 25.5 g/L; citric acid, anhydrous 3.27 g/L; monobasic sodium phosphate, monohydrate, 2.22 g/L) was collected following informed consent from healthy volunteers of both genders aged from18 to 60 years that had no history of CV disease. Blood was treated with 100 μM acetylsalicylic acid and 25 ml buffy coat was centrifuged at 280 *g* for 15 min at room temperature to obtain platelet-rich plasma (PRP), which was further centrifuged at 650 *g* for 10 min at room temperature. The pelleted platelets were suspended in 8 ml washing buffer (mM composition: citric acid monohydrate 39, glucose monohydrate 5, KCl 5, $CaCl_2$ 2, $MgCl_2$ x $6H_2O$ 1, NaCl 103, pH 6.5), centrifuged at 650 g for 15 min at room temperature, and finally resuspended in 15 ml of Hank's Balance Salt Solution (HBSS): $CaCl_2 \cdot 2H_2O$ 0.185 g/L; KCl 0.40 g/L; KH_2PO_4 0.06 g/L; $MgCl_2 \cdot 6H_2O$ 0.10 g/L; $MgSO_4 \cdot 7H_2O$ 0.10 g/L; NaCl 8.00 g/L; $NaHCO_3$ 0.35 g/L; Na_2HPO_4 0.048 g/L; D-glucose 1.00 g/L). The concentration was adjusted at approximately $2x10^8$ cell mL^{-1} and platelet aggregation was assessed with a Chrono-

Log aggregometer (Mascia Brunelli, Milano, Italy), using the Born Turbidimetric assay at 37°C in a 0.5 mL sample. After incubation with drug or vehicle Dimethyl sulfoxide (DMSO), maximum 0.2%, v:v) for 5 min at 37°C, platelet aggregation was induced by U46619 (0.1 μM) under continuous stirring and monitored for 5 minutes. Experiments were repeated at least in triplicate using platelets from different subjects. The anti-aggregating activity of each compound emerged by comparison with a control aggregation, recorded immediately before and after drug testing due to the inter-subject variability of the platelet response to the agonist challenge.

COX-2 inhibitory activity (lympho-monocytes)

The study of COX-2 activity was carried out in a lympho-monocytes HBSS suspension, in order to avoid compound binding to plasma-protein. Lympho-monocytes were isolated from buffy coat (diluted in NaCl 0.9% 1:1) Ficoll-Paque gradient density centrifugation (400 *g* for 30 min at 10°C); enriched cell ring was collected and twice saline washing (280 *g* for 15 min at 10°C) performed to remove the remaining suspended platelets. Soon after, a lysis buffer (NaCl 0.2% weight/volume, w/v) was added to remove the remaining erythrocytes, immediately balanced with an equal volume of equilibrating solution (NaCl 1.6% + saccharose 0.2%, w/v). Lympho-monocytes were then resuspended in HBSS and COX-2 inhibition was evaluated quantifying PGE_2 production in 24h LPS challenged preparations pretreated (30 min, 37°C) with increasing concentration of the tested compound. PGE_2 determination was carried out by EIA, according to the manufacturer's instructions, or mass spectrometry as described below.

COX-1 inhibitory activity (human platelets)

Human platelets were recovered from PRP after centrifugation at 650 *g* for 15 min at room temperature. Their concentration was adjusted at 2×10^8 cells mL^{-1}. Platelets were treated with increasing concentration of the tested compounds, and incubated at 37°C in a Dubnoff bath for 30 min. In order to stimulate the TXB_2 production by platelet degranulation, 2μM calcium ionophore A23187 was added to each test tube sample for 10 min at 37° C. Following centrifugation at 15000 *g* for 5 min, TXB_2

production was evaluated in the supernatant by mass spectrometry as described below.

Mass spectrometry determination of eicosanoids

PGE_2 and TXB_2 concentrations were evaluated by liquid chromatography-tandem mass spectrometry using the isotopic dilution of the deuterated internal standards $[d_4]PGE_2$ and $[d_4]TXB_2$. Briefly, samples were spiked with internal standards and an aliquot injected into a liquid chromatograph Agilent 1100 (Agilent Technologies, Santa Clara, CA). Chromatography was carried out using a reverse phase column (Synergi 4 µm Hydro-RP, 150x2 mm; Phenomenex, Torrance, CA). The column was eluted with a linear gradient from 25 to 100% solvent B (Methanol: Acetonitrile, 65:35) over 10 min (Solvent A: 0.05% acetic acid pH 6 with ammonia). The effluent from the High-performance liquid chromatography (HPLC) column was directly infused into an API4000 triple quadrupole operated in negative ion mode, monitoring the following specific transitions: m/z 351>271 for PGE_2, m/z 355>275 for $[d_4]PGE_2$, m/z 369>169 TXB_2 and m/z 373>173 for $[d_4]TXB_2$. Quantitation was carried out using standard curves obtained with synthetic standards (Cayman Chemical, Ann Arbor, MI).

Determination of dissociation constants

The ionization constants of compounds were determined by potentiometric titration with the GLpKa apparatus (Sirius Analytical Instruments Ltd., Forest Row, East Sussex, UK) as previously described (24). Briefly, because of the low aqueous solubility, compounds required titrations in the presence of MeOH as co-solvent: at least five different hydro-organic solutions (ionic strength adjusted to 0.15m with KCl) of the compounds (20 mL, ca. 0.5 mM in 20–60 wt% MeOH) were initially acidified to pH 1.8 with 0.5N HCl; the solutions were then titrated with standardized 0.5N KOH to pH 12.2 at 25°C under N_2.

The apparent ionization constants in the H_2O–MeOH mixtures (psKa) were obtained and aqueous pKa values were calculated by extrapolation to zero content of the co-solvent, following the Yasuda–Shedlovsky procedure (Avdeef et al., 1993).

Determination of lipophilicity descriptors

Calculated partition coefficients of compounds in neutral form (clog P) were obtained by using Bio-Loom for Windows v.1.5 (BioByte Corp. Claremont, CA, USA).

The distribution coefficient at pH 7.4 (log $D^{7.4}$) of the compounds between *n*-octanol and water was experimentally obtained by shake-flask technique at room temperature. In the shake-flask experiments phosphate 50 mM buffer with ionic strength adjusted to 0.15 M with KCl, was used as aqueous phase; the organic (*n*-octanol) and aqueous phase were mutually saturated by shaking for 4 h. The compounds were solubilised in the buffered aqueous phase at a concentration of about 0.1 mM and an appropriate amount of *n*-octanol was added. The two phases were shaken for about 20 min, by which time the partitioning equilibrium of solutes is reached, and then centrifuged (1100 g, 10 min). The concentration of the solutes was measured in the aqueous phase by HPLC. Each log D value is an average of at least six measurements. All the experiments were performed avoiding exposure to light.

Solubility assessment in phosphate buffered saline (PBS) and simulated gastric fluid (SGF)

The solubility of compounds **7**, **18**, **20**, **32** and lumiracoxib was studied in simulated gastric fluid (SGF-without pepsin) and phosphate buffered saline (PBS) 0.05 M to evaluate the solubility of compounds in acid (pH 1.5 for SGF) and neutral conditions (7.4 pH for PBS) to simulate the gastric and the body fluid environment respectively (Table 5) (Kerns et al., 2008).

Stock solutions of compounds lumiracoxib, **7**, **18**, **20** and **32** (10 mM) were prepared in DMSO. Eight point calibration standards (1, 5, 10, 20, 50, 100, 200 and 500 μM) were prepared from each 10 mM stock solution by dilution in HPLC mobile phase and analyzed by HPLC. 100 μL of each test compound (stock solution 10 mM in DMSO) were added to 1900 μL of PBS and SGF in glass tubes in triplicate and shaken for 90 min at 100 rpm at room temperature. The samples were filtered using 0.45 μL PTFE filters and analysed by HPLC.

HPLC analysis were performed with a HP 1100 chromatograph system (Agilent Technologies, Palo Alto, CA, USA) equipped with a quaternary pump (model G1311A), a membrane degasser (G1379A), a diode-array detector (DAD) (model G1315B) integrated in the HP1100 system. Data analysis was processed using a HP ChemStation system (Agilent Technologies). The analytical column was a Tracer Excel C18 (250×4.6 mm, 5 μm; Teknokroma). The mobile phase consisting of acetonitrile/HCOOH 0.1% 70/30 (v/v) at flow-rate = 1.0 mL/min. The injection volume was 20 μL (Rheodyne, Cotati, CA). The column effluent was monitored at 254 nm and 280 nm referenced against a 800 nm wavelength. Quantitation of compounds was done using calibration curves of compounds; the linearity of the calibration curves was determined in a concentration range of 1-500 μM ($r^2 > 0.99$).

Stability in human serum

A solution of each compound (10 mM) in DMSO was added to human serum (from human male AB plasma, USA origin, sterile-filtered, Sigma-Aldrich) preheated at 37°C; the final concentration of the compound was 100 μM. Resulting solution were incubated at 37 ± 0.5°C and at appropriate time intervals (2, 6, 24 hours) 300 μL of the reaction mixture was withdrawn and added to 300 μL of acetonitrile containing 0.1% trifluoroacetic acid in order to deproteinize the proteins. Sample was sonicated, vortexed and then centrifuged for 10 min at 2150 g, The clear supernatant was filtered by 0.45 μm PTFE filters (Alltech) and analyzed by RP-HPLC with method previously described for solubility assessment.

Statistical analysis

pA_2 were calculated accordingly to the following set of equations as described in Prism 5 (GraphPad Software Inc., San Diego, CA):

1) Agonist response = Bottom + (Top-Bottom)/(1+10^((LogEC$_{50}$-X)*HillSlope))

2) Antagonist response = Bottom+(Top-Bottom)/(1+(Antag/FixedAg)^HillSlope)

3) Antag = (10^LogEC$_{50}$)*(1+((10^X)/(10^(-1*pA$_2$)))^SchildSlope)

Where X is the Log concentration of the agonist, Bottom is the response when X = 0, Top is the response for an infinite concentration of X, EC_{50} is the concentrations of the agonist that produce half of the response, Hill Slope is the slopes of the curves,

FixedAg is the initial fixed concentration of the agonist used in the determination of the antagonist inhibition curve. The concentration-response curves of platelet aggregation were analysed by Prism-5 software utilizing the four-parameter logistic model as described in the ALLFIT program (De Lean et al., 1978). Parameter errors are all expressed in percentage coefficient of variation (% CV) and calculated by simultaneous analysing at least three different independent experiments performed in duplicate or triplicate. $P<0.05$ was set as the statistical level of significance. All curves shown are computer generated.

References

Acharya S and Karnik SS (1996) Modulation of GDP release from transducin by the conserved Glu134-Arg135 sequence in rhodopsin. *J Biol Chem* **271**(41): 25406-25411.

Acquaviva A, Vecchio D, Arezzini B, Comporti M and Gardi C (2013) Signaling pathways involved in isoprostane-mediated fibrogenic effects in rat hepatic stellate cells. *Free Radic Biol Med* **65**: 201-207.

Ambrosio M, Fanelli F, Brocchetti S, Raimondi F, Mauri M, Rovati GE and Capra V (2010) Superactive mutants of thromboxane prostanoid receptor: functional and computational analysis of an active form alternative to constitutively active mutants. *Cell Mol Life Sci* **67**(17): 2979-2989.

Ariëns EJ (1954) Affinity and intrinsic activity in the theory of competitive inhibition. *Arch Internat Pharmacodyn Therap* **99**: 32-49.

Armstrong RA and Wilson NH (1995) Aspects of the thromboxane receptor system. *Gen Pharmacol* **26**(3): 463-472.

Audet M and Bouvier M (2012) Restructuring g-protein- coupled receptor activation. *Cell* **151**(1): 14-23.

Audoly LP, Rocca B, Fabre JE, Koller BH, Thomas D, Loeb AL, Coffman TM and FitzGerald GA (2000) Cardiovascular responses to the isoprostanes iPF(2alpha)-III and iPE(2)-III are mediated via the thromboxane A(2) receptor in vivo. *Circulation* **101**(24): 2833-2840.

Avdeef A, Comer JEA and Thomson SJ (1993) pH-Metric log P. 3. Glass electrode calibration in methanol-water, applied to pKa determination of water-insoluble substances. *Anal Chem* **65**(1): 42-49.

Ballatore C, Soper JH, Piscitelli F, James M, Huang L, Atasoylu O, Huryn DM, Trojanowski JQ, Lee VM, Brunden KR and Smith AB (2011) Cyclopentane-1,3-dione: a novel isostere for the carboxylic acid functional group. Application to the design of potent thromboxane (A2) receptor antagonists. *J Med Chem* **54**(19): 6969-6983.

Ballesteros JA, Jensen AD, Liapakis G, Rasmussen SG, Shi L, Gether U and Javitch JA (2001) Activation of the beta 2-adrenergic receptor involves disruption of an ionic lock between the cytoplasmic ends of transmembrane segments 3 and 6. *J Biol Chem* **276**(31): 29171-29177.

Barak LS, Oakley RH, Laporte SA and Caron MG (2001) Constitutive arrestin-mediated desensitization of a human vasopressin receptor mutant associated with nephrogenic diabetes insipidus. *Proc Natl Acad Sci U S A* **98**(1): 93-98.

Bartzatt R (2012) Anti-inflammatory drugs and prediction of new structures by comparative analysis. *Antiinflamm Antiallergy Agents Med Chem* **11**(2): 151-160.

Bartzatt R (2014) Drug analogs of COX-2 selective inhibitors lumiracoxib and valdecoxib derived from in silico search and optimization. *Antiinflamm Antiallergy Agents Med Chem* **13**(1): 17-28.

Bauer J, Ripperger A, Frantz S, Ergun S, Schwedhelm E and Benndorf RA (2014) Pathophysiology of isoprostanes in the cardiovascular system: implications of isoprostane-mediated thromboxane A2 receptor activation. *Br J Pharmacol* **171**(13): 3115-3131.

Benndorf RA, Schwedhelm E, Gnann A, Taheri R, Kom G, Didie M, Steenpass A, Ergun S and Boger RH (2008) Isoprostanes inhibit vascular endothelial growth factor-induced endothelial cell migration, tube formation, and cardiac vessel sprouting in vitro, as well as angiogenesis in vivo via activation of the thromboxane A(2) receptor: a potential link between oxidative stress and impaired angiogenesis. *Circ Res* **103**(9): 1037-1046.

Bertinaria M, Shaikh MA, Buccellati C, Cena C, Rolando B, Lazzarato L, Fruttero R, Gasco A, Hoxha M, Capra V, Sala A and Rovati GE (2012) Designing Multitarget Anti-inflammatory Agents: Chemical Modulation of the Lumiracoxib Structure toward Dual Thromboxane Antagonists-COX-2 Inhibitors. *ChemMedChem* **7**(9): 1647-1660.

Bhattacharya S and Vaidehi N (2014) Differences in allosteric communication pipelines in the inactive and active states of a GPCR. *Biophys J* **107**(2): 422-434.

Blobaum AL and Marnett LJ (2007) Molecular determinants for the selective inhibition of cyclooxygenase-2 by lumiracoxib. *J Biol Chem* **282**(22): 16379-16390.

Bockenhauer S, Furstenberg A, Yao XJ, Kobilka BK and Moerner WE (2011) Conformational dynamics of single G protein-coupled receptors in solution. *J Phys Chem B* **115**(45): 13328-13338.

Bombardier C, Laine L, Reicin A, Shapiro D, Burgos-Vargas R, Davis B, Day R, Ferraz MB, Hawkey CJ, Hochberg MC, Kvien TK, Schnitzer TJ and Group VS (2000) Comparison of upper gastrointestinal toxicity of rofecoxib and naproxen in patients with rheumatoid arthritis. VIGOR Study Group. *N Engl J Med* **343**(21): 1520-1528, 1522 p following 1528.

Bousser MG, Amarenco P, Chamorro A, Fisher M, Ford I, Fox KM, Hennerici MG, Mattle HP, Rothwell PM, de Cordoue A, Fratacci MD and Investigators PS (2011) Terutroban versus aspirin in patients with cerebral ischaemic events (PERFORM): a randomised, double-blind, parallel-group trial. *Lancet* **377**(9782): 2013-2022.

Breyer MD and Breyer RM (2000) Prostaglandin receptors: their role in regulating renal function. *Curr Opin Nephrol Hypertens* **9**(1): 23-29.

Brink C, Dahlen SE, Drazen J, Evans JF, Hay DW, Nicosia S, Serhan CN, Shimizu T and Yokomizo T (2003) International Union of Pharmacology XXXVII. Nomenclature for leukotriene and lipoxin receptors. *Pharmacol Rev* **55**(1): 195-227.

Bruijnzeel PL, Warringa RA, Kok PT and Kreukniet J (1990) Inhibition of neutrophil and eosinophil induced chemotaxis by nedocromil sodium and sodium cromoglycate. *Br J Pharmacol* **99**(4): 798-802.

Burstein ES, Spalding TA and Brann MR (1998) The second intracellular loop of the m5 muscarinic receptor is the switch which enables G-protein coupling. *J Biol Chem* **273**(38): 24322-24327.

Campbell WB and Falck JR (2007) Arachidonic acid metabolites as endothelium-derived hyperpolarizing factors. *Hypertension* **49**(3): 590-596.

Cannon GW and Breedveld FC (2001) Efficacy of cyclooxygenase-2-specific inhibitors. *Am J Med* **110 Suppl 3A**: 6S-12S.

Capra V, Busnelli M, Perenna A, Ambrosio M, Accomazzo MR, Gales C, Chini B and Rovati GE (2013) Full and partial agonists of thromboxane prostanoid receptor unveil fine tuning of receptor superactive conformation and G protein activation. *PLoS One* **8**(3): e60475.

Capra V, Mauri M, Guzzi F, Busnelli M, Accomazzo MR, Gaussem P, Nisar SP, Mundell SJ, Parenti M and Rovati GE (2016) Impaired thromboxane receptor dimerization reduces signaling efficiency: A potential mechanism for reduced platelet function in vivo. *Biochem Pharmacol*.

Capra V, Veltri A, Foglia C, Crimaldi L, Habib A, Parenti M and Rovati GE (2004) Mutational analysis of the highly conserved ERY motif of the thromboxane A2 receptor: alternative role in G protein-coupled receptor signaling. *Mol Pharmacol* **66**(4): 880-889.

Carroll MA, Doumad AB, Li J, Cheng MK, Falck JR and McGiff JC (2006) Adenosine2A receptor vasodilation of rat preglomerular microvessels is mediated by EETs that activate the cAMP/PKA pathway. *Am J Physiol Renal Physiol* **291**(1): F155-161.

Catella-Lawson F, Reilly MP, Kapoor SC, Cucchiara AJ, DeMarco S, Tournier B, Vyas SN and FitzGerald GA (2001) Cyclooxygenase inhibitors and the antiplatelet effects of aspirin. *N Engl J Med* **345**(25): 1809-1817.

Cayatte AJ, Du Y, Oliver-Krasinski J, Lavielle G, Verbeuren TJ and Cohen RA (2000) The thromboxane receptor antagonist S18886 but not aspirin inhibits atherogenesis in apo E-deficient mice: evidence that eicosanoids other than thromboxane contribute to atherosclerosis. *Arterioscler Thromb Vasc Biol* **20**(7): 1724-1728.

Chiamvimonvat N, Ho CM, Tsai HJ and Hammock BD (2007) The soluble epoxide hydrolase as a pharmaceutical target for hypertension. *J Cardiovasc Pharmacol* **50**(3): 225-237.

Chung DA, Wade SM, Fowler CB, Woods DD, Abada PB, Mosberg HI and Neubig RR (2002a) Mutagenesis and peptide analysis of the DRY motif in the alpha2A adrenergic receptor: evidence for alternate mechanisms in G protein-coupled receptors. *Biochem Biophys Res Commun* **293**(4): 1233-1241.

Chung DA, Wade SM, Fowler CB, Woods DD, Abada PB, Mosberg HI and Neubig RR (2002b) Mutagenesis and peptide analysis of the DRY motif in the alpha2A adrenergic receptor: evidence for alternate mechanisms in G protein-coupled receptors. *Biochem Biophys Res Commun* **293**(4): 1233-1241.

Clark AJ (1937) General pharmacology, in *Handbuch der experimentellen Parmakologie*, Springer-Verlag, Berlin.

Coleman RA, Grix SP, Head SA, Louttit JB, Mallett A and Sheldrick RL (1994) A novel inhibitory prostanoid receptor in piglet saphenous vein. *Prostaglandins* **47**(2): 151-168.

Conklin BR, Farfel Z, Lustig KD, Julius D and Bourne HR (1993) Substitution of three amino acids switches receptor specificity of Gq alpha to that of Gi alpha. *Nature* **363**(6426): 274-276.

Conklin BR, Herzmark P, Ishida S, Voyno-Yasenetskaya TA, Sun Y, Farfel Z and Bourne HR (1996) Carboxyl-terminal mutations of Gq alpha and Gs alpha that alter the fidelity of receptor activation. *Mol Pharmacol* **50**(4): 885-890.

Corey EJ, Niwa H, Falck JR, Mioskowski C, Arai Y and Marfat A (1980) Recent studies on the chemical synthesis of eicosanoids. *Adv Prostaglandin Thromboxane Res* **6**: 19-25.

Costa T and Herz A (1989) Antagonists with negative intrinsic activity at delta opioid receptors coupled to GTP-binding proteins. *Proc Natl Acad Sci U S A* **86**(19): 7321-7325.

Costa T, Ogino Y, Munson PJ, Onaran HO and Rodbard D (1992) Drug efficacy at guanine nucleotide-binding regulatory protein-linked receptors: thermodynamic interpretation of negative antagonism and of receptor activity in the absence of ligand. *Mol Pharmacol* **41**(3): 549-560.

Cotecchia S, Bjorklof K, Rossier O, Stanasila L, Greasley P and Fanelli F (2002) The alpha1b-adrenergic receptor subtype: molecular properties and physiological implications. *J Recept Signal Transduct Res* **22**(1-4): 1-16.

Csoma Z, Kharitonov SA, Balint B, Bush A, Wilson NM and Barnes PJ (2002) Increased leukotrienes in exhaled breath condensate in childhood asthma. *Am J Respir Crit Care Med* **166**(10): 1345-1349.

Daniel TO, Liu H, Morrow JD, Crews BC and Marnett LJ (1999) Thromboxane A2 is a mediator of cyclooxygenase-2-dependent endothelial migration and angiogenesis. *Cancer Res* **59**(18): 4574-4577.

De Lean A, Munson PJ and Rodbard D (1978) Simultaneous analysis of families of sigmoidal curves: application to bioassay, radioligand assay, and physiological dose-response curves. *Am J Physiol* **235**: E97-E102.

De Lean A, Stadel JM and Lefkowitz RJ (1980a) A ternary complex model explains the agonist-specific binding properties of the adenylate cyclase-coupled b-adrenergic receptor. *J Biol Chem* **255**: 7108-7117.

De Lean A, Stadel JM and Lefkowitz RJ (1980b) A ternary complex model explains the agonist-specific binding properties of the adenylate cyclase-coupled beta-adrenergic receptor. *J Biol Chem* **255**(15): 7108-7117.

Del Castillo J and Katz B (1957) Interaction at end-plate receptors between different choline derivatives. *Proc R Soc Lond B Biol Sci* **146**(924): 369-381.

Deupi X and Kobilka BK (2010) Energy landscapes as a tool to integrate GPCR structure, dynamics, and function. *Physiology (Bethesda)* **25**(5): 293-303.

Devillier P and Bessard G (1997) Thromboxane A2 and related prostaglandins in airways. *Fundam Clin Pharmacol* **11**(1): 2-18.

DeWitt DL (1999) Cox-2-selective inhibitors: the new super aspirins. *Mol Pharmacol* **55**(4): 625-631.

Egan KM, Lawson JA, Fries S, Koller B, Rader DJ, Smyth EM and Fitzgerald GA (2004) COX-2-derived prostacyclin confers atheroprotection on female mice. *Science* **306**(5703): 1954-1957.

Egan KM, Wang M, Fries S, Lucitt MB, Zukas AM, Pure E, Lawson JA and FitzGerald GA (2005) Cyclooxygenases, thromboxane, and atherosclerosis: plaque destabilization by cyclooxygenase-2 inhibition combined with thromboxane receptor antagonism. *Circulation* **111**(3): 334-342.

Fanelli F, Mauri M, Capra V, Raimondi F, Guzzi F, Ambrosio M, Rovati GE and Parenti M (2011) Light on the structure of thromboxane A(2) receptor heterodimers. *Cell Mol Life Sci* **68**(18): 3109-3120.

Fiessinger JN, Bounameaux H, Cairols MA, Clement DL, Coccheri S, Fletcher JP, Hoffmann U, Turpie AG and investigators T (2010) Thromboxane

Antagonism with terutroban in Peripheral Arterial Disease: the TAIPAD study. *J Thromb Haemost* **8**(11): 2369-2376.

Figueroa DJ, Breyer RM, Defoe SK, Kargman S, Daugherty BL, Waldburger K, Liu Q, Clements M, Zeng Z, O'Neill GP, Jones TR, Lynch KR, Austin CP and Evans JF (2001) Expression of the cysteinyl leukotriene 1 receptor in normal human lung and peripheral blood leukocytes. *Am J Respir Crit Care Med* **163**(1): 226-233.

FitzGerald GA (1991) Mechanisms of platelet activation: thromboxane A2 as an amplifying signal for other agonists. *Am J Cardiol* **68**(7): 11B-15B.

Fitzgerald GA (2004) Coxibs and cardiovascular disease. *N Engl J Med* **351**(17): 1709-1711.

FitzGerald GA (2007) COX-2 in play at the AHA and the FDA. *Trends Pharmacol Sci* **28**(7): 303-307.

FitzGerald GA and Patrono C (2001) The coxibs, selective inhibitors of cyclooxygenase-2. *N Engl J Med* **345**(6): 433-442.

Fredriksson R, Lagerstrom MC, Lundin LG and Schioth HB (2003) The G-protein-coupled receptors in the human genome form five main families. Phylogenetic analysis, paralogon groups, and fingerprints. *Mol Pharmacol* **63**(6): 1256-1272.

Funk CD (2001) Prostaglandins and leukotrienes: advances in eicosanoid biology. *Science* **294**(5548): 1871-1875.

Gaussem P, Reny JL, Thalamas C, Chatelain N, Kroumova M, Jude B, Boneu B and Fiessinger JN (2005) The specific thromboxane receptor antagonist S18886: pharmacokinetic and pharmacodynamic studies. *J Thromb Haemost* **3**(7): 1437-1445.

Geoffroy J, Benzoni D and Sassard J (1989) Antihypertensive effect of thromboxane A2 receptor blockade in genetically hypertensive rats of the Lyon strain. *J Hypertens Suppl* **7**(6): S272-273.

Gross GJ, Gauthier KM, Moore J, Falck JR, Hammock BD, Campbell WB and Nithipatikom K (2008) Effects of the selective EET antagonist, 14,15-EEZE, on cardioprotection produced by exogenous or endogenous EETs in the canine heart. *Am J Physiol Heart Circ Physiol* **294**(6): H2838-2844.

Grosser T, Fries S and FitzGerald GA (2006) Biological basis for the cardiovascular consequences of COX-2 inhibition: therapeutic challenges and opportunities. *J Clin Invest* **116**(1): 4-15.

Habib A, FitzGerald GA and Maclouf J (1999) Phosphorylation of the thromboxane receptor alpha, the predominant isoform expressed in human platelets. *J Biol Chem* **274**(5): 2645-2651.

Hamm HE, Deretic D, Arendt A, Hargrave PA, Koenig B and Hofmann KP (1988) Site of G protein binding to rhodopsin mapped with synthetic peptides from the alpha subunit. *Science* **241**(4867): 832-835.

Hao CM and Breyer MD (2007) Physiologic and pathophysiologic roles of lipid mediators in the kidney. *Kidney Int* **71**(11): 1105-1115.

Hartley P (1909) On the nature of the fat contained in the liver, kidney and heart: Part II. *J Physiol* **38**(5): 353-374.

Haurand M and Ullrich V (1985) Isolation and characterization of thromboxane synthase from human platelets as a cytochrome P-450 enzyme. *J Biol Chem* **260**(28): 15059-15067.

Hay DW, Torphy TJ and Undem BJ (1995) Cysteinyl leukotrienes in asthma: old mediators up to new tricks. *Trends Pharmacol Sci* **16**(9): 304-309.

Heise CE, O'Dowd BF, Figueroa DJ, Sawyer N, Nguyen T, Im DS, Stocco R, Bellefeuille JN, Abramovitz M, Cheng R, Williams DL, Jr., Zeng Z, Liu Q, Ma L, Clements MK, Coulombe N, Liu Y, Austin CP, George SR, O'Neill GP, Metters KM, Lynch KR and Evans JF (2000) Characterization of the human cysteinyl leukotriene 2 receptor. *J Biol Chem* **275**(39): 30531-30536.

Higashi N, Taniguchi M, Mita H, Ishii T and Akiyama K (2003) Nasal blockage and urinary leukotriene E4 concentration in patients with seasonal allergic rhinitis. *Allergy* **58**(6): 476-480.

Hirai H, Tanaka K, Yoshie O, Ogawa K, Kenmotsu K, Takamori Y, Ichimasa M, Sugamura K, Nakamura M, Takano S and Nagata K (2001) Prostaglandin D2 selectively induces chemotaxis in T helper type 2 cells, eosinophils, and basophils via seven-transmembrane receptor CRTH2. *J Exp Med* **193**(2): 255-261.

Hirata M, Hayashi Y, Ushikubi F, Yokota Y, Kageyama R, Nakanishi S and Narumiya S (1991) Cloning and expression of cDNA for a human thromboxane A2 receptor. *Nature* **349**(6310): 617-620.

Howard PA and Delafontaine P (2004) Nonsteroidal anti-Inflammatory drugs and cardiovascular risk. *J Am Coll Cardiol* **43**(4): 519-525.

Hoxha M, Buccellati C, Capra V, Garella D, Cena C, Rolando B, Fruttero R, Carnevali S, Sala A, Rovati GE and Bertinaria M (2016) In vitro pharmacological evaluation of multitarget agents for thromboxane prostanoid receptor antagonism and COX-2 inhibition. *Pharmacol Res* **103**: 132-143.

Huang H, Morisseau C, Wang J, Yang T, Falck JR, Hammock BD and Wang MH (2007) Increasing or stabilizing renal epoxyeicosatrienoic acid production attenuates abnormal renal function and hypertension in obese rats. *Am J Physiol Renal Physiol* **293**(1): F342-349.

Huber J, Bochkov VN, Binder BR and Leitinger N (2003) The isoprostane 8-iso-PGE2 stimulates endothelial cells to bind monocytes via cyclic AMP- and p38 MAP kinase-dependent signaling pathways. *Antioxid Redox Signal* **5**(2): 163-169.

Iizuka Y, Yokomizo T, Terawaki K, Komine M, Tamaki K and Shimizu T (2005) Characterization of a mouse second leukotriene B4 receptor, mBLT2: BLT2-dependent ERK activation and cell migration of primary mouse keratinocytes. *J Biol Chem* **280**(26): 24816-24823.

Imig JD (2005) Epoxide hydrolase and epoxygenase metabolites as therapeutic targets for renal diseases. *Am J Physiol Renal Physiol* **289**(3): F496-503.

Kamohara M, Takasaki J, Matsumoto M, Matsumoto S, Saito T, Soga T, Matsushime H and Furuichi K (2001) Functional characterization of cysteinyl leukotriene CysLT(2) receptor on human coronary artery smooth muscle cells. *Biochem Biophys Res Commun* **287**(5): 1088-1092.

Kamohara M, Takasaki J, Matsumoto M, Saito T, Ohishi T, Ishii H and Furuichi K (2000) Molecular cloning and characterization of another leukotriene B4 receptor. *J Biol Chem* **275**(35): 27000-27004.

Kawabe J, Ushikubi F and Hasebe N (2010) Prostacyclin in vascular diseases. - Recent insights and future perspectives. *Circ J* **74**(5): 836-843.

Kenakin T (2004) Principles: receptor theory in pharmacology. *Trends Pharmacol Sci* **25**(4): 186-192.

Kenakin TP and Morgan PH (1989) Theoretical effects of single and multiple transducer receptor coupling proteins on estimates of the relative potency of agonists. *Mol Pharmacol* **35**(2): 214-222.

Kennedy I, Coleman RA, Humphrey PP, Levy GP and Lumley P (1982) Studies on the characterisation of prostanoid receptors: a proposed classification. *Prostaglandins* **24**(5): 667-689.

Kerns EH, Di L and Carter GT (2008) In vitro solubility assays in drug discovery. *Curr Drug Metab* **9**(9): 879-885.

Kinsella BT, O'Mahony DJ and Fitzgerald GA (1997) The human thromboxane A2 receptor alpha isoform (TP alpha) functionally couples to the G proteins Gq and G11 in vivo and is activated by the isoprostane 8-epi prostaglandin F2 alpha. *J Pharmacol Exp Ther* **281**(2): 957-964.

Kjelsberg MA, Cotecchia S, Ostrowski J, Caron MG and Lefkowitz RJ (1992) Constitutive activation of the alpha 1B-adrenergic receptor by all amino acid substitutions at a single site. Evidence for a region which constrains receptor activation. *J Biol Chem* **267**(3): 1430-1433.

Kobayashi T, Tahara Y, Matsumoto M, Iguchi M, Sano H, Murayama T, Arai H, Oida H, Yurugi-Kobayashi T, Yamashita JK, Katagiri H, Majima M, Yokode M, Kita T and Narumiya S (2004) Roles of thromboxane A(2) and prostacyclin in the development of atherosclerosis in apoE-deficient mice. *J Clin Invest* **114**(6): 784-794.

Konig P, Krasteva G, Tag C, Konig IR, Arens C and Kummer W (2006) FRET-CLSM and double-labeling indirect immunofluorescence to detect close association of proteins in tissue sections. *Lab Invest* **86**(8): 853-864.

Kromer BM and Tippins JR (1996) Coronary artery constriction by the isoprostane 8-epi prostaglandin F2 alpha. *Br J Pharmacol* **119**(6): 1276-1280.

Lagerstrom MC and Schioth HB (2008) Structural diversity of G protein-coupled receptors and significance for drug discovery. *Nat Rev Drug Discov* **7**(4): 339-357.

Larsen BT, Campbell WB and Gutterman DD (2007) Beyond vasodilatation: non-vasomotor roles of epoxyeicosatrienoic acids in the cardiovascular system. *Trends Pharmacol Sci* **28**(1): 32-38.

Larsen BT, Gutterman DD, Sato A, Toyama K, Campbell WB, Zeldin DC, Manthati VL, Falck JR and Miura H (2008) Hydrogen peroxide inhibits cytochrome p450 epoxygenases: interaction between two endothelium-derived hyperpolarizing factors. *Circ Res* **102**(1): 59-67.

Leff P, Dougall IG, Harper DH and Dainty IA (1990) Errors in agonist affinity estimation: do they and should they occur in isolated tissue experiments? *Trends Pharmacol Sci* **11**(2): 64-67.

Lefkowitz RJ (2007a) Seven transmembrane receptors: a brief personal retrospective. *Biochim Biophys Acta* **1768**(4): 748-755.

Lefkowitz RJ (2007b) Seven transmembrane receptors: something old, something new. *Acta Physiol (Oxf)* **190**(1): 9-19.

Lefkowitz RJ, Cotecchia S, Samama P and Costa T (1993) Constitutive activity of receptors coupled to guanine nucleotide regulatory proteins. *Trends in Pharmacological Sciences* **14**(8): 303-307.

Leitinger N, Huber J, Rizza C, Mechtcheriakova D, Bochkov V, Koshelnick Y, Berliner JA and Binder BR (2001) The isoprostane 8-iso-PGF(2alpha) stimulates endothelial cells to bind monocytes: differences from thromboxane-mediated endothelial activation. *FASEB J* **15**(7): 1254-1256.

Lesault PF, Boyer L, Pelle G, Covali-Noroc A, Rideau D, Akakpo S, Teiger E, Dubois-Rande JL and Adnot S (2011) Daily administration of the TP receptor antagonist terutroban improved endothelial function in high-cardiovascular-risk patients with atherosclerosis. *Br J Clin Pharmacol* **71**(6): 844-851.

Liel N, Nathan I, Yermiyahu T, Zolotov Z, Lieberman JR, Dvilansky A and Halushka PV (1993) Increased platelet thromboxane A2/prostaglandin H2 receptors in patients with pregnancy induced hypertension. *Thromb Res* **70**(3): 205-210.

Liu M and Yokomizo T (2015) The role of leukotrienes in allergic diseases. *Allergol Int* **64**(1): 17-26.

Lu T, Katakam PV, VanRollins M, Weintraub NL, Spector AA and Lee HC (2001) Dihydroxyeicosatrienoic acids are potent activators of Ca(2+)-activated K(+) channels in isolated rat coronary arterial myocytes. *J Physiol* **534**(Pt 3): 651-667.

Lu ZL, Curtis CA, Jones PG, Pavia J and Hulme EC (1997) The role of the aspartate-arginine-tyrosine triad in the m1 muscarinic receptor: mutations of aspartate 122 and tyrosine 124 decrease receptor expression but do not abolish signaling. *Mol Pharmacol* **51**(2): 234-241.

Lynch KR, O'Neill GP, Liu Q, Im DS, Sawyer N, Metters KM, Coulombe N, Abramovitz M, Figueroa DJ, Zeng Z, Connolly BM, Bai C, Austin CP, Chateauneuf A, Stocco R, Greig GM, Kargman S, Hooks SB, Hosfield E, Williams DL, Jr., Ford-Hutchinson AW, Caskey CT and Evans JF (1999) Characterization of the human cysteinyl leukotriene CysLT1 receptor. *Nature* **399**(6738): 789-793.

Maclouf J, Folco G and Patrono C (1998) Eicosanoids and iso-eicosanoids: constitutive, inducible and transcellular biosynthesis in vascular disease. *Thromb Haemost* **79**(4): 691-705.

Malik RU, Ritt M, DeVree BT, Neubig RR, Sunahara RK and Sivaramakrishnan S (2013) Detection of G protein-selective G protein-coupled receptor (GPCR) conformations in live cells. *J Biol Chem* **288**(24): 17167-17178.

Martin C, Uhlig S and Ullrich V (2001) Cytokine-induced bronchoconstriction in precision-cut lung slices is dependent upon cyclooxygenase-2 and thromboxane receptor activation. *Am J Respir Cell Mol Biol* **24**(2): 139-145.

Masso Gonzalez EL, Patrignani P, Tacconelli S and Garcia Rodriguez LA (2010) Variability among nonsteroidal antiinflammatory drugs in risk of upper gastrointestinal bleeding. *Arthritis Rheum* **62**(6): 1592-1601.

McAdam BF, Catella-Lawson F, Mardini IA, Kapoor S, Lawson JA and FitzGerald GA (1999) Systemic biosynthesis of prostacyclin by cyclooxygenase (COX)-2: the human pharmacology of a selective inhibitor of COX-2. *Proc Natl Acad Sci U S A* **96**(1): 272-277.

Miggin SM and Kinsella BT (1998) Expression and tissue distribution of the mRNAs encoding the human thromboxane A2 receptor (TP) alpha and beta isoforms. *Biochim Biophys Acta* **1425**(3): 543-559.

Minuz P, Andrioli G, Degan M, Gaino S, Ortolani R, Tommasoli R, Zuliani V, Lechi A and Lechi C (1998) The F2-isoprostane 8-epiprostaglandin F2alpha increases platelet adhesion and reduces the antiadhesive and antiaggregatory effects of NO. *Arterioscler Thromb Vasc Biol* **18**(8): 1248-1256.

Moro O, Lameh J, Hogger P and Sadee W (1993) Hydrophobic amino acid in the i2 loop plays a key role in receptor-G protein coupling. *J Biol Chem* **268**(30): 22273-22276.

Morrow JD, Awad JA, Boss HJ, Blair IA and Roberts LJ, 2nd (1992) Non-cyclooxygenase-derived prostanoids (F2-isoprostanes) are formed in situ on phospholipids. *Proc Natl Acad Sci U S A* **89**(22): 10721-10725.

Morrow JD, Harris TM and Roberts LJ, 2nd (1990a) Noncyclooxygenase oxidative formation of a series of novel prostaglandins: analytical ramifications for measurement of eicosanoids. *Anal Biochem* **184**(1): 1-10.

Morrow JD, Hill KE, Burk RF, Nammour TM, Badr KF and Roberts LJ, 2nd (1990b) A series of prostaglandin F2-like compounds are produced in vivo in humans by a non-cyclooxygenase, free radical-catalyzed mechanism. *Proc Natl Acad Sci U S A* **87**(23): 9383-9387.

Morrow JD, Minton TA, Mukundan CR, Campbell MD, Zackert WE, Daniel VC, Badr KF, Blair IA and Roberts LJ, 2nd (1994) Free radical-induced generation of isoprostanes in vivo. Evidence for the formation of D-ring and E-ring isoprostanes. *J Biol Chem* **269**(6): 4317-4326.

Nakahata N (2008) Thromboxane A2: physiology/pathophysiology, cellular signal transduction and pharmacology. *Pharmacol Ther* **118**(1): 18-35.

Narumiya S (2007) Physiology and pathophysiology of prostanoid receptors. *Proc Jpn Acad Ser B Phys Biol Sci* **83**(9-10): 296-319.

Narumiya S, Sugimoto Y and Ushikubi F (1999) Prostanoid receptors: structures, properties, and functions. *Physiol Rev* **79**(4): 1193-1226.

Needleman P, Moncada S, Bunting S, Vane JR, Hamberg M and Samuelsson B (1976) Identification of an enzyme in platelet microsomes which generates thromboxane A2 from prostaglandin endoperoxides. *Nature* **261**(5561): 558-560.

Ng VY, Morisseau C, Falck JR, Hammock BD and Kroetz DL (2006) Inhibition of smooth muscle proliferation by urea-based alkanoic acids via peroxisome proliferator-activated receptor alpha-dependent repression of cyclin D1. *Arterioscler Thromb Vasc Biol* **26**(11): 2462-2468.

Nothacker HP, Wang Z, Zhu Y, Reinscheid RK, Lin SH and Civelli O (2000) Molecular cloning and characterization of a second human cysteinyl leukotriene receptor: discovery of a subtype selective agonist. *Mol Pharmacol* **58**(6): 1601-1608.

Nusing RM, Hirata M, Kakizuka A, Eki T, Ozawa K and Narumiya S (1993) Characterization and chromosomal mapping of the human thromboxane A2 receptor gene. *J Biol Chem* **268**(33): 25253-25259.

Ohnishi H, Miyahara N, Dakhama A, Takeda K, Mathis S, Haribabu B and Gelfand EW (2008) Corticosteroids enhance CD8+ T cell-mediated airway hyperresponsiveness and allergic inflammation by upregulating leukotriene B4 receptor 1. *J Allergy Clin Immunol* **121**(4): 864-871 e864.

Oldham WM and Hamm HE (2008) Heterotrimeric G protein activation by G-protein-coupled receptors. *Nat Rev Mol Cell Biol* **9**(1): 60-71.

Pal B and Hossain MA (1985) Non-steroidal anti-inflammatory drugs and adverse renal effects. *Ann Rheum Dis* **44**(3): 212-213.

Palczewski K, Kumasaka T, Hori T, Behnke CA, Motoshima H, Fox BA, Le Trong I, Teller DC, Okada T, Stenkamp RE, Yamamoto M and Miyano M (2000) Crystal structure of rhodopsin: A G protein-coupled receptor. *Science* **289**(5480): 739-745.

Patrono C, Coller B, Dalen JE, FitzGerald GA, Fuster V, Gent M, Hirsh J and Roth G (2001) Platelet-active drugs : the relationships among dose, effectiveness, and side effects. *Chest* **119**(1 Suppl): 39S-63S.

Pawlosky N (2013) Cardiovascular risk: Are all NSAIDs alike? *Can Pharm J (Ott)* **146**(2): 80-83.

Peters-Golden M, Gleason MM and Togias A (2006) Cysteinyl leukotrienes: multi-functional mediators in allergic rhinitis. *Clin Exp Allergy* **36**(6): 689-703.

Rao VR and Oprian DD (1996) Activating mutations of rhodopsin and other G protein-coupled receptors. *Annu Rev Biophys Biomol Struct* **25**: 287-314.

Rasenick MM, Watanabe M, Lazarevic MB, Hatta S and Hamm HE (1994) Synthetic peptides as probes for G protein function. Carboxyl-terminal G alpha s peptides mimic Gs and evoke high affinity agonist binding to beta-adrenergic receptors. *J Biol Chem* **269**(34): 21519-21525.

Raychowdhury MK, Yukawa M, Collins LJ, McGrail SH, Kent KC and Ware JA (1994) Alternative splicing produces a divergent cytoplasmic tail in the human endothelial thromboxane A2 receptor [published erratum appears in J Biol Chem 1995 Mar 24;270(12):7011]. *Journal of Biological Chemistry* **269**(30): 19256-19261.

Robinson PR, Cohen GB, Zhukovsky EA and Oprian DD (1992) Constitutively active mutants of rhodopsin. *Neuron* **9**(4): 719-725.

Rocca B, Secchiero P, Ciabattoni G, Ranelletti FO, Catani L, Guidotti L, Melloni E, Maggiano N, Zauli G and Patrono C (2002) Cyclooxygenase-2 expression is induced during human megakaryopoiesis and characterizes newly formed platelets. *Proc Natl Acad Sci U S A* **99**(11): 7634-7639.

Rodbell M, Krans HM, Pohl SL and Birnbaumer L (1971) The glucagon-sensitive adenyl cyclase system in plasma membranes of rat liver. IV. Effects of guanylnucleotides on binding of 125I-glucagon. *J Biol Chem* **246**(6): 1872-1876.

Roman RJ (2002) P-450 metabolites of arachidonic acid in the control of cardiovascular function. *Physiol Rev* **82**(1): 131-185.

Rordorf CM, Choi L, Marshall P and Mangold JB (2005) Clinical pharmacology of lumiracoxib: a selective cyclo-oxygenase-2 inhibitor. *Clin Pharmacokinet* **44**(12): 1247-1266.

Rovati GE, Capra V and Neubig RR (2007) The highly conserved DRY motif of class A G protein-coupled receptors: beyond the ground state. *Mol Pharmacol* **71**(4): 959-964.

Rovati GE, Sala A, Capra V, Dahlen SE and Folco G (2010) Dual COXIB/TP antagonists: a possible new twist in NSAID pharmacology and cardiovascular risk. *Trends Pharmacol Sci* **31**(3): 102-107.

Rowlinson SW, Kiefer JR, Prusakiewicz JJ, Pawlitz JL, Kozak KR, Kalgutkar AS, Stallings WC, Kurumbail RG and Marnett LJ (2003) A novel mechanism of

cyclooxygenase-2 inhibition involving interactions with Ser-530 and Tyr-385. *J Biol Chem* **278**(46): 45763-45769.

Sabirsh A, Bristulf J and Owman C (2004) Exploring the pharmacology of the leukotriene B4 receptor BLT1, without the confounding effects of BLT2. *Eur J Pharmacol* **499**(1-2): 53-65.

Sakariassen KS, Femia EA, Daray FM, Podda GM, Razzari C, Pugliano M, Errasti AE, Armesto AR, Nowak W, Alberts P, Meyer JP, Sorensen AS, Cattaneo M and Rothlin RP (2012) EV-077 in vitro inhibits platelet aggregation in type-2 diabetics on aspirin. *Thromb Res* **130**(5): 746-752.

Salvo F, Fourrier-Reglat A, Bazin F, Robinson P, Riera-Guardia N, Haag M, Caputi AP, Moore N, Sturkenboom MC, Pariente A and Investigators of Safety of Non-Steroidal Anti-Inflammatory Drugs SOSP (2011) Cardiovascular and gastrointestinal safety of NSAIDs: a systematic review of meta-analyses of randomized clinical trials. *Clin Pharmacol Ther* **89**(6): 855-866.

Samama P, Cotecchia S, Costa T and Lefkowitz RJ (1993a) A mutation-induced activated state of the beta 2-adrenergic receptor. Extending the ternary complex model. *Journal of Biological Chemistry* **268**(7): 4625-4636.

Samama P, Cotecchia S, Costa T and Lefkowitz RJ (1993b) A mutation-induced activated state of the beta 2-adrenergic receptor. Extending the ternary complex model. *J Biol Chem* **268**(7): 4625-4636.

Samuelsson B, Dahlen SE, Lindgren JA, Rouzer CA and Serhan CN (1987) Leukotrienes and lipoxins: structures, biosynthesis, and biological effects. *Science* **237**(4819): 1171-1176.

Scheer A, Costa T, Fanelli F, De Benedetti PG, Mhaouty-Kodja S, Abuin L, Nenniger-Tosato M and Cotecchia S (2000) Mutational analysis of the highly conserved arginine within the Glu/Asp-Arg-Tyr motif of the alpha(1b)-adrenergic receptor: effects on receptor isomerization and activation. *Mol Pharmacol* **57**(2): 219-231.

Scheer A, Fanelli F, Costa T, De Benedetti PG and Cotecchia S (1996) Constitutively active mutants of the alpha 1B-adrenergic receptor: role of highly conserved polar amino acids in receptor activation. *EMBO Journal* **15**(14): 3566-3578.

Scheer A, Fanelli F, Costa T, De Benedetti PG and Cotecchia S (1997a) The activation process of the alpha1B-adrenergic receptor: potential role of protonation and hydrophobicity of a highly conserved aspartate. *Proc Natl Acad Sci U S A* **94**(3): 808-813.

Scheer A, Fanelli F, Costa T, De Benedetti PG and Cotecchia S (1997b) The activation process of the alpha1B-adrenergic receptor: potential role of protonation and hydrophobicity of a highly conserved aspartate. *Proceedings of the National Academy of Sciences of the United States of America* **94**(3): 808-813.

Schnitzer TJ, Burmester GR, Mysler E, Hochberg MC, Doherty M, Ehrsam E, Gitton X, Krammer G, Mellein B, Matchaba P, Gimona A, Hawkey CJ and Group TS (2004) Comparison of lumiracoxib with naproxen and ibuprofen in the Therapeutic Arthritis Research and Gastrointestinal Event Trial (TARGET), reduction in ulcer complications: randomised controlled trial. *Lancet* **364**(9435): 665-674.

Schoneberg T, Schulz A, Biebermann H, Hermsdorf T, Rompler H and Sangkuhl K (2004) Mutant G-protein-coupled receptors as a cause of human diseases. *Pharmacol Ther* **104**(3): 173-206.

Schultheiss G and Diener M (1999) Inhibition of spontaneous smooth muscle contractions in rat and rabbit intestine by blockers of the thromboxane A2 pathway. *Zentralbl Veterinarmed A* **46**(2): 123-131.

Schwedhelm E, Tsikas D, Durand T, Gutzki FM, Guy A, Rossi JC and Frolich JC (2000) Tandem mass spectrometric quantification of 8-iso-prostaglandin F2alpha and its metabolite 2,3-dinor-5,6-dihydro-8-iso-prostaglandin F2alpha in human urine. *J Chromatogr B Biomed Sci Appl* **744**(1): 99-112.

Selg E, Buccellati C, Andersson M, Rovati GE, Ezinga M, Sala A, Larsson AK, Ambrosio M, Lastbom L, Capra V, Dahlen B, Ryrfeldt A, Folco GC and Dahlen SE (2007) Antagonism of thromboxane receptors by diclofenac and lumiracoxib. *Br J Pharmacol* **152**(8): 1185-1195.

Serhan CN and Prescott SM (2000) The scent of a phagocyte: Advances on leukotriene b(4) receptors. *J Exp Med* **192**(3): F5-8.

Seubert JM, Zeldin DC, Nithipatikom K and Gross GJ (2007) Role of epoxyeicosatrienoic acids in protecting the myocardium following ischemia/reperfusion injury. *Prostaglandins Other Lipid Mediat* **82**(1-4): 50-59.

Shen RF and Tai HH (1986) Monoclonal antibodies to thromboxane synthase from porcine lung. Production and application to development of a tandem immunoradiometric assay. *J Biol Chem* **261**(25): 11585-11591.

Silverstein FE, Faich G, Goldstein JL, Simon LS, Pincus T, Whelton A, Makuch R, Eisen G, Agrawal NM, Stenson WF, Burr AM, Zhao WW, Kent JD, Lefkowith JB, Verburg KM and Geis GS (2000) Gastrointestinal toxicity with celecoxib vs nonsteroidal anti-inflammatory drugs for osteoarthritis and rheumatoid arthritis: the CLASS study: A randomized controlled trial. Celecoxib Long-term Arthritis Safety Study. *JAMA* **284**(10): 1247-1255.

Simonet S, Descombes JJ, Vallez MO, Dubuffet T, Lavielle G and Verbeuren TJ (1997) S 18886, a new thromboxane (TP)-receptor antagonist is the active isomer of S 18204 in all species, except in the guinea-pig. *Adv Exp Med Biol* **433**: 173-176.

Six DA and Dennis EA (2000) The expanding superfamily of phospholipase A(2) enzymes: classification and characterization. *Biochim Biophys Acta* **1488**(1-2): 1-19.

Smith WL, DeWitt DL and Garavito RM (2000) Cyclooxygenases: structural, cellular, and molecular biology. *Annu Rev Biochem* **69**: 145-182.

Smyth EM, Grosser T, Wang M, Yu Y and FitzGerald GA (2009) Prostanoids in health and disease. *J Lipid Res* **50 Suppl**: S423-428.

Sousa AR, Parikh A, Scadding G, Corrigan CJ and Lee TH (2002) Leukotriene-receptor expression on nasal mucosal inflammatory cells in aspirin-sensitive rhinosinusitis. *N Engl J Med* **347**(19): 1493-1499.

Spector AA (2009) Arachidonic acid cytochrome P450 epoxygenase pathway. *J Lipid Res* **50 Suppl**: S52-56.

Spector AA and Norris AW (2007) Action of epoxyeicosatrienoic acids on cellular function. *Am J Physiol Cell Physiol* **292**(3): C996-1012.

Stephenson RP (1956) A modification of receptor theory. *British Journal of Pharmacology* **11**: 379-393.

Sternweis PC, Northup JK, Smigel MD and Gilman AG (1981) The regulatory component of adenylate cyclase. Purification and properties. *J Biol Chem* **256**(22): 11517-11526.

Sumimoto H, Takeshige K and Minakami S (1984) Superoxide production of human polymorphonuclear leukocytes stimulated by leukotriene B4. *Biochim Biophys Acta* **803**(4): 271-277.

Sun FF, Chapman JP and McGuire JC (1977) Metabolism of prostaglandin endoperoxide in animal tissues. *Prostaglandins* **14**(6): 1055-1074.

Takasaki J, Kamohara M, Matsumoto M, Saito T, Sugimoto T, Ohishi T, Ishii H, Ota T, Nishikawa T, Kawai Y, Masuho Y, Isogai T, Suzuki Y, Sugano S and Furuichi K (2000) The molecular characterization and tissue distribution of the human cysteinyl leukotriene CysLT(2) receptor. *Biochem Biophys Res Commun* **274**(2): 316-322.

Teller DC, Okada T, Behnke CA, Palczewski K and Stenkamp RE (2001) Advances in determination of a high-resolution three-dimensional structure of rhodopsin, a model of G-protein-coupled receptors (GPCRs). *Biochemistry* **40**(26): 7761-7772.

Tyndall JD and Sandilya R (2005) GPCR agonists and antagonists in the clinic. *Med Chem* **1**(4): 405-421.

Ushikubi F, Nakajima M, Hirata M, Okuma M, Fujiwara M and Narumiya S (1989) Purification of the thromboxane A2/prostaglandin H2 receptor from human blood platelets. *J Biol Chem* **264**(28): 16496-16501.

van der Sterren S and Villamor E (2011) Contractile effects of 15-E2t-isoprostane and 15-F2t-isoprostane on chicken embryo ductus arteriosus. *Comp Biochem Physiol A Mol Integr Physiol* **159**(4): 436-444.

Wang M, Zukas AM, Hui Y, Ricciotti E, Pure E and FitzGerald GA (2006) Deletion of microsomal prostaglandin E synthase-1 augments prostacyclin and retards atherogenesis. *Proc Natl Acad Sci U S A* **103**(39): 14507-14512.

Warner TD, Giuliano F, Vojnovic I, Bukasa A, Mitchell JA and Vane JR (1999) Nonsteroid drug selectivities for cyclo-oxygenase-1 rather than cyclo-oxygenase-2 are associated with human gastrointestinal toxicity: a full in vitro analysis. *Proc Natl Acad Sci U S A* **96**(13): 7563-7568.

Weber G (1972) Ligand binding and internal equilibria in proteins. *Biochemistry* **11**(5): 864-878.

Weiss JM, Morgan PH, Lutz MW and Kenakin TP (1996a) The cubic ternary complex receptor-occupancy model I. Model Description. *J Theor Biol* **178**(2): 151-167.

Weiss JM, Morgan PH, Lutz MW and Kenakin TP (1996b) The cubic ternary complex receptor-occupancy model. II. Understanding apparent affinity. *J Theor Biol* **178**(2): 169–182.

Weiss JM, Morgan PH, Lutz MW and Kenakin TP (1996c) The cubic ternary complex receptor-occupancy model. III. resurrecting efficacy. *J Theor Biol* **181**(4): 381-397.

Wenzel SE, Trudeau JB, Kaminsky DA, Cohn J, Martin RJ and Westcott JY (1995) Effect of 5-lipoxygenase inhibition on bronchoconstriction and airway

inflammation in nocturnal asthma. *Am J Respir Crit Care Med* **152**(3): 897-905.

Wess J (1998) Molecular basis of receptor/G-protein-coupling selectivity. *Pharmacol Ther* **80**(3): 231-264.

Whittle BJ (2003) Gastrointestinal effects of nonsteroidal anti-inflammatory drugs. *Fundam Clin Pharmacol* **17**(3): 301-313.

Xu D, Li N, He Y, Timofeyev V, Lu L, Tsai HJ, Kim IH, Tuteja D, Mateo RK, Singapuri A, Davis BB, Low R, Hammock BD and Chiamvimonvat N (2006) Prevention and reversal of cardiac hypertrophy by soluble epoxide hydrolase inhibitors. *Proc Natl Acad Sci U S A* **103**(49): 18733-18738.

Yamamoto Y, Kamiya K and Terao S (1993) Modeling of human thromboxane A2 receptor and analysis of the receptor-ligand interaction. *J Med Chem* **36**(7): 820-825.

Yokomizo T, Izumi T, Chang K, Takuwa Y and Shimizu T (1997) A G-protein-coupled receptor for leukotriene B4 that mediates chemotaxis. *Nature* **387**(6633): 620-624.

Yokomizo T, Kato K, Terawaki K, Izumi T and Shimizu T (2000) A second leukotriene B(4) receptor, BLT2. A new therapeutic target in inflammation and immunological disorders. *J Exp Med* **192**(3): 421-432.

Yu Y, Fan J, Chen XS, Wang D, Klein-Szanto AJ, Campbell RL, FitzGerald GA and Funk CD (2006) Genetic model of selective COX2 inhibition reveals novel heterodimer signaling. *Nat Med* **12**(6): 699-704.